

Aus der Abteilung Neurologie Max-Planck-Institut für Kognitions- und
Neurowissenschaften Leipzig

DISSERTATION

Non-invasive electrophysiological biomarkers of aging and
Parkinson's disease

Nicht-invasive elektrophysiologische Biomarker des Alterns und
der Parkinson-Krankheit

zur Erlangung des akademischen Grades
Doctor rerum medicinalium (Dr. rer. medic.)

vorgelegt der Medizinischen Fakultät
Charité – Universitätsmedizin Berlin

von

Juanli Zhang

Datum der Promotion: 30.11.2023

Table of Contents

List of figures.....	3
List of abbreviations.....	4
Abstract.....	6
1 Introduction.....	9
1.1 Parkinson’s disease (PD): symptoms and treatment.....	9
1.2 Pathology of PD.....	10
1.3 Electrophysiological neuronal biomarkers of PD.....	13
1.4 PD and normal aging.....	20
1.4.1 Risk factors for PD and markers for prodromal PD.....	20
1.4.2 Aging is the primary risk factor for PD.....	22
1.5 Rationale of the studies.....	24
2 Methods.....	27
2.1 Experimental design.....	27
2.2 Spectral analysis.....	28
2.3 Phase-amplitude coupling.....	28
2.4 Beta burst characteristics.....	28
2.5 Spectral slope.....	30
2.6 Functional Connectivity (FC) and network properties.....	30
2.7 Source reconstruction.....	32
2.8 Statistical tests.....	32
3 Results.....	32
3.1 PAC over the motor-related area is elevated in healthy aging.....	32
3.2 Stronger association between PAC and reaction time with more advanced age.....	33
3.3 Healthy aging is accompanied by longer bursts with a higher incidence rate.....	34
3.4 Spectral slope is deeper after medication administration in patients with PD.....	35
3.5 Functional connectivity is enhanced due to medication intake.....	36
3.6 Graph properties of functional brain network are not responsive to dopaminergic medication.....	36
3.7 Spectral slope is closely related to global network efficiency in Off medication state.....	37
4 Discussion.....	37
5 Conclusions.....	45
Reference list.....	47
Statutory Declaration.....	63
Declaration of your own contribution to the publications.....	64
Excerpt from Journal Summary List.....	66
Printing copies of the publications.....	69
Curriculum Vitae.....	102
Publication list.....	104
Acknowledgments.....	105

List of figures

Figure 1: A simplified schematic illustration of three motor pathways in PD.....13

Figure 2: A schematic model describing the relationship between normal aging and PD in the dopamine system proposed by Collier et al. (2011).....24

Figure 3: A schematic illustration of PAC and beta burst definition.....29

Figure 4: A schematic illustration of the methodology in study 2.....31

Figure 5: An extended model describing the relationship between normal aging and PD.....40

Figure 6: Local E/I impacts the global network integration (modified figure from the study (Zhou et al., 2021)).....43

Figure 7: Overview of the two studies and outlook for the future study designs.....45

List of abbreviations

EEG	Electroencephalography
PD	Parkinson's disease
MDS	Movement Disorder Society
DAT-SPECT	Dopamine Transporter-Single-Photon Emission Computed Tomography
DBS	Deep Brain Stimulation
L-DOPA	Levodopa
CNS	Central Nervous System
STN	Subthalamic Nucleus
GPI	Internal Globus Pallidus
GPe	External Globus Pallidus
SNC	Substantia Nigra Pars Compacta
LBs	Lewy Bodies
BGTC	Basal Ganglia-Thalamus-Cortex
MC	Motor Cortex
PMC	Premotor Cortex
SMA	Supplementary Motor Cortex
CMA	Cingulate Motor Area
LFPs	Local Field Potentials
MEG	Magnetoencephalography
PSD	Power Spectral Density
PAC	Phase Amplitude Coupling
ECoG	Electrocorticography
UPDRS	Unified Parkinson's disease Rating Scale

M1	Primary Motor Cortex
fMRI	Functional Magnetic Resonance Imaging
ADHD	Attention Deficit Hyperactivity Disorder
TMS	Transcranial Magnetic Stimulation
HMM	Hidden Markov Model
PSG	Polysomnogram
REM	Rapid Eye Movement
PET	Positron Emission Tomography
LRs	Likelihood Ratios
EO	Eyes-Open
EC	Eyes-Closed
GE	Global Efficiency
CC	Clustering Coefficient
eLORETA	Exact Low Resolution Brain Electromagnetic Tomography
ROIs	Regions of Interest
MI	Modulation Index
FC	Functional Connectivity
HRV	Heart Rate Variability
HEPs	Heart Evoked Potentials
E/I	Excitation/Inhibition
MSNs	Medium Spine Neurons
SNR	Signal-to-Noise Ratio

Abstract

Parkinson's disease (PD) is a frequent neurodegenerative disorder. It mainly affects motor functions and it has a long preclinical phase. Dopaminergic medication is an effective treatment but also comes with adverse effects. Therefore, investigating early biomarkers of PD and effects of dopaminergic medication is crucial for advancing the understanding and treatment of this disease. In my dissertation, two studies are presented that contribute to this field.

In the first study, we studied PD-related neuronal biomarkers, including excessive PAC (phase-amplitude coupling) between the beta phase and amplitude from broadband gamma and abnormal beta burst dynamics in a group of young (N=71, age 20–35 years) and apparently healthy elderly (N=66, age 59–77 years) subjects with electroencephalography (EEG) recordings. In the second study, based on a group of patients with PD (N=15), we investigated the effects of dopaminergic medication on non-oscillatory component of the neural activity (estimated by the spectral slope), the inter-areal functional connectivity and functional network's configuration properties.

The results from the first study confirmed that the elderly subjects show elevated PAC compared to the younger ones; and this effect is most pronounced in motor-related areas. In addition, the elderly are characterized by prolonged and more often bursting beta activity compared to the young subjects. In the second study, we observed that the spectral slope is steeper after dopaminergic medication intake. Moreover, the medication administration induces an up-regulation of the inter-regional connectivity in the beta band, mainly in fronto-centro-parietal regions. However, there is no evidence showing a significant alteration in the global properties of the functional network. Interestingly, we found that only in the Off medication state there is a close association between the spectral slope and the integrative ability of the brain network. These effects are consistently present in the centro-parietal region.

These findings provide evidence that the electrophysiological biomarkers associated with PD are also present in a group of presumably healthy elderly compared to a young one. This, in turn, indicates that these biomarkers might be *promising* for the detection

of a pre-clinical stage of PD given a close relationship between aging and PD. Future prospective studies should test their unique predictive value in the development of PD. Furthermore, dopaminergic medication induces changes not only locally in the spectral slope but also in the interaction between the areas with a specific spatial interaction pattern. Crucially, the spectral slope (which may index the local excitation/inhibition ratio) appears to be essential in forming the global network's ability to integrate information from remote areas in PD. This could be relevant for the interventional studies directed at non-invasive modulation of neuronal activity in these areas.

Zusammenfassung

Die Parkinson-Krankheit (PK) ist eine neurodegenerative Störung. Sie betrifft die motorischen Funktionen und hat eine lange präklinische Phase. Dopaminerge Medikamente (DM) sind eine wirksame Behandlung, haben aber auch Nebenwirkungen. Daher ist die Untersuchung früher Biomarker für PK und der Auswirkungen DM von Bedeutung, um das Verständnis und die Behandlung dieser Krankheit voranzutreiben. In meiner Dissertation werden zwei Studien vorgestellt, die einen Beitrag zu diesem Thema leisten.

In Studie 1 nutzten wir Elektroenzephalografie (EEG) und untersuchten neuronale PD-bezogene Biomarker, einschließlich erhöhter PAC (Phasen-Amplituden-Kopplung) zwischen der Beta-Phase und der Breitband-Gamma-Amplitude und abnormaler Beta-Burst-Dynamik in jungen (N=71, Alter 20-35 Jahre) und gesunden älteren (N=66, Alter 59–77 Jahre) Probanden. In Studie 2 mit PK-Patienten (N=15) untersuchten wir die Auswirkungen von DM auf die nicht-oszillatorische Komponente der neuronalen Aktivität, die interareale funktionelle Konnektivität und dessen Konfigurationseigenschaften.

Die Ergebnisse von Studie 1 bestätigten, dass ältere Probanden eine erhöhte PAC aufweisen; dieser Effekt ist in den motorischen Bereichen am stärksten ausgeprägt. Darüber hinaus weisen ältere Probanden eine verlängerte und häufiger auftretende Bursting-Beta-Aktivität auf. In Studie 2 beobachteten wir, dass die spektrale Steigung

nach der DM-Einnahme steiler ist. Außerdem führt DM zu einer Hochregulierung der Konnektivität im Betaband, vor allem in fronto-zentral-parietalen Regionen. Es gibt jedoch keine Hinweise auf eine signifikante Veränderung der globalen Eigenschaften des funktionellen Netzwerks. Interessanterweise haben wir festgestellt, dass nur im Zustand „ohne“ DM ein enger Zusammenhang zwischen der spektralen Steigung und der Integrationsfähigkeit des Netzwerks besteht. Diese Effekte sind durchweg in der zentro-parietalen Region vorzufinden.

Diese Ergebnisse belegen, dass die EEG-Biomarker, die mit PK in Verbindung gebracht werden, auch in gesunden, älteren Menschen vorhanden sind. Dies wiederum deutet darauf hin, dass diese Biomarker vielversprechend für die Erkennung eines präklinischen Stadiums der PK sein könnten. Künftige prospektive Studien sollten ihren prädiktiven Wert in der Entwicklung der PK untersuchen. Darüber hinaus induzieren DM Veränderungen nicht nur lokal in der spektralen Steigung, sondern auch in der Interaktion zwischen den Bereichen mit einem bestimmten räumlichen Interaktionsmuster. Entscheidend ist, dass die spektrale Steigung (die möglicherweise das lokale Verhältnis zwischen Erregung und Hemmung anzeigt) für die Fähigkeit des globalen Netzwerks, Informationen aus entfernten Bereichen zu integrieren, bei der PK von Bedeutung ist. Dies könnte für interventionelle Studien relevant sein, die auf eine nicht-invasive Modulation der neuronalen Aktivität in diesen Bereichen abzielen.

1 Introduction

1.1 Parkinson's disease (PD): symptoms and treatment

PD is a chronic neurodegenerative disorder with a prevalence ranging from 0.25% to 4% for people aged between 65 and 80 years (de Lau et al., 2004; de Lau and Breteler, 2006; Pringsheim et al., 2014). PD demonstrates major motor symptoms and also non-motor ones. Typical motor-related symptoms include stiffness of the limbs and trunk, resting tremor, gait imbalance and bradykinesia. Symptoms usually start to be present on one side of the body and progress to the other, and eventually show presence on both sides. However, one side of the symptoms is still more severe than the other, which is often called the dominant side of the symptoms. Non-motor symptoms also appear, which may include, e.g., depression (and other affective disorders), sleep problems, olfactory loss, difficulties in swallowing and speaking, etc. Although typical PD symptoms are well defined, their progression rate over time differs from patient to patient. Even though PD is clinically defined as a movement disorder, the non-motor manifestations are demonstrated to start even from a very early stage and are present in most patients. Thus, some of them have been incorporated into the current diagnostic criteria for prodromal PD (Berg et al., 2015).

Motor symptoms remain the core feature by which PD is diagnosed clinically. Total diagnostic certainty is impossible in life; a varied accuracy between 75% to 95% of the patients diagnosed by clinical experts have been confirmed only by autopsy (A. J. Hughes et al., 1992; Andrew J. Hughes et al., 2002). This variability can be attributed to the disease duration, age, the expertise of the clinician, and advancement in disease understanding. The diagnosis of PD can be robust in most cases, particularly with a stringent use of the criteria by an experienced neurologist. However, it has been suggested that imaging modalities for instance dopamine transporter single-photon emission computed tomography (DAT-SPECT) could be a helpful diagnostic tool in routine clinical practice by identifying the presynaptic nigrostriatal dysfunction (Poewe & Scherfler, 2003).

Current treatment of PD mainly includes dopaminergic medication and surgical DBS (deep brain stimulation). Drugs, for instance, Levodopa (L-DOPA), are prescribed to enhance the dopamine concentration in the brain of patients. The precursor for the neurotransmitters, L-DOPA, can pass the protective blood-brain barrier, unlike dopamine, which is not able to do so. L-DOPA is converted not only by the neurons in the central nervous system (CNS), but also by the cells in the peripheral nervous system. This leads to an undesired increase in dopamine signaling in the periphery as well, thus resulting in many adverse effects (for instance nausea, vomiting, low blood pressure and restlessness). L-DOPA is typically administered along with other medications, including carbidopa, to stop the peripheral synthesis of dopamine from L-DOPA. In addition, the administration of dopamine can lead to changes in the brain regions affected by PD and in the non-PD related regions (Gershman & Uchida, 2019). For instance, prior studies on PD have shown that overdose administration of dopaminergic medication can cause adverse cognitive effects (A. A. MacDonald et al., 2013; P. A. MacDonald et al., 2011; Voon et al., 2010). Therefore, rational management of dopaminergic medication remains an important topic and is still challenging. Identifying biomarkers, particularly derived from non-invasive recordings, underlying changes corresponding to the improvement of clinical symptoms due to dopaminergic medication is of great interest.

With the accumulation of the medication effects, at some point, patients might become much less or even not responsive to medications anymore. Then, they are subject to an invasive treatment that involves a surgical procedure - deep brain stimulation (DBS). DBS involves insertion of electrodes into the sub-cortical part (typically in the subthalamic nucleus (STN) or internal globus pallidus (GPI)) of the brain and connecting the electrodes via cables to a device that is placed in the chest. By programming the device depending on the severity and symptoms of the patient, stimulating the brain structure can usually effectively improve the motor symptoms (Sobesky et al., 2022).

1.2 Pathology of PD

The loss of dopaminergic neurons in the substantia nigra pars compacta (SNc) is the primary cause of PD. Cardinal PD symptoms are believed to become clinically present when around 50%–70% of the dopaminergic cells in the SNc degenerate (Antonini et

al., 2002; Carvey et al., 2006; Ransmayr et al., 2001). The presence of fibrillar aggregates known as Lewy bodies (LBs) is one of the primary characteristics of PD. Lewy bodies are the abnormal aggregation of protein that develop inside nerve cells. In PD, α -synuclein, a protein from the pre-synaptic nerve terminal (Iwai et al., 1995), makes up a significant component of Lewy bodies (Wakabayashi et al., 2007, 2013). The role of LBs concerning neuronal loss in PD is still under debate. LB production has previously been thought to be a sign for neuronal degeneration; however, recent research has suggested that fibrillar aggregates of LBs might instead function as a cytoprotective mechanism in PD (Wakabayashi et al., 2013).

Previous studies have demonstrated that the early pathology of PD begins in substantia nigra (SN) (Damier et al., 1999; Fearnley & Lees, 1991). However, following the α -synuclein pathology, it has been recognized that the progression of PD follows caudorostral propagation from the peripheral nervous system to the CNS. Previous studies have shown that the substantia nigra is not the first structure in the brain to develop PD-related lesions (Del Tredici et al., 2002). In 2003, Braak and his colleagues proposed a model that describes PD's pathological staging scheme (Braak et al., 2003). There, they suggest that pathology starts in the dorsal nucleus of vagal nerves and olfactory bulb in stages 1–2. In stages 3–4, it progresses into pontine tegmentum and midbrain, neostriatum, and medial temporal cortex. Then its invasion into the higher order sensory association and prefrontal areas and further the whole neocortex is considered as a final stage of 5–6. Although this model is commonly recognized, very recent work by (Blesa et al., 2022) suggests that early involvement of the nigrostriatal system in this bottom-up progression model is a prominent component of pathological mechanism for PD.

In terms of brain function, PD mainly affects the basal ganglia-thalamus-cortex (BGTC) circuitry. In this loop, through innervation of glutamatergic neurons in the striatum, the cortex provides excitatory input to the striatum, which then projects back to the cortex via the thalamus (Hammond et al., 2007). The loops can be generally separated into five functional zones based on the differential input from distinct cortical areas: the motor, the dorsolateral prefrontal, the lateral orbitofrontal, the anterior cingulate, and the

oculomotor loop (Alexander, 1986). Evidence has demonstrated that these circuits rather interact with each other instead of functioning in a segregated manner via projections within the striatum (DeLong & Wichmann, 2009; Saint-Cyr, 1995). In PD, investigating the motor-related circuit is crucial for understanding its pathology. It comprises three major pathways: direct, indirect, and hyperdirect pathways (see own representation: Figure 1). MSNs (medium spiny neurons) within the striatum project different nodes within the loop: D1 receptors give rise to the direct pathway, while the MSNs expressing D2 receptors constitute an indirect pathway (Schwarz et al., 2004; Wichmann et al., 2011). The striatum projects GABAergic inhibitory input onto GPi directly through a direct pathway and indirectly excitatory input onto the GPi by involving the GPe (external globus pallidus; gets inhibitory input from the striatum) and the STN (gets the inhibitory input from the GPe) via the indirect pathway. In addition, a direct connection from the motor-related cortices (sensorimotor cortex, premotor cortex, supplementary motor cortex, and cingulate motor area) to the STN forms another pathway: the hyperdirect pathway, which bypasses other nodes in the circuit and thus can transmit information faster (Hammond et al., 2007). It was previously believed that the direct pathway is essential for motor initiation and promotion, while the indirect pathway is involved more in the termination of movement (DeLong & Wichmann, 2009). However, this mechanism could not account for concurrent activation of both pathways during movement. Recent findings suggest that both pathways are rather structurally and functionally interconnected through the coordination in the striatum (Calabresi et al., 2014). In a healthy state, activities of direct and indirect pathways are balanced. Motor irregularities have been linked to a disruption in the ability of the striatum to maintain the balance between excitation and inhibition (Gittis et al., 2010; Oran & Bar-Gad, 2018). Besides, animal PD models and computational work have shown that PD is characterized by an overactive hyperdirect pathway (Ahn et al., 2015; Oswal et al., 2021; Shi et al., 2021). While a large body of studies focuses on the BG, the cortex, and their interaction, cortico-cortical interaction is also a crucial part of this pathological loop. This notion can be evidenced by a very recent study showing that the functional connectivity between the subcortical regions and a variety of cortical regions (not only those mentioned above) closely relates to the movement improvement in PD (Sobesky et al., 2022).

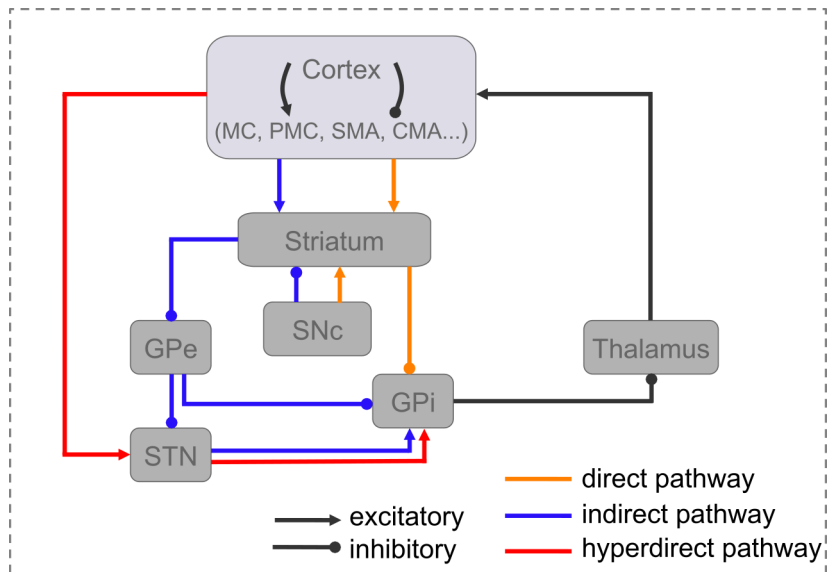


Figure 1. A simplified schematic illustration of three motor pathways in PD. The striatum receives excitatory input from particular cortical regions (MC, PMC, SMA, and CMA). It exerts inhibitory output to GPi via the direct pathway and GPe, and STN via the indirect pathway. Two pathways merge at GPi and inhibit the thalamus with excitatory output projecting back to the cortex. In addition, the cortex directly projects to the STN through a hyperdirect pathway. Note, apart from these pathways, cortico-cortical interaction is an important component of the loop which, nevertheless, is less a focus of previous studies.

1.3 Electrophysiological neuronal biomarkers of PD

Local Field potentials (LFPs) can be produced by the synchronous electrical activity of multiple neurons in a given area of tissue. They can be recorded by placing a microelectrode nearby the population of neurons of interest (in cortical and subcortical regions). In addition, there is a lot of interest in employing non-invasive measurements, such as MEG (Magnetoencephalography) and EEG, to identify potential biomarkers related to PD. This could be valuable for PD diagnosis, dopaminergic drug administration, tracking the development of disease, and as control signals for closed-loop DBS therapy (A. M. Miller et al., 2019). Compared to a local activity captured by LFPs, EEG recording captures the summed electrical activity, generated along the whole cortex and transmits through layers of tissues (cerebrospinal fluid, skull, scalp skin). The primary source of neuronal activity recorded by EEG is the excitatory and inhibitory postsynaptic potentials from the pyramidal cells in the cortex (Speckmann et

al., 2012). Besides, synchronized neuronal currents induce magnetic fields which can be captured by MEG recording. Electrophysiological biomarkers of PD can be studied with LFPs recorded in the basal ganglia or non-invasive scalp MEG/EEG recordings or simultaneous LFPs-MEG/EEG.

Electrophysiologically, it has been consistently reported that a pathological neuronal synchronization characterizes PD through the BGTC circuit (DeLong & Wichmann, 2009; Hirschmann et al., 2011; Litvak et al., 2011; Silberstein et al., 2005; Waschke et al., 2017; Weinberger et al., 2006), and this abnormal synchronization is mainly reflected in a specific frequency range: beta (13–30 Hz) frequency band. Therefore, particular attention has been given to this frequency band. The most prominent electrophysiological markers associated with PD are summarized below.

Beta power. The power of oscillatory activity can be estimated with spectrum density (PSD) or mean squared amplitude over a specific frequency range when using band-pass filtered signals. Beta band activity is typically referred to as a narrow band of 13–30 Hz. It has been shown that neurons in the STN can fire rhythmically at the beta frequency band (Levy et al., 2000), and further evidence demonstrates that oscillations in the STN LFP reflect synchronous population activity of local neurons (Brown et al., 2001; A. A. Kühn et al., 2004; Andrea A. Kühn et al., 2005; Ray et al., 2008). In PD, studies using local field potentials of the STN showed that excessive neuronal synchronization is observed in the beta frequency range (Brown et al., 2003; Chen et al., 2010; Andrea A. Kühn et al., 2006). Crucially, both dopaminergic medications (Alonson-Frech et al., 2006; Cassidy et al., 2002; Andrea A. Kühn et al., 2004; Ozturk, Abosch, et al., 2020; Ozturk, Kaku, et al., 2020; Ray et al., 2008; Tinkhauser, Pogosyan, Tan, et al., 2017; Weinberger et al., 2006) and DBS (Müller and Robinson, 2018; Ray et al., 2008; Tinkhauser, Pogosyan, Little, et al., 2017; Wingeier et al., 2006) can effectively interfere with this excessive beta synchronization, and an improvement in motor symptoms (amelioration of PD symptoms) is closely correlated with the beta oscillation suppression. In addition, cortical beta power has been intensively investigated; however, a link between cortical beta power and parkinsonian state is less consistently reported than that from the subcortical region. More specifically, some

studies have demonstrated an increase of beta power in the PD Off state (Gong et al., 2021) and a decrease after dopaminergic medication, while other studies showed no power difference in the PD Off compared to healthy controls and no alteration by the dopaminergic medication (George et al., 2013; A. M. Miller et al., 2019; Silberstein et al., 2005; Stoffers et al., 2008; Swann et al., 2015; Zhang et al., 2022).

Beta-gamma PAC (Phase-amplitude coupling). PAC is one of the commonly used forms of cross-frequency coupling with amplitude from the higher frequency activity being modulated by the phase of lower oscillations. Previous studies, particularly in attention control tasks, have suggested the role of PAC in coordinating the activity between different associative brain areas (Szczepanski et al., 2014). In addition, it has been shown that the thalamus regulates the exchange with cortical regions via PAC (Malekmohammadi et al., 2015).

As mentioned earlier, aberrant synchronization in the beta frequency band of the basal ganglia has been commonly recognized as the major neuronal sign characterizing PD. In the context of PD, in 2013, de Hemptinne and colleagues showed that in patients with PD, an existence of abnormal coupling of the beta rhythm phase and amplitude of broadband gamma activity (beta-gamma PAC, referred to as PAC in the context of PD in the rest of the text) as recorded with subdural electrocorticography (ECoG) (De Hemptinne et al., 2013). Compared to patients with craniocervical dystonia and patients with epilepsy, in patients with PD, excessive PAC was evident not only in the local LFPs of the primary motor cortex (M1) but also between the LFPs from the STN and the M1 cortex. Significantly, this abnormal cortical coupling could be effectively suppressed by DBS. Later, more investigations have demonstrated the existence of excessive PAC in cortical recordings from patients with PD (De Hemptinne et al., 2015; Malekmohammadi et al., 2018; van Wijk et al., 2016). This enhanced PAC has also been identified using non-invasive EEG measurement in PD (Jackson et al., 2019; A. M. Miller et al., 2019; Swann et al., 2015). PAC was also reduced by dopaminergic medication (A. M. Miller et al., 2019; Swann et al., 2015). Previous studies on PAC used data from sensor space, reflecting mixed signals from different brain regions due to volume conduction. A more recent study solved this issue by utilizing an advanced source reconstruction

methodology based on individual head models (Gong et al., 2021). The authors further proposed that beta and gamma signals originating from distinct sub-networks instead of from the same network components demonstrate more relevance for understanding pathology in PD. Moreover, this study has demonstrated a close relation between this inter-regional PAC and motor symptoms measured with UPDRS III (unified Parkinson's disease rating scale). To date, one very recent study further confirmed the crucial role of cortical PAC about movement deficit (particularly gait freezing) by using ECoG recording at the motor cortex in patients with PD. Here the authors demonstrated an occurrence of abnormally elevated PAC in freezing trials, and DBS targeting STN could effectively decouple the oscillations at the cortex, thus alleviating freezing (Yin et al., 2022). Besides, it is worth noting that all these electrophysiological markers described (above and below) were only demonstrated on a group level (i.e., not everyone having a high PAC will be diagnosed with PD). So far, only one study examined the diagnostic utility of PAC at a single subject level, and their analyses showed moderate potential for this purpose (Swann et al., 2015). Although PAC is far from being an ideal non-invasive biomarker of PD (with high specificity and sensitivity), it does appear to have some intriguing features of being a very promising biomarker characterizing PD. Yet, its full potential should be explored further.

Beta burst dynamics. Earlier in this section, I have mentioned that previous studies showed a direct link between basal ganglia beta oscillations and the severity of motor symptoms (Brown, 2003) as well as a reduction in beta power after dopaminergic medication administration or during DBS (Andrea A. Kühn et al., 2006, 2009; Neumann et al., 2018; Oswal et al., 2016; Trager et al., 2016). In the meantime, increasing evidence has shown that physiological beta activity is composed of brief bursting episodes in the motor circuit (Feingold et al., 2015; Murthy & Fetz, 1992). Breakthrough evidence was presented by human MEG data, computational modeling, and laminar recordings, suggesting that neocortical beta activity emerges as short bursts (Sherman et al., 2016). In 2017, Tinkhauser and colleagues, for the first time, demonstrated that in PD, spontaneous beta activity in the STN is rather transient and occurs in bursts with a large portion lasting 150–200 ms. Their experimental studies with PD patients suggest that pathological beta activity in PD is related to prolonged duration along with a more

frequent incidence of beta bursting activity. Importantly, this pathological phenomenon could be alleviated by re-distributing the beta bursts into shorter, less frequent (or, in other words, more physiological) ones through either dopaminergic medication or adaptive DBS, where long beta bursts were selectively targeted and fragmented (Tinkhauser, Pogosyan, Little, et al., 2017; Tinkhauser, Pogosyan, Tan, et al., 2017). These abnormal burst dynamics observed in STN LFPs were further present in the motor cortex using ECoG at M1 by (O’Keefe et al., 2020) in PD patients. Simultaneous local field potentials in the STN and EEG over the motor cortex confirmed that beta bursts take place locally and are also connected to a between-structure coupling in the basal ganglia-cortical motor network (Tinkhauser et al., 2018). This coupling exerts a greater impact on burst periods as opposed to non-bursting episodes, and longer beta bursts than the shorter ones. This finding raises the possibility that beta bursts have a role in the phasic coupling between sites within the network as well as in the increased local synchronization, which implies a further impact on the motor-related circuits’ ability to encode information in PD.

Spectral slope (also referred to as 1/f slope). Electrophysiological brain signals are composed of oscillatory activities and an aperiodic component in the frequency domain. In the brain, recordings with LFPs, EEG, and fMRI (functional magnetic resonance imaging) have all demonstrated this characteristic (Bullmore et al., 2001; Bullmore & Sporns, 2012; Freeman & Zhai, 2009). It has been suggested that this non-oscillatory aspect of brain activity can shed more light on the complex neuronal dynamics that are taking on at various temporal scales (He et al., 2010; Voytek et al., 2015). In computational modeling and animal studies, this measure has been shown to have a close association with the ratio of excitation/inhibition (E/I) from the recorded site (Gao et al., 2017). Represented by the fitted slope in the log-log space, the aperiodic part of neural activity (referred to as spectral slope or 1/f) is associated with development, healthy aging, dynamic cognitive performance, and neurological diseases like schizophrenia and ADHD (Attention deficit hyperactivity disorder) (Donoghue et al., 2020; Molina et al., 2020; Peterson et al., 2017; Robertson et al., 2019; Voytek et al., 2015). Moreover, clinical studies showed this spectral slope becoming more negative during anesthesia (Colombo et al., 2019; Gao et al., 2017). While many studies have

focused on changes in oscillatory activity, the non-oscillatory part of brain signal has remained unexplored in PD. It is important to mention that previous studies have demonstrated that a flattening of the spectral slope is observed with healthy aging (Cesnaite et al., 2021; Voytek et al., 2015). Even though this measure is not yet investigated in PD studies, based on a close relationship between normal aging and PD, it seems rational to hypothesize that the flattened slope can also be present in PD (as shown in healthy aging). Additionally, previous studies using TMS (transcranial magnetic stimulation), with which excitation and inhibition of the neuronal activity can be directly measured, have demonstrated that PD is associated with alterations in cortical excitability (Cantello et al., 2002; Ridding et al., 1995); therefore, such alterations can also be potentially captured with aperiodic $1/f$ component.

Distributed beta connectivity (coherence). Coherence is a metric that gauges how strongly the signals are phase-synchronized over a certain frequency and is one of the typical approaches for quantifying connectivity. Although the exact mechanism of the generation and the propagation of abnormal oscillatory activity remains unclear, it is commonly recognized that PD is a network pathology (West et al., 2018). The abnormal oscillation could propagate through the basal ganglia-cortical network's connected structures. Previous studies have shown that coherent activity exists within the basal ganglia (DeLong & Wichmann, 2009; S. Little et al., 2012; Oswal et al., 2013; Shimamoto et al., 2013; Weinberger et al., 2006) and between the subcortical region and the motor cortex (Hirschmann et al., 2013; Lalo et al., 2008; Simon Little et al., 2013; Litvak et al., 2011; West et al., 2018). In addition, abnormal cortico-cortical interactions are also involved in this pathological loop. Prior work has shown that beta coherence between cortical regions is exaggerated in PD and could be effectively reduced by L-DOPA (George et al., 2013; Silberstein et al., 2005). A recent study, however, did not replicate this finding, and conversely, no difference was found between healthy controls and PD patients or between the PD Off medication and On state (A. M. Miller et al., 2019). It might imply that excessive synchrony between the basal ganglia and the cortex does not necessarily indicate an increase in connectivity between cortical regions in PD. This assumption seems to be supported by a very recent study using combined STN LFPs-MEG recordings. By applying a time-resolved Hidden Markov

Model (HMM) to study whole brain interactions, including the STN and whole cortex, the authors provided evidence showing that after dopamine administration, beta activity shifted from being mediated by a STN to being mediated by a cortico-cortical (frontoparietal-motor) network in PD (Sharma et al., 2021). Critical engagement of cortical interactions has also been implied in work by (Gong et al., 2021), where the authors reported a distributed presence of PAC over a variety of cortical regions, especially over the somatosensory cortex. Although it has previously been suggested that the hyperdirect tract is required for excessive PAC production (De Hemptinne et al., 2013), this new finding might indicate that the abnormal PAC does not exclusively involve the hyperdirect pathway – it is very likely to engage other pathways in the BGTC network (direct and indirect pathways) or cortico-cortical connections.

What do these biomarkers imply in the context of PD pathology? The abnormal PAC in PD involves the beta-band phase and amplitude from broadband gamma activity. Broadband gamma amplitude is proposed to reflect local non-synchronous spiking of neural populations (Manning et al., 2009; K. J. Miller et al., 2009); therefore, excessive PAC indicates a neural recruiting pattern in which the local spiking activity is preferably activated by some specific phase of lower frequency rhythm (i.e., beta oscillation). PAC in a healthy state is dynamic, task-related, and responsive to changes in cognition and behavior (Ryan T. Canolty et al., 2010; Ryan T. Canolty & Knight, 2010). In PD, however, the elevation of PAC might render the neurons in an inflexible state, thus preventing the necessary changes for a dynamic behavior (Jackson et al., 2019). As pointed out by other studies (Aru et al., 2015; Kramer et al., 2008; Lozano-Soldevilla et al., 2016), one important note is that the non-sinusoidality of the signals could confound the estimation of PAC. Therefore, a cautious interpretation of the PAC-related finding is warranted. Similarly, since spectral coherence in the beta band can serve as an index for communication between regions through the coherence hypothesis (Fries, 2005, 2015), an increase in beta band coherence might also indicate excessive synchrony throughout the network (Swann et al., 2015). As proposed by (Jackson et al., 2019; Swann et al., 2015), different measures might pick up differential aspects of the exact pathophysiology — excessive beta synchronization and neural entrainment within the motor network. For beta burst dynamics, since increasing local

field potential amplitude reflects the increasing local neural synchronization (Tinkhauser et al., 2018), more frequent prolonged beta bursts (also naturally with higher amplitude) in PD may index the excessively synchronous periods. Consequently, the synchronized neurons are less likely to carry diverse information, and therefore, the capacity of information coding of the network is constrained. Interestingly, a recent study was dedicated to investigating the relationship between oscillatory power, bursting, synchrony, and PAC over the motor cortex using ECoG (O’Keeffe et al., 2020). The authors hypothesized that in PD, individual differences in beta power and PAC may be explained by beta burst dynamics, evidenced by a higher PAC or beta power relating to longer bursting periods. However, in my opinion, more work should be performed to validate or provide more direct evidence for this claim.

In summary, current research tends to interpret these differential biomarkers as a partial (thus imperfect) manifestation of the same pathological process underlying PD. Despite this conclusion, one should acknowledge that none of these biomarkers can completely explain each other. Therefore, investigating differential biomarkers characterizing PD is an ongoing research topic, and it is crucial for understanding the pathology of PD reflected in these biomarkers.

1.4 PD and normal aging

1.4.1 Risk factors for PD and markers for prodromal PD

PD is a chronic disorder, and it progresses through an early stage, where the neurodegeneration has already commenced. This early period usually lasts from several years to decades before the onset of the cardinal motor symptoms, based on which a definite diagnosis of PD can be made. During this prodromal phase, neurodegeneration has already started and spread throughout the nervous system (Berg et al., 2014). Notably, a broad range of motor and non-motor signs characterize the prodromal phase, and they might progress and evolve further to a fully developed PD (Berg et al., 2015; Louis & Bennett, 2007). Even though mild symptoms are present, these signs do not yet match the criteria for a clinical PD diagnosis. According to the definition of PD by the International Parkinson and Movement Disorder Society Task Force (Berg et al., 2014), PD should be categorized into three stages: *preclinical*

(neurodegeneration has started but without evident symptoms) (Stern et al., 2012), *prodromal* (symptoms are present, but they do not meet the criteria for diagnosis) and *clinical PD* (cardinal symptoms are present and they are sufficient for clinical diagnosis). Understanding the origin underlining these features during the early stages and their pathological evolution may be crucial for the development of potential neuroprotective treatment, which might halt the development and progression of PD.

The risk factors for developing PD, which have been established by previous work, include age, male sex, regular occupational exposure to pesticides or solvents, non-use of caffeine, non-smoking, family history with PD (sibling and first-degree family), and known genetic mutation (such as GBA/LRRK2 mutation carriers) (Liu et al., 2012; Noyce et al., 2012; Pezzoli & Cereda, 2013). Except for these risk markers with a broad consensus, according to the first published criteria, multiple prodromal markers have been identified and quantified to indicate a likely ongoing neurodegeneration process (Berg et al., 2015). These prodromal markers comprise PSG (polysomnogram)-proven RBD (rapid eye movement (RBM) sleep behavior disorder), clearly abnormal dopaminergic PET (positron emission tomography)/SPECT (single-photon emission computed tomography) to quantify the extent of striatal dopaminergic denervation, possible subthreshold parkinsonism (or abnormal motor testing), depression, severe erectile dysfunction, urinary dysfunction, constipation, olfactory loss, excessive daytime sleepiness and symptomatic hypotension. As pointed out by (Berg et al., 2015), since new data from different fields (neurobiology, genetics, neuroimaging, etc.) are constantly generated, factors or markers used for defining prodromal PD require re-updating continuously. In 2019, an update, which includes newly defined risk factors (for instance, polygenetic risk factor, SN hyperechogenicity, diabetes mellitus, physical inactivity, and low plasma urate levels) and identified prodromal markers (for instance, global cognitive deficit) was then published (Heinzel et al., 2019). According to this latest update, one of the promising candidate markers (not yet added to the criteria due to lack of evidence from prospective studies), is neuroimaging biomarkers (Heinzel et al., 2019). These candidate biomarkers (including neuroimaging ones) could be suggested by their associations with RBD, carriers of genetic mutation, dementia with Lewy bodies, and PD (Barber et al., 2017). Therefore, from this point of view,

theoretically, electrophysiological biomarkers which have been associated with PD, as mentioned above (section 1.3), may also potentially serve as prodromal markers for PD.

1.4.2 Aging is the primary risk factor for PD

Except for the risk factors mentioned above, we focus here on age which remains the primary risk factor for developing PD (Bennett et al., 1996; Hindle, 2010; Morens et al., 1996). Both healthy aging and PD are associated with dopamine loss (Cheng et al., 2010; Darden, 2007). The mild symptoms present in the prodromal phase of PD have often been demonstrated in the healthy elderly (Louis & Bennett, 2007). The published criteria for prodromal PD can also evidence a close relationship between aging and PD: the prior probability and required minimum total LR_s (likelihood ratios that highlight a diagnostic test's potency: A positive LR_s shows how much the likelihood of PD increases with a positive test result) for defining a prodromal PD is clearly age-dependent (Berg et al., 2015). For instance, for people aged between 50–54, the prior probability (the prevalence of prodromal PD) is 0.4%, and the corresponding required LR_s is 1000, while for the ones who are older than 80, the prior probability increases to 4.0%, and the total LR_s for defining a prodromal PD decreases to 95. Another piece of evidence comes from the age-dependent penetrance of intermediate-strength genetic mutations associated with PD. For example, the cumulative PD risk of an LRRK2 mutation carrier is ~42% at the age of 80 years, while only 4% in the general population (Heinzel et al., 2019; Lee et al., 2017). Crucially, evidence from non-human primates has demonstrated a close link in the cellular mechanisms between aging and PD (see Figure 2 below, from Collier et al., 2011) (Collier et al., 2011). Specifically, it has been proposed that in the dopaminergic system, aging and PD share multiple biological features (the accumulation of cellular markers in aging occurs, mimicking the pattern observed in PD). Healthy aging induces a pre-parkinsonian state, and PD develops in a way that is an accelerated normal aging process due to genetic, environmental and other factors (Collier et al., 2011, 2017).

Moreover, data from PD mice models have shown that electrophysiological properties of dopaminergic neurons are altered, and notably many of the effects are dependent on age (Branch et al., 2016). In addition, neuroimaging studies have shown that age remains the most substantial contributor to the first identified latent variable of brain

atrophy derived from patients with PD (Zeighami et al., 2019). In a longitudinal study, both healthy aging and PD data were acquired, and it was found that during one year, both healthy aging and PD are accompanied by cortical thinning. Additionally, PD showed a more pronounced alteration than what was observed in healthy aging (Yau et al., 2018). These structural changes shared by both healthy aging and PD seem to additively support the theory that PD is an accelerated or exaggerated aging process. Based on the evidence from different lines of research, aging has repeatedly been shown to be the primary risk factor for the onset of PD. In this context, we follow the logic that aging might represent a process *potentially* associated with a preclinical/prodromal PD, which might in turn provide a window through which appropriate biomarkers may relate to early signs of neurodegeneration (which may progress further to fully developed clinical PD).

Given a close relation between normal aging and PD, aging-related neuronal biomarkers may prove useful to index an early stage of PD. These promising biomarkers may appear in the normal aging process and can be further amplified throughout the development of PD. Therefore, an important question arises: Are the biomarkers associated with a fully developed PD also present during seemingly “healthy” aging and could probably eventually reach a pathological level when PD is fully developed? This question could be accessed by looking at the neurophysiological changes in both healthy aging and PD.

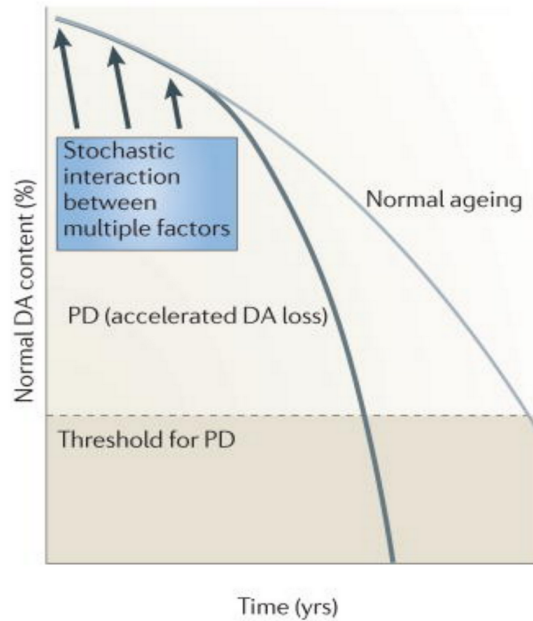


Figure 2. A schematic model describing the relationship between normal aging and PD in the dopamine system proposed by Collier et al. (2011). With time passing, both normal aging and PD are characterized by dopamine loss. However, due to a stochastic interaction between multiple factors (for instance, genetic, inflammation, environment, unknown factors, etc.), in PD an accelerated dopamine loss results in dysfunction passing eventually the clinical threshold for PD.

1.5 Rationale of the studies

I have investigated electrophysiological biomarkers during apparently healthy aging (perhaps indicating pre-clinical or prodromal PD) (study 1) and during dopaminergic medication-induced On- and Off-states in PD patients (study 2).

Study 1: We hypothesized that the electrophysiological neuronal biomarkers associated with PD are also present in healthy aging. To address whether the electrophysiological biomarkers for PD are also present during healthy aging, we have analyzed an open dataset that includes a large number of resting-state EEG recordings from healthy young (age 20–35 years) and elderly (age 59–77 years). We hypothesized that electrophysiological biomarkers of PD, that is, PAC between beta phase and amplitude of broadband gamma activity, and the occurrence of longer beta bursts, are more pronounced in the elderly in comparison to the young subjects. These biomarkers are chosen based on the fact that they are consistently reported in previous studies about

PD. In addition, these effects are expected to be strongest in the sensorimotor cortex. A methodological overview of this study is shown in Figure 3 (own representation) below.

Although regional alterations may provide a in-depth understanding of the underlying local circuit, the brain operates as a distributed network. Additionally, as we have mentioned above, PD is a network pathology. While our first study has demonstrated the presence of PAC and prolonged beta bursts in healthy aging, similar to what has been shown in PD, the effect was not manifested only in the sensorimotor areas. Instead, these effects were found to be present in multiple cortical areas (for instance, the primary motor cortex, the somatosensory cortex, the cingulate cortex, the frontal cortex, the temporal cortex, etc.). It is worth noting that the areas demonstrating increased electrophysiological biomarkers in a healthy aging brain in our first study are consistent with the recent data from patients with PD, where the authors showed the elevation of PAC in similar cortical regions (Gong et al., 2021). Due to this observation, I became interested in the interaction between cortical regions and moved beyond the within-areal biomarkers. Besides, since it has been shown that a flattening of the spectral slope is observed with healthy aging (Cesnaite et al., 2021; Voytek et al., 2015), I anticipated this effect should also be present in PD. These factors contribute to the motivation to carry out study 2, which I will introduce below.

Study 2: In this study, we hypothesized that dopaminergic Off and On medication administration is accompanied by alterations locally in the non-oscillatory component (represented by spectral slope) and globally in the brain network. To test this hypothesis, we analyzed an open-access dataset that includes a patients' cohort with On and Off dopaminergic medication states. Specifically, here, we aimed to address the following questions. What impact does dopaminergic medication have on functional connectivity? In addition, from the perspective of graph theory, the following research question was formulated: Does dopaminergic medication produce changes in the global network architecture? Based on the previous finding of the flattening of spectral slope observed in healthy aging (Cesnaite et al., 2021; Voytek et al., 2015), we assume that this measure can also serve as a potential index for the parkinsonian state. We further wondered: In PD, how does the spectral slope alter after the administration of

dopaminergic medication? Moreover, based on a hypothesis of excitation/inhibition balance of spectral slope (Colombo et al., 2019; Gao et al., 2017), we hypothesized that the local non-oscillatory activity should relate to the functional connectivity of the brain network since local excitation can define and shape the transmission of the activation locally and globally (Deco et al., 2014; S. Zhou & Yu, 2018). A methodological overview of this study is shown in Figure 4 (own representation) below.

Before further details are presented, I would like to clarify a few possible ambiguities. First, as mentioned above, all the summarized biomarkers associated with PD have not yet been rigorously tested for their specificity and sensitivity (except for PAC in one study (Swann et al., 2015)). These “biomarkers” were only demonstrated at group level and are not yet proven as a feasible application at single subject level in clinical practice. As a result, a statement like “a subject demonstrating high PAC should be diagnosed with PD” is *not* the intended interpretation. Rather, we focus currently on the interpretation of the effects on a group basis. Secondly, healthy aging (or normal aging), in contrast to pathological aging, here refers to a natural process during which the subjects age without developing any clinically diagnosed disease including PD. It is unclear, though, whether some of the seemingly “healthy elderly” subjects are already in the stage of the preclinical/prodromal PD. This problem is not resolved in my work as is also the case for the earlier PD studies (where elderly are often recruited for a control group). However, through performing these studies, some specific suggestions could be provided so that such an issue could be possibly addressed in the future studies. Last but not least, it may appear counterintuitive that a biomarker characterizing PD is hypothesized to be also present in “healthy aging”. However, it should be emphasized once more that the neuronal loss and cellular dysfunction in dopamine system is a common feature of both aging and PD. Nevertheless, the magnitude of the effects accessed in a longitudinal manner (i.e., the absolute value of PAC increase for instance) should also be considered in relation to the particular effects we examined in aging and PD, in addition to the question of whether or not the biomarkers are present as such (i.e., a PAC elevation or not for instance).

2 Methods

In this section, I will briefly introduce the methodologies we have utilized in this dissertation. For a detailed description of all these methods, one can refer to the attached original publications (Zhang et al., 2021, 2022).

2.1 Experimental design

The data analyzed in the first study is an open public dataset that was acquired in a previous study (Babayan et al., 2019). Participants were instructed to sit calmly in a chair, and recordings were performed in a sound-shielded room. A 62-channel EEG cap (BrainAmp MR-plus amplifiers using ActiCAP electrodes) was used to acquire the data. The recording included eyes-open (EO) and eyes-closed (EC) sessions, with each condition (EO or EC) lasting 8 minutes in total. In our study, we only pooled the data from the eyes-closed condition since, usually, this condition has a higher SNR (signal-to-noise ratio). The final dataset included an elderly group (with 66 subjects aged 59–77 years, 31 females) and a gender-matched younger group (71 subjects aged 20–35 years, 24 females). Additionally, we also included measurements from a behavioral task. The Alertness subtest of TAP (Test of Attentional Performance, Zimmermann & Fimm, 2002) measures the reaction speed and alertness. Participants were asked to respond to the randomly appearing cross with varying intervals on the screen as quickly as possible. As a final measure for intrinsic alertness, the mean reaction time for each subject was calculated: the higher the reaction time, the lower the behavioral performance.

Data analyzed in the second study is open-source data which can be acquired with this link: <https://openneuro.org/datasets/ds002778/versions/1.0.5>. Fifteen patients with PD were recruited and measured on two days for dopaminergic medication: On and Off conditions in a counterbalanced manner. The EEG recordings include approximately 3 minutes of resting-state obtained with a 32-channel EEG cap with the BioSemi ActiveTwo system. During the recordings, participants were told to be calmly seated in front of a screen that displayed a cross in the center. For more details, one could refer to this original study (George et al., 2013).

2.2 Spectral analysis

Power spectral density was computed by the *'pwelch'* function from Matlab with a Hamming window size of 1s (512 samples) and 50% overlap. By averaging the PSD values over the corresponding frequency range, 13–30 Hz, beta band power was attained. For the detection of individual beta peaks, we used the function *'findpeaks'* from Matlab over the frequency range of the beta band.

2.3 Phase-amplitude coupling

To quantify the degree of phase-amplitude modulation, modulation index (MI) based PAC was computed (Tort et al., 2008). It estimates the deviation of the normalized amplitude distribution based on the sorted phase bins. The MI value ranges from 0 to 1: 0 indicates no coupling and 1 indicates a perfect coupling. To visualize the possible coupling pattern in a broad range of frequencies, as described in Zhang et al. (2021), we computed MI across the 4–50 Hz for phase providing frequency (in the step of 2 Hz with a bandwidth of 2 Hz) and 4–170 Hz for amplitude providing frequency (in the step of 4 Hz with a bandwidth equal to the slower oscillation's center frequency), which is also called a phase-amplitude comodulogram. To obtain the phase and amplitude envelope information, Hilbert transform was applied to the band-pass filtered time series. A PAC value was accessed by taking the mean of the MI values over the frequency of interest within the comodulogram. In our case, MI values over the phase-providing frequency range of 13–30 Hz and amplitude-providing frequency range of 50–150 Hz were determined for further statistical analyses. A simplified illustration of PAC is shown in Figure 3 (own representation).

2.4 Beta burst characteristics

Referring to the proposed methods by previous studies (Tinkhauser, Pogosyan, Little, et al., 2017; Tinkhauser, Pogosyan, Tan, et al., 2017), a beta burst was defined as an event that exceeds a certain threshold of the amplitude envelope and lasts more than 100 ms (at least two cycles of beta oscillations; see own representation: Figure 3) above the threshold. For demonstrating the main findings, as described in Zhang et al. (2021), we used a fixed threshold which in this case was the 65th percentile. In addition, to verify the robustness of our results, we also incorporated the analysis encompassing

a variety of thresholds (percentiles 50th-90th in a step of 5%). To characterize how long the bursts are and how often they emerge, two parameters were estimated to quantify the dynamic features of the beta burst event. One is the percentage of the beta burst with different durations, and the other one is the burst incidence rate. A normalized histogram was plotted to show the percentage distribution of bursts with different durations: 0.1–0.2 s, 0.2–0.3 s, 0.3–0.4 s, 0.4–0.5 s, 0.5–0.6 s, 0.6–0.7 s, 0.7–0.8 s, 0.8–0.9 s. The incidence rate was obtained by counting the number of bursts over a time unit (bursts/second).

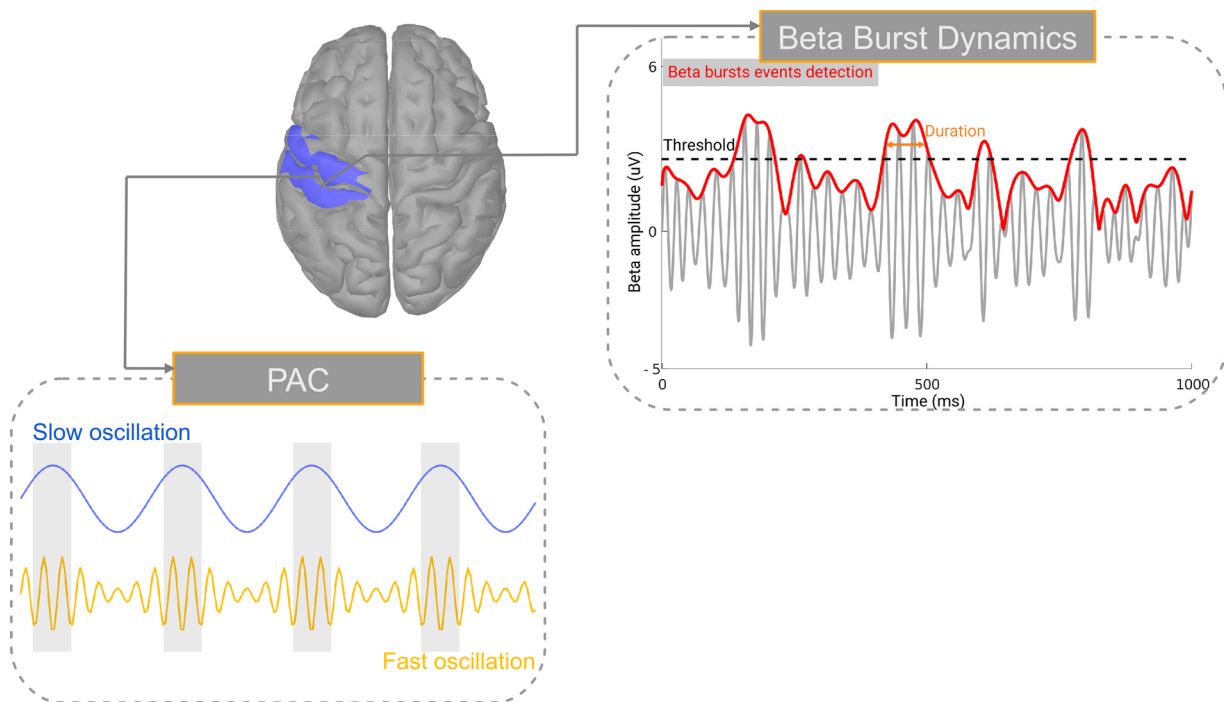


Figure 3. A schematic illustration of PAC and beta burst definition. PAC is calculated based on the degree to which the phase of beta oscillation modulates the amplitude from the broadband gamma activity. As illustrated in the PAC panel, the amplitude of the fast oscillation (in the orange line) is always the highest when the slower oscillation (in the blue line) reaches a specific phase (in this case, it is a positive peak). For the beta-burst detection, the amplitude envelope of beta oscillation is obtained, and then a particular percentile-based threshold (for instance, 65th) is applied. An episode that is above this threshold and lasts longer than two cycles is defined as a beta burst event. We predominantly focus on motor-related areas for both measures, both in sensor and source space.

2.5 Spectral slope

Following the recommendation of a previous study (Colombo et al., 2019), we estimated the spectral slope using a robust three-step regression method. The regression was performed on the computed PSD (power spectral density) over a wide range of frequencies (2–45 Hz) of the signal. As described in Zhang et al. (2022), briefly, a line was fitted to the raw PSD in the log-log space using Matlab's function 'robustfit'. Then, oscillatory peaks were identified and excluded based on the deviation of the PSD residuals according to the fitted line. Lastly, the remaining of frequency bins are fitted for a second time. The slope of the second fitted line was taken to be a final measure of the spectral slope (see own representation: Figure 4). This approach is similar to how the $1/f$ slope is quantified using built-in functions based on the toolbox FOOOF (<https://foof-tools.github.io/foof/>).

2.6 Functional Connectivity (FC) and network properties

To eliminate the spurious connectivity due to the volume conduction, lagged coherence (Pascual-Marqui, 2007; Pascual-Marqui et al., 2011) was used to estimate the functional connectivity by excluding zero-lag phase coupling. As mentioned in Zhang et al. (2022), with a step of 1 Hz, connectivity between all of the channel pairs was calculated over a frequency range of 1–35 Hz. By averaging the values of lagged coherence over the frequency range of interest, functional connectivity in a particular oscillatory frequency band was measured. Eventually, a functional connectivity map (functional network) could be represented by a symmetrical 32×32 matrix.

In addition, we estimated theoretical graph measures for the functional network. As described in Zhang et al. (2022), the nodal degree was estimated by the node centrality, which quantifies the importance of the node in a network by the number and weight of the connected node edges. To further characterize the network's structure, we calculated global efficiency (GE, which can be obtained by the inverse of the shortest path length, and the shortest path length between two nodes is the path with the fewest links) and clustering coefficient (CC, which can be calculated by the number of triangles dividing by the total number of triples, and a triple means a subgraph consisting of three nodes and at least two edges) to quantify the global network's integration and

segregation, respectively. Before doing so, a sparse connection matrix and further a binary network was obtained by applying a proportional thresholding for the estimation of the network features based on graph theory. We examined a series of thresholds that may produce networks with 20 to 200 links, ranging from 36% to 4%. Next, these graph theory-based metrics (GE and CC) were computed using the functions as implemented in the Brain Connectivity Toolbox (Rubinov & Sporns, 2010). The greater the functional integration (segregation) of the network, the larger the GE (CC).

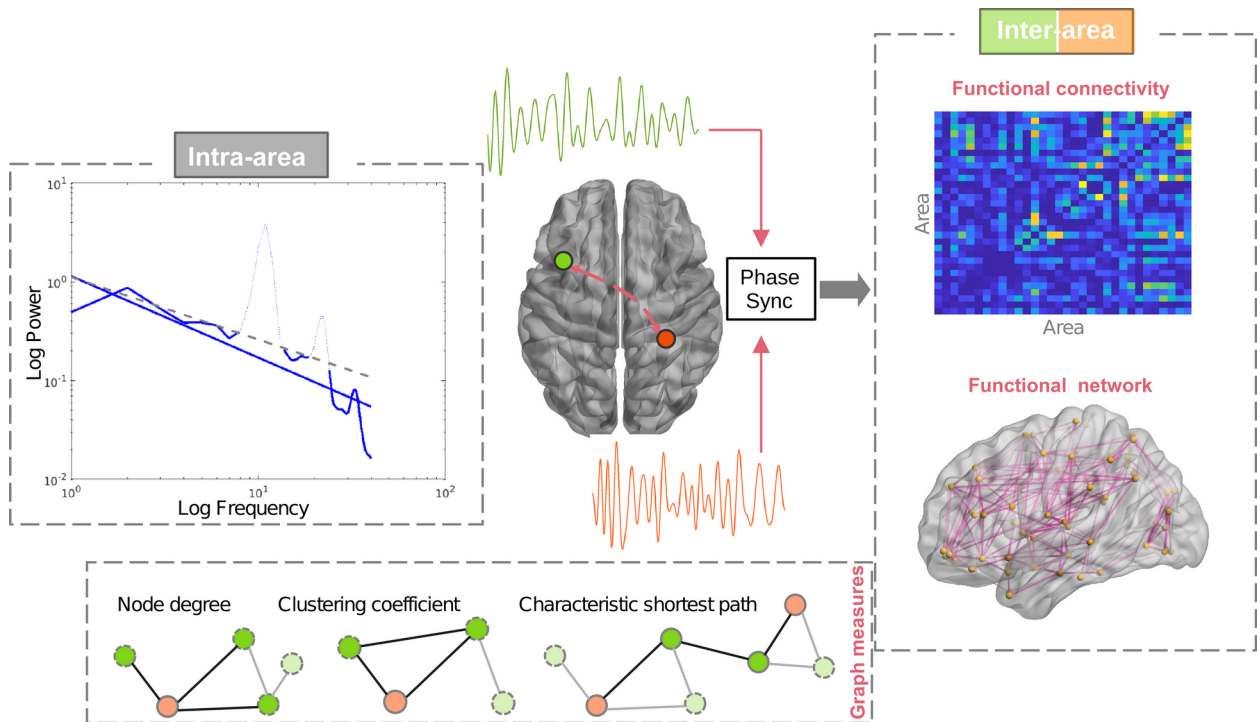


Figure 4. A schematic illustration of the methodology in study 2. The spectral slope is measured in a log-log space within each area without including the prominent oscillatory peaks. Besides, phase coupling in the beta frequency band between two areas is estimated, and a symmetric matrix (32×32) representing the functional brain network is obtained. Graph theory-based network measures are employed to quantify the local and global properties of the network. Specifically, node degree quantifies the strength of connections of one node based on the number (and the weight in some cases) of the edges (for instance, in the bottom of Figure 4, the node degree of the orange one is 3 which is unweighted by the edge strength, only for illustration purpose). The clustering coefficient quantifies a network’s ability for functional segregation. It is defined as the ratio of present triangles to the total possible number of triangles for each node (for instance, in the bottom of Figure 4, the clustering coefficient of the orange-colored node

is 1). Global efficiency is the inverse of shortest path length between two nodes, which is the path with the fewest edges (for instance, in the bottom of Figure 4, the shortest path length between the two orange-colored nodes is 3). The functional network's global properties (CC and GE) are obtained by averaging the estimations over all the nodes constituting a network.

2.7 Source reconstruction

To project the sensor data to cortical source space, we employed the New York head model to acquire the lead field matrix (Huang et al., 2016) and the eLORETA (exact low-resolution brain electromagnetic tomography) algorithm for inverse modeling. Further, 96 ROIs (regions of interest) were created by grouping the vertices according to the Harvard-Oxford brain atlas (Desikan et al., 2006).

2.8 Statistical tests

We performed statistical comparisons between groups using non-parametric tests. Specifically, Wilcoxon signed-rank test was performed for within-subject and Wilcoxon rank-sum test was applied for between-subject comparisons. To correct for multiple tests, FDR (false discovery rate) procedure was employed (Yoav Benjamini & Yosef Hochberg, 1995). In addition, for MI comodulograms in study 1, we applied a cluster-based permutation test ("*Monte Carlo*", implemented in FieldTrip (Oostenveld et al., 2011)) to account for the multiple tests within the two-dimensional frequency-frequency space (Zhang et al., 2021). Similarly, in both studies, to account for multiple tests conducted over all the channels in channel space, the cluster-based permutation was used. Finally, we provided cluster-level statistics in the empirical data in comparison to the null distribution derived from the permuted data (1000 times). Clusters with p values less than 0.05 (two-tailed) were deemed significant.

3 Results

3.1 PAC over the motor-related area is elevated in healthy aging

Following the previous PD studies, we computed the MI comodulogram over the sensorimotor area which electrodes C3 and C4 can represent. As shown in Figure 2A in study 1 (Zhang et al., 2021), one can see a pronounced coupling over the phase from

beta extending to low gamma frequency range and amplitude from broadband gamma band in healthy elderly compared to the younger ones. To test whether there is a significant difference in the PAC value between the beta (13–30 Hz) phase and broadband gamma (50–150 Hz) amplitude similar to what has already been described in the PD studies, we averaged PAC over these frequency ranges within the MI map. A Wilcoxon rank-sum test demonstrated a significant enhancement in beta-broadband gamma PAC in healthy elderly compared to healthy young group ($p=0.0147$).

To further characterize the spatial origin of the PAC effect, we performed similar analyses for all the channels as we described for channel C3 above. Statistical analysis revealed a dominant distribution over the centro-temporal regions in the left-hemisphere with extension to frontal areas (see Figure 3A in the study of Zhang et al., 2021). In addition, we calculated PAC values for each region of interest for each subject in the source space. Comparison between the two age groups in the source space confirmed a spatial pattern where the most pronounced difference originated from left pre- and post-central gyri (see Figure 3B in the study of Zhang et al., 2021), consistent with what we have observed at the sensor level. Crucially, to rule out the confounds from the non-sinusoidality of the beta waveform to the observed PAC effect, we performed additional analyses (phase-phase coupling and regression analysis), showing that beta-gamma The non-sinusoidality of the waveform of beta oscillations is unlikely to be the primary drive of PAC (for details see supplemental analysis 1 in the study of Zhang et al., 2021). Similarly, the PAC effect was not associated with the power of beta oscillation itself, either (see supplemental analysis 2 in the study of Zhang et al., 2021).

3.2 Stronger association between PAC and reaction time with more advanced age

Next, due to the previous suggestion of a link between PAC and the severity of motor impairment in PD patients, we also examined a possible link between the magnitude of PAC and behavioral movement readiness which can be indicated by the mean reaction time in a TAP-alertness task. We took an average of PAC values from the precentral gyri (left and right) as a reliable measure of PAC for each subject. By increasing the age-onset for inclusion of the subgroup to calculate the correlation between PAC and the behavioral reaction times within each age group (elderly and young), we observed an increasing correlation strength between PAC and the reaction times with more

advanced age onset in the elderly, but not in the young group (see Figure 4 in the study of Zhang et al., 2021). It demonstrates that for the elderly with more advanced age, there is a stronger positive association between PAC and reaction time. This means that if we only take a sub-sample of elderly participants, a higher PAC associates with a slower reaction and this association becomes even stronger when the included participants are older. Importantly, by performing a permutation test, we showed that the observed tendency was not due to the sub-sampling procedure.

3.3 Healthy aging is accompanied by longer bursts with a higher incidence rate

Properties of beta burst events were investigated as well. Beta bursts were classified into nine windows (0.1–0.9 s with steps of 0.1 s and longer than 0.9 s) based on their duration, consistent with how it was done in previous PD studies (Tinkhauser, Pogosyan, Little, et al., 2017; Tinkhauser, Pogosyan, Tan, et al., 2017). In the centro-parietal region (represented by channel CP3), we found that the proportion of shorter bursts (0.1–0.2 s) in the young group was higher than that of the elderly group ($p=0.0122$ after FDR correction). In comparison, the percentage of longer bursts (0.2–0.3 s, 0.3–0.4 s, 0.4–0.5 s) are lower than that from the elderly group ($p=0.0132$, 0.0132, 0.0184 after FDR correction, respectively) (see Figure 5A in the study of Zhang et al., 2021). Further, we estimated the percentage of longer bursts (0.2–0.5 s) for each channel and each subject to examine the spatial pattern of the effect, and statistical analysis indicated that a higher percentage of longer bursts in elder subjects, in comparison to young subjects, were present in the bilateral frontal and centro-parietal sites (see Figure 5B in the study of Zhang et al., 2021). In addition, the same analysis from the source reconstructed signals revealed a spatial pattern with the most pronounced difference located in bilateral pre- and post-central gyri (see Figure 5C in the study of Zhang et al., 2021).

Except for the proportion of short and long bursts, another critical characteristic of beta burst events is the burst incidence rate. Between the two groups, there is no significant difference in the burst incidence rate for shorter bursts; however, a significant increase was found in longer bursts (0.2–0.3 s, 0.3–0.4 s, 0.4–0.5 s) for the elderly compared to the younger group. The difference topographies were distributed over the centro-parietal regions across the longer bursts with various durations (0.2–0.3 s, 0.3–0.4 s,

0.4–0.5 s) at the sensor level (see Figure 6A in the study of Zhang et al., 2021). In the source space, we contrasted the two groups' mean incidence rate of longer bursts (0.2–0.5 s), and the analysis further confirmed a spatial localization over multiple cortical areas with the strongest effects in the bilateral pre- and post-central gyri (see Figure 6B in the study of Zhang et al., 2021).

Of note, the primary analyses for beta burst dynamics were based on the burst definition with the representative threshold of the 65th percentile. Additionally, to address whether the effect was dependent on this specific threshold applied, we examined two primary parameters of beta bursts, that is, overall burst duration and amplitude across a range of thresholds ranging from the 50th to 90th percentile with a step of 5%. This analysis demonstrated that, in general, the elderly participants have longer bursts with higher amplitude than the young group, regardless of the thresholds for the definition of a burst event (see Figure S5 in the supplemental material in the study of Zhang et al., 2021).

3.4 Spectral slope is deeper after medication administration in patients with PD

In the second study, we examined the changes in the local aperiodic component and global network alterations in PD patients in On and Off medication states. Regarding the regional non-oscillatory component measured by the spectral slope based on the PSD over a wide band of frequency (2–45 Hz). We found a spatial specificity for both groups: a steeper power spectra distribution along the front-center-parietal midline of the brain compared to other regions (see Figure 2B of Zhang et al., 2022). Statistical analysis revealed an increase of spectral slope (flattening) in the Off condition compared to the On condition (see Figure 2C of Zhang et al., 2022). The effect was primarily localized in the left central site (Monte-Carlo, $p=0.0220$). Furthermore, we investigated the differences in oscillatory beta power between the two conditions for scenarios both with and without taking the overall slope effect into account. The result showed a lack of significant difference in beta power between conditions for these both scenarios (see Figure 3 of Zhang et al., 2022), despite the fact that after correcting for the slope, there was a tendency for a decline in the beta power in centro-parietal regions (Off versus On, Monte-Carlo, $p=0.0739, 0.0939$).

3.5 Functional connectivity is enhanced due to medication intake

Next, we examined the functional coupling between pairs of regions which can be approximately represented by the corresponding channels. We predominantly focused on the connectivity between sensorimotor regions which typically includes C3 and C4 (or frontal regions covered by Fz) and other areas. With a resolution of 1 Hz in a frequency range of 1–35 Hz, FC between C3 (or Fz) and Pz (one of the parietal region's representative channels) showed clear peaks for both conditions (see Figure 4A in the study of Zhang et al., 2022). Using a channel-space cluster permutation test, we performed a seed-based beta band connectivity comparison between medication conditions after averaging the FC values over the beta frequency range. We found there is a significant increase in the On in comparison to the Off condition in the beta band FC between C3 (or Fz) and parieto-occipital (or centro-parietal) regions (see Figure 4B in the study of Zhang et al., 2022). However, no difference was observed for C4-based connectivity between conditions. This analysis was then repeated for all the rest of the channels, and eventually, we were able to show a whole head profile (see Figure 4C in the study of Zhang et al., 2022). The head-in-head topography demonstrated that there was a synchronization up-regulation between the frontal, central, and parieto-occipital regions after dopaminergic medication administration.

3.6 Graph properties of functional brain network are not responsive to dopaminergic medication

To gain a better understanding of the properties of functional networks based on theoretical graph analysis, we estimated the local and global features of functional brain networks. First, we calculated the node degree for each channel and each subject. A spatial specificity was revealed by a grand average of node degree across patients within each group: In comparison to other regions, central regions had a higher level of node degree (see Figure 5A in Zhang et al., 2022). Statistical comparison between the two conditions revealed an increase of node degree primarily in the centro-parietal region in the On condition compared to the Off condition (Monte-Carlo, $p=0.0140$, see Figure 5B in Zhang et al., 2022). Further, we examined a possible change in the global configuration/organization of functional networks: Clustering coefficient measures global segregation, while global efficiency measures global integration. Statistical analyses did

not indicate a difference across a broad range of thresholding values in either of these measures (see Figure 6 in Zhang et al., 2022).

3.7 Spectral slope is closely related to global network efficiency in Off medication state

To answer the question of whether the local activity can define the whole network's organization, we also looked into a possible association between global network metrics and spectral slope. Firstly, we conducted the analyses using an example thresholding value of 20% to derive the functional network metrics. The global slope (averaged across all the channels for each subject) was found to be negatively correlated with the GE of the functional brain network ($r=-0.7643$, $p<0.001$). This relation was only present for the Off condition. Further, to investigate the spatial specificity of this relation, we took each slope value from each channel and performed a correlation analysis across all the electrodes. The investigation revealed a topographical pattern where the left centro-parietal region showed the most pronounced effect (see Figure 7B in the study of Zhang et al., 2022). Again, in the On condition, no significant association was found between the local spectral slope and GE of the network. Next, the correlation analysis between global slope and GE in the Off condition was extended using a broad range of thresholding values ranging from 36% to 4%. Consistently, negative relations were present across almost all these thresholds (36%–6%: $p<0.05$, 4%: $p=0.33$) (see Figure 7C in Zhang et al., 2022).

4 Discussion

This doctoral thesis consists of two studies. The first study demonstrates that the typical electrophysiological biomarkers associated with PD are also present in an elderly group in comparison with a group of younger subjects. This might indicate that these biomarkers, i.e., amplified PAC (between beta phase and amplitude of broadband gamma activity) and prolonged beta burst with higher incidence, could be indicators of preclinical or prodromal stages of PD. Consistent with this notion, with higher age, there is an increasing correspondence between PAC and slowing of reaction times derived from an alertness task (with increasing age of elderly, the positive correlation between PAC and behavioral reaction time increases). This relationship did not show existence

in a young group which we investigated, thus indicating a functional relevance of PAC increase in the elderly. Additionally, the elevation of PAC and prolonged beta bursts are found to be most prominent over the motor regions, which might reflect abnormal motor circuitry pathology. These findings may help facilitate the early detection of electrophysiological markers of neuronal degeneration, which might eventually progress and evolve to meet a clinical diagnosis of PD later.

Apart from demonstrating the presence of PAC in healthy aging, in addition, we were able to show a preferred phase specificity across the young and elderly groups. It means that the high-frequency amplitude increases at a specific phase of beta oscillation for the elderly and young subjects. We assume that in PD, this phase specificity will remain or become even more pronounced. Since it has been shown that a phase-dependent DBS treatment could suppress the beta amplitude in a more efficient manner (Holt et al., 2019), it would be intriguing to test, at an individual level in a patients' cohort, whether at the preferred beta phase the stimulating effect could be even further improved.

In agreement with the proposal from previous studies on non-human primates (Collier et al., 2011, 2017) demonstrating that aging and PD share the cellular markers and aging creates a pre-parkinsonian state, our study further shows that healthy aging and PD share similar pathophysiological processes reflected in the electrophysiological biomarkers. It seems reasonable to assume that electrophysiological biomarkers of PD can be found in elderly people who are apparently healthy, and are further amplified in patients with PD. This, specifically, leads to an assumption that the elevation of PAC and prolonged beta bursts would be even more pronounced in PD compared to healthy aging. However, due to a lack of inclusion of patients' data in the first study, it was impossible to have a straightforward comparison of the effects shared by healthy aging and PD. In the first study (Zhang et al., 2021), we were only able to demonstrate that both healthy aging and PD share the same directionality of the electrophysiological changes in the brain, which are typically associated with PD. These shared characteristics have spectral and spatial specificity. We did observe an overlap of the PAC effect in our data with what has been reported in the previous PD studies.

Increased PAC in the beta frequency range at the left sensorimotor cortical region, has been consistently shown in healthy aging (Zhang et al., 2021) and PD (Gong et al., 2021; A. M. Miller et al., 2019; Swann et al., 2015).

Methodologically, a critical contribution of this study also points to a novel way of controlling for the spurious PAC attributed to the non-sinusoidality of beta oscillations. Our data showed that the observed PAC effect was only partially (less than 10% of the variance) explained by the non-sinusoidality of the beta waveform. Separating these two phenomena is crucial for understanding the underlying physiological processes. A typical PAC, by definition, is used to quantify the interaction between two independent processes. It has been commonly linked to the assumption that phase from low-frequency oscillation modulates the local spiking probability (R. T. Canolty et al., 2006; De Hemptinne et al., 2013, 2015; Lisman & Jensen, 2013). Instead, a non-sinusoidal wave-shaped beta oscillation, according to a recent simulation and experimental work, may suggest a level of input synchronization onto the cortical pyramidal cells (Sherman et al., 2016). In particular, to disentangle whether the observed PAC is mainly attributed to the non-sinusoidality of slower oscillation, we adopted a methodology of disassociating the harmonic versus non-harmonic driven PAC. For PAC calculation, the harmonics of base frequency signal with a non-sinusoidal waveshape could lead to spurious amplitude modulation of higher frequency signal. This spurious coupling could be picked up by the measurement algorithms for PAC detection. I speculate that estimated PAC value on cortical activity recorded with EEG/MEG is a mixture of genuine and spurious ones. The core idea is to determine whether the PAC of interest is *mainly* or *mildly* attributed to the non-sinusoidality of the lower frequency oscillation. We demonstrated one example of possibilities (see supplemental analysis 1 of Zhang et al., 2021) to disentangle to what degree the non-sinusoidality of beta oscillations drives PAC.

Concerning the beta burst dynamics, the average duration of long beta bursts in healthy elderly and PD patients is around 0.2–0.3 s, and the prolongation of beta bursts is commonly reported in motor regions (O’Keefe et al., 2020; Tinkhauser, Pogosyan, Tan, et al., 2017; Zhang et al., 2021). In future work, it would be crucial to test how these

effects are overlapping *quantitatively* while differentiating PD from healthy aging. An illustration of further evidence provided by our study on the previously proposed model is shown in Figure 5 (modified from Collier et al., 2011). In agreement with this model, we added further evidence from the electrophysiological perspective, demonstrating that both healthy aging and PD indeed share the biomarkers typically found in PD.

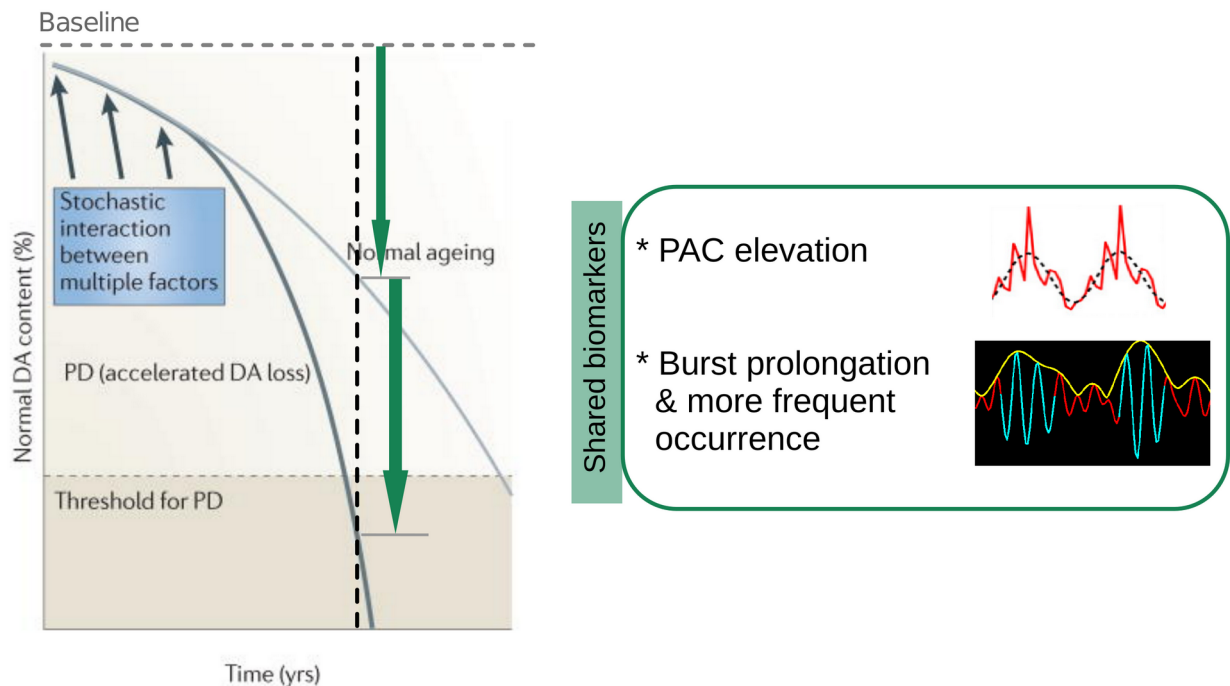


Figure 5. An extended model describing the relationship between normal aging and PD. It is adapted from the figure in the study by Collier et al. (2011). Here, we have added one further piece of evidence showing that electrophysiological biomarkers related to PD are also present in normal aging. These biomarkers include PAC elevation (beta modulating broadband gamma) and abnormal beta burst dynamics (prolonged and more frequent beta bursts). This might imply that the processes underlined these biomarkers take place in normal aging and may be further amplified in PD.

Considering the limitations of our first study, we are also interested in validating and extending our findings with comprehensive data, which would allow a quantitative comparison of the effects between normal aging and PD. Currently, we are conducting a third study based on a large LIFE cohort (<https://www.uniklinikum-leipzig.de/einrichtungen/life>). With this study (in progress) by inclusion of three groups (healthy young, elderly and patients with PD), we aim to test

the hypothesis that both aging (healthy elderly versus young) and PD (patients with PD versus age-matched elderly control) share the directionality of changes in these markers and further the magnitude of the effects (obtained through a longitudinal design or by cross-sectionally comparing both PD patients and healthy elderly subjects with a common baseline measure) can differ between PD and healthy aging - the effects will be more pronounced in PD compared to healthy aging. Additionally, we would also investigate other potential early biomarkers of PD from the autonomic system and heart-brain interaction, for instance, heart rate variability (HRV) and heart evoked potentials (HEPs).

In the second study (Zhang et al., 2022), we focused on 1) non-oscillatory activity and 2) cross-regional interaction in a group of PD patients. Specifically, we investigated the local and global brain changes in response to dopaminergic medication in PD. In our study, we demonstrated that the aperiodic property of electrophysiological activity underwent a significant change with the administration of dopaminergic medication. We observed a flattening of the spectral slope in the Off compared to the On condition. The changes are most prominent in the left central area, including the sensorimotor cortex. This finding implies that the wideband background arrhythmic activity is a sensitive marker for the medication-induced alterations. This finding complements previous studies showing that a flattening of the spectral slope is observed with healthy aging (Cesnaite et al., 2021; Voytek et al., 2015). These findings are important considering that PD is pathological aging which is believed to be an accelerated aging process (Collier et al., 2011, 2017). We postulate a similar change – a flatter slope, also occurs in PD. Importantly, spectral slope, or power-law exponent of arrhythmic activity, has been shown to differ across brain regions and to be impacted by task performance (He et al., 2010; Voytek et al., 2015). Dopaminergic medication might bring the flattened spectral slope in PD back to a normal state (steepened by dopaminergic medication). In my thesis, a complete picture of the changes related to PD was presented for the first time: both the arrhythmic (scale-free activity represented by spectral slope) and the nested temporal pattern (in terms of PAC) were demonstrated in PD.

Moreover, we investigated the cortical functional network changes in different medication (On and Off) states. An increase in the connectivity between fronto-centro-parietal regions in the beta frequency band was identified in the On compared to Off medication condition. This finding agrees with a previous report where the authors demonstrated that dopamine medication modulates the global brain networks in a way shifting an STN-cortex mediated motor network towards a cortico-cortical (fronto-parietal) mediated one (Sharma et al., 2021). An increase in the cortico-cortical connectivity after dopamine administration might be due to a reduction in the coherence between the STN and the cortex since at rest PD is associated with increased cortex-STN synchrony (Hirschmann et al., 2013; Sharma et al., 2021), and such excessive synchrony could prevent or limit the communication between cortical structures (Cruz et al., 2009; Holt et al., 2019). Moreover, we did not observe any significant difference in the network global architectures between the medication states, specifically in the global segregation or integration of the functional networks. It may indicate that modulation by dopaminergic medication only exhibits limited impact on the interactions between some specific regions rather than at the global network's structural level. Future work should address whether a successful modulation of the network properties relates to an even more effective improvement of clinical symptoms than an unsuccessful one (as shown in this data). Given that we only access the network at sensor space with a rather low-density setup, we did not further quantify other aspects of the cortical networks, for instance, small-world and scale-free characteristics. If one can appropriately address the concerns regarding quantifying the network's structures (Kaminski & Blinowska, 2018), future work should also investigate a possible change in these specific characteristics of functional networks to gain more insights into the global network features in On and Off medication states.

Finally, our data presented a link between local aperiodic activity and global network efficiency in patients with PD. This result can be interpreted in a framework of regional excitation/inhibition balance shaping the information transmission through the global network. Spectral slope has been closely related to excitation/inhibition balance at the recorded site (Gao et al., 2017), with shallower slopes corresponding to stronger excitation over inhibition. Relating our findings of spectral slope to the E/I

(excitation/inhibition) balance hypothesis, a steeper slope in the On condition might imply that there was a stronger inhibition in comparison to the Off condition. This line of interpretation is consistent with the previous studies using TMS (transcranial magnetic stimulation) showing that in PD at rest in Off condition, there is a reduced inhibition which can be up-modulated by the intake of dopaminergic medication (Cantello, 2002; Casula et al., 2017; Hanajima et al., 1996). Our observation regarding the association between spectral slope and the functional networks' GE in PD Off condition implies that local E/I balance could define the network's ability of global integration. This is in agreement with a previous study proposing that a degree of E/I ratio is negatively correlated with the global network's property (X. Zhou et al., 2021) (see Figure 6, modified from X. Zhou et al., 2021). We assume that the PD Off condition is characterized by an imbalanced state (more excitation against inhibition) and thus exhibits a close association with the network's global integration. Dopaminergic medication gains a more balanced state, which positions the network in a rather stable point achieving the optimal network configuration (specifically in integration). In addition, surprisingly, our data did show a difference in E/I dynamics (indexed by the spectral slope) between the two medication conditions, although not exhibiting a difference in the network's GE property. As illustrated in Figure 6, one intriguing possibility of interpretation would be that the left side of the inverted-U shaped function (GE vs. E/I) is perhaps where the PD Off state located, and GE grows rather slowly for rapidly changing E/I ratio. Thus, along the GE axis, the network in the Off condition is situated relatively near to the network in the On state. The networks from the two conditions remain farther apart along the E/I axis.

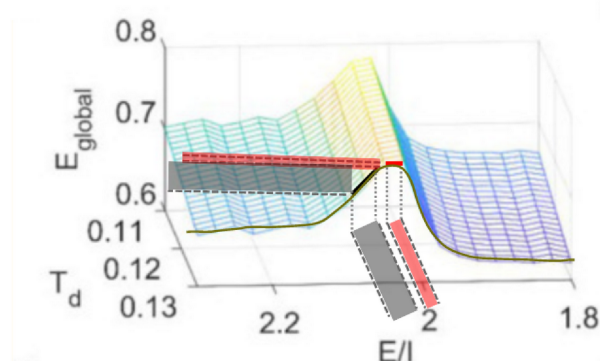


Figure 6. Local E/I impacts the global network integration (modified figure from the study

(X. Zhou et al., 2021)). The dark line and grey areas represent the data samples in the Off condition, while the red colored ones show the scenario from the On medication condition. E_{global} represents the global efficiency, and T_d means the thresholding values for binarizing the network to compute the GE.

Interestingly, combining all the findings concerning local spectral slope, connectivity, and graph measures of the functional network, we found that the left centro-parietal area is consistently present for all these effects. Therefore, we can speculate that this region might be a critical area involved in the alterations due to dopaminergic medication. Regulating the level of excitation of this area might influence not only local activity but also distributed network activity. Finally, we are refraining from drawing too strong conclusions from the current findings, and we suggest that future studies should further validate these effects in the source space and with a larger sample size.

Taking these two studies together, one limitation of this thesis is that for neither study, we have a comprehensive dataset that simultaneously includes the groups of healthy young, healthy elderly, and PD patients in Off and On medication states (see own representation: Figure 7). This setup would allow us to investigate the measures (PAC, beta burst dynamics, spectral slope, functional connectivity, and graph-based representations of the network) straightforwardly in healthy aging (healthy elderly compared to young subjects), PD development (patients with PD compared to healthy elderly control), and medication-induced effects (medication On compared to Off in PD patients). In addition, these biomarkers should be further validated longitudinally.

A refined elderly group should be considered for future work since the inclusion of an elderly group without PD does *not* exclude the presence of a preclinical or a prodromal PD state. Ideally, in a future study elderly people should be screened neurologically for early preclinical signs of PD. Based on this, subgroups of elderly who are completely parkinsonism-free and subgroups where the elderly show mild parkinsonian signs could be defined. For this purpose, the set of criteria for defining prodromal PD proposed by the MDS could be applied (for instance, by integrating the identified risk factors and markers of prodromal PD published in 2015 and 2019). This way, it would become

possible to differentiate a “truly healthy aging” process from a preclinical/prodromal PD and a clinical PD. It will be interesting to test how the neuronal biomarkers presented here will differ in these refined groups and whether those biomarkers could continuously trace the development and progression of parkinsonian state. Also, one could test whether a subgroup of elderly subjects with a higher LRs (indicating a higher probability of prodromal PD) would show a similar effect in comparison to a lower-LRs subgroup, as we have demonstrated in the elderly in comparison to young group in study 1.

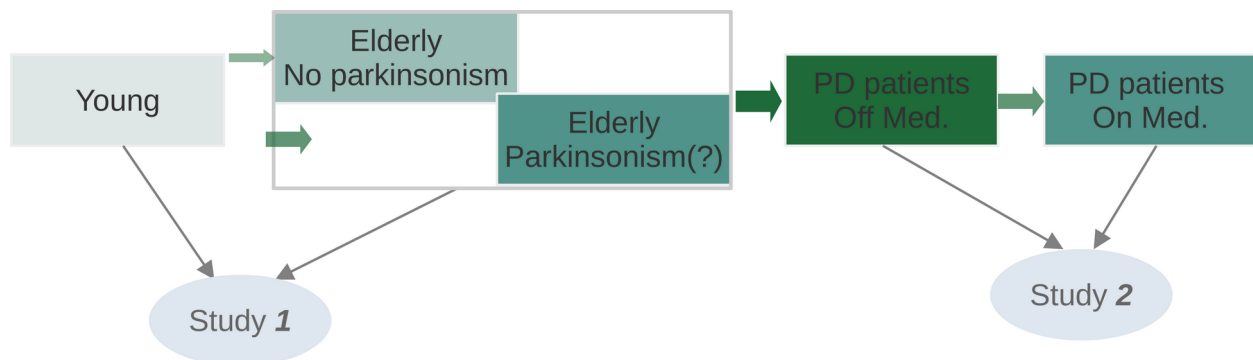


Figure 7. Overview of the two studies and outlook for future study designs. In study 1, we only included apparently healthy young and elderly groups to investigate the general aging effect on the neuronal biomarkers associated with PD in the previous literature. Note, in the literature, all the PD-related results were indicated by comparing the patients with PD to a general healthy control group (without defining the level of parkinsonism). In study 2, we only investigated the dopaminergic medication-induced effects in a cohort of patients with PD. In future studies, a comprehensive design including all the groups would be desirable for answering the research question as to whether the identified neuronal biomarkers could indeed indicate different stages of PD (“completely healthy” versus “preclinical/prodromal PD” versus “clinical PD” versus “medication relieved parkinsonian state”).

5 Conclusions

My doctoral thesis shows that electrophysiological neuronal biomarkers associated with PD can also be present and detectable in the apparently healthy elderly people without PD in comparison to younger subjects, supporting the hypothesis that aging might be related to a pre-parkinsonian state, as evidenced previously in non-human primate studies. Specifically, aging-related changes in PAC and beta burst dynamics share the

directionality that accompanies the PD development. Our findings suggest that future prospective studies should be carried out to test their predictive values as early biomarkers of PD development. In addition to these effects, which focus on the oscillatory activities (specifically in the beta band), local non-oscillatory wide-band activity (estimated by spectral slope) can also be a marker differentiating medication-induced states in PD. We further show that dopaminergic medication not only induces changes within the local cortical areas which are related to the movement control but also in the functional interaction across remote areas. Lastly, linking the local and global network changes, the local spectral slope appears crucial in defining the network's integrative property in PD. Taken together, these findings contribute to identifying early biomarkers of PD and differentiating or even tracking the progression course of parkinsonian state.

Reference list

- Ahn, S., Zauber, S. E., Worth, R. M., Witt, T., & Rubchinsky, L. L. (2015). Interaction of synchronized dynamics in cortex and basal ganglia in Parkinson's disease. *European Journal of Neuroscience*, 42(5), 2164–2171. <https://doi.org/10.1111/ejn.12980>
- Alexander, G. (1986). Parallel Organization of Functionally Segregated Circuits Linking Basal Ganglia and Cortex. *Annual Review of Neuroscience*, 9(1), 357–381. <https://doi.org/10.1146/annurev.neuro.9.1.357>
- Alonso-Frech, F., Zamarbide, I., Alegre, M., Rodríguez-Oroz, M. C., Guridi, J., Manrique, M., Valencia, M., Artieda, J., & Obeso, J. A. (2006). Slow oscillatory activity and levodopa-induced dyskinesias in Parkinson's disease. *Brain*, 129(7), 1748–1757. <https://doi.org/10.1093/brain/awl103>
- Antonini, A., Moresco, R. M., Gobbo, C., De Notaris, R., Panzacchi, A., Barone, P., Bonifati, V., Pezzoli, G., & Fazio, F. (2002). Striatal dopaminergic denervation in early and late onset Parkinson's disease assessed by PET and the tracer [11C]FECIT: Preliminary findings in one patient with autosomal recessive parkinsonism (Park2). *Neurological Sciences*, 23(SUPPL. 2), 51–52. <https://doi.org/10.1007/s100720200065>
- Aru, J., Aru, J., Priesemann, V., Wibral, M., Lana, L., Pipa, G., Singer, W., & Vicente, R. (2015). Untangling cross-frequency coupling in neuroscience. *Current Opinion in Neurobiology*, 31, 51–61. <https://doi.org/10.1016/j.conb.2014.08.002>
- Babayan, A., Erbey, M., Kumral, D., Reinelt, J. D., Reiter, A. M. F., Röbbig, J., Lina Schaare, H., Uhlig, M., Anwander, A., Bazin, P. L., Horstmann, A., Lampe, L., Nikulin, V. V., Okon-Singer, H., Preusser, S., Pampel, A., Rohr, C. S., Sacher, J., Thöne-Otto, A., ... Villringer, A. (2019). Data descriptor: A mind-brain-body dataset of MRI, EEG, cognition, emotion, and peripheral physiology in young and old adults. *Scientific Data*, 6, 1–21. <https://doi.org/10.1038/sdata.2018.308>
- Barber, T. R., Klein, J. C., Mackay, C. E., & Hu, M. T. M. (2017). Neuroimaging in pre-motor Parkinson's disease. *NeuroImage: Clinical*, 15(December 2016), 215–227. <https://doi.org/10.1016/j.nicl.2017.04.011>
- Bennett, D. A., Beckett, L. A., Murray, A. M., Shannon, K. M., Goetz, C. G., Pilgrim, D. M., & Evans, D. A. (1996). Prevalence of parkinsonian signs and associated mortality in a community population of older people. *The New England Journal of Medicine*, 334(2), 71–76. <https://doi.org/10.1056/NEJM199601113340202>

- Berg, D., Postuma, R. B., Adler, C. H., & Bloem, B. R. (2015). *CME MDS Research Criteria for Prodromal Parkinson's Disease Key Definition Features of Prodromal PD*. 30(12), 1600–1609. <https://doi.org/10.1002/mds.26431>
- Berg, D., Postuma, R. B., Bloem, B., & Chan, P. (2014). *FEATUR ED Time to Redefine PD? Introductory Statement of the MDS Task Force on the Definition of Parkinson's Disease What Is the Gold Standard for the Definition of PD?* 29(4), 454–462. <https://doi.org/10.1002/mds.25844>
- Blesa, J., Foffani, G., Dehay, B., Bezard, E., Obeso, J. A. (2022). Motor and non-motor circuit disturbances in early Parkinson disease: which happens first? *Nat Rev Neurosci*, 23(2), 115-128. <https://doi.org/10.1038/s41583-021-00542-9>
- Braak, H., Del Tredici, K., Rüb, U., De Vos, R. A. I., Jansen Steur, E. N. H., & Braak, E. (2003). Staging of brain pathology related to sporadic Parkinson's disease. *Neurobiology of Aging*, 24(2), 197–211. [https://doi.org/10.1016/S0197-4580\(02\)00065-9](https://doi.org/10.1016/S0197-4580(02)00065-9)
- Branch, S. Y., Chen, C., Sharma, R., Lechleiter, J. D., Li, S., & Beckstead, M. J. (2016). Dopaminergic neurons exhibit an age-dependent decline in electrophysiological parameters in the MitoPark mouse model of Parkinson's disease. *Journal of Neuroscience*, 36(14), 4026–4037. <https://doi.org/10.1523/JNEUROSCI.1395-15.2016>
- Brown, P. (2003). Oscillatory nature of human basal ganglia activity: Relationship to the pathophysiology of parkinson's disease. *Movement Disorders*, 18(4), 357–363. <https://doi.org/10.1002/mds.10358>
- Brown, P., Oliviero, A., Mazzone, P., Insola, A., Tonali, P., & Di Lazzaro, V. (2001). Dopamine dependency of oscillations between subthalamic nucleus and pallidum in Parkinson's disease. *Journal of Neuroscience*, 21(3), 1033–1038. <https://doi.org/10.1523/jneurosci.21-03-01033.2001>
- Bullmore, E., Long, C., Suckling, J., Fadili, J., Calvert, G., Zelaya, F., Carpenter, A., & Brammer, M. (2001). Colored noise and computational inference in fMRI time series analysis: resampling methods in time and wavelet domains. *NeuroImage*, 13(6), 86. [https://doi.org/10.1016/s1053-8119\(01\)91429-6](https://doi.org/10.1016/s1053-8119(01)91429-6)
- Bullmore, E., & Sporns, O. (2012). The economy of brain network organization. *Nature Reviews Neuroscience*, 13(5), 336–349. <https://doi.org/10.1038/nrn3214>
- Calabresi, P., Picconi, B., Tozzi, A., Ghiglieri, V., & Di Filippo, M. (2014). Direct and indirect pathways of basal ganglia: A critical reappraisal. *Nature Neuroscience*, 17(8), 1022–1030. <https://doi.org/10.1038/nn.3743>

- Canolty, R. T., Edwards, E., Dalal, S. S., Soltani, M., Nagarajan, S. S., Kirsch, H. E., Berger, M. S., Barbare, N. M., & Knight, R. T. (2006). High gamma power is phase-locked to theta oscillations in human neocortex. *Science*, *313*(5793), 1626–1628. <https://doi.org/10.1126/science.1128115>
- Canolty, Ryan T., Ganguly, K., Kennerley, S. W., Cadieu, C. F., Koepsell, K., Wallis, J. D., & Carmena, J. M. (2010). Oscillatory phase coupling coordinates anatomically dispersed functional cell assemblies. *Proceedings of the National Academy of Sciences of the United States of America*, *107*(40), 17356–17361. <https://doi.org/10.1073/pnas.1008306107>
- Canolty, Ryan T., & Knight, R. T. (2010). The functional role of cross-frequency coupling. *Trends in Cognitive Sciences*, *14*(11), 506–515. <https://doi.org/10.1016/j.tics.2010.09.001>
- Cantello, R. (2002). Applications of transcranial magnetic stimulation in movement disorders. *Journal of Clinical Neurophysiology*, *19*(4), 272–293. <https://doi.org/10.1097/00004691-200208000-00003>
- Carvey, P. M., Punati, A., & Newman, M. B. (2006). Progressive dopamine neuron loss in Parkinson's disease: The multiple hit hypothesis. *Cell Transplantation*, *15*(3), 239–250. <https://doi.org/10.3727/000000006783981990>
- Cassidy, M., Mazzone, P., Oliviero, A., Insola, A., Tonali, P., Di Lazzaro, V., & Brown, P. (2002). Movement-related changes in synchronization in the human basal ganglia. *Brain*, *125*(6), 1235–1246. <https://doi.org/10.1093/brain/awf135>
- Casula, E. P., Stampanoni Bassi, M., Pellicciari, M. C., Ponzio, V., Veniero, D., Peppe, A., Brusa, L., Stanzione, P., Caltagirone, C., Stefani, A., & Koch, G. (2017). Subthalamic stimulation and levodopa modulate cortical reactivity in Parkinson's patients. *Parkinsonism and Related Disorders*, *34*, 31–37. <https://doi.org/10.1016/j.parkreldis.2016.10.009>
- Cesnaite, E., Steinfath, P., Idaji, M. J., Stephani, T., Haufe, S., Sander, C., Hensch, T., Hegerl, U., Riedel-heller, S., Röhr, S., Schroeter, M. L., Witte, A. V., Villringer, A., & Nikulin, V. V. (2021). Alterations in rhythmic and non-rhythmic resting-state EEG activity and their link to cognition in older age. *BioRxiv*, 1–34.
- Chen, C. C., Hsu, Y. T., Chan, H. L., Chiou, S. M., Tu, P. H., Lee, S. T., Tsai, C. H., Lu, C. S., & Brown, P. (2010). Complexity of subthalamic 13-35Hz oscillatory activity directly correlates with clinical impairment in patients with Parkinson's disease. *Experimental Neurology*, *224*(1), 234–240. <https://doi.org/10.1016/j.expneurol.2010.03.015>

- Cheng, H. C., Ulane, C. M., & Burke, R. E. (2010). Clinical progression in Parkinson disease and the neurobiology of axons. *Annals of Neurology*, *67*(6), 715–725. <https://doi.org/10.1002/ana.21995>
- Collier, T. J., Kanaan, N. M., & Kordower, J. H. (2011). Ageing as a primary risk factor for Parkinson's disease: Evidence from studies of non-human primates. *Nature Reviews Neuroscience*, *12*(6), 359–366. <https://doi.org/10.1038/nrn3039>
- Collier, T. J., Kanaan, N. M., & Kordower, J. H. (2017). Aging and Parkinson's disease: Different sides of the same coin? *Movement Disorders*, *32*(7), 983–990. <https://doi.org/10.1002/mds.27037>
- Colombo, M. A., Napolitani, M., Boly, M., Gosseries, O., Casarotto, S., Rosanova, M., Brichant, J. F., Boveroux, P., Rex, S., Laureys, S., Massimini, M., Chiergato, A., & Sarasso, S. (2019). The spectral exponent of the resting EEG indexes the presence of consciousness during unresponsiveness induced by propofol, xenon, and ketamine. *NeuroImage*, *189*(December 2018), 631–644. <https://doi.org/10.1016/j.neuroimage.2019.01.024>
- Cruz, A. V., Mallet, N., Magill, P. J., Brown, P., & Averbeck, B. B. (2009). Effects of dopamine depletion on network entropy in the external globus pallidus. *Journal of Neurophysiology*, *102*(2), 1092–1102. <https://doi.org/10.1152/jn.00344.2009>
- Damier, P., Hirsch, E. C., Agid, Y., & Graybiel, A. M. (1999). The substantia nigra of the human brain: II. Patterns of loss of dopamine-containing neurons in Parkinson's disease. *Brain*, *122*(8), 1437–1448. <https://doi.org/10.1093/brain/122.8.1437>
- Darden, L. (2007). Mechanisms and models. *The Cambridge Companion to the Philosophy of Biology*, *39*, 139–159. <https://doi.org/10.1017/CCOL9780521851282.008>
- De Hemptinne, C., Ryapolova-Webb, E. S., Air, E. L., Garcia, P. A., Miller, K. J., Ojemann, J. G., Ostrem, J. L., Galifianakis, N. B., & Starr, P. A. (2013). Exaggerated phase-amplitude coupling in the primary motor cortex in Parkinson disease. *Proceedings of the National Academy of Sciences of the United States of America*, *110*(12), 4780–4785. <https://doi.org/10.1073/pnas.1214546110>
- De Hemptinne, C., Swann, N. C., Ostrem, J. L., Ryapolova-Webb, E. S., San Luciano, M., Galifianakis, N. B., & Starr, P. A. (2015). Therapeutic deep brain stimulation reduces cortical phase-amplitude coupling in Parkinson's disease. *Nature Neuroscience*, *18*(5), 779–786. <https://doi.org/10.1038/nn.3997>
- de Lau, L. M. L., Giesbergen, P. C. L. M., de Rijk, M. C., Hofman, A., Koudstaal, P. J., & Breteler, M. M. B. (2004). Incidence of parkinsonism and Parkinson disease in a

- general population. *Neurology*, 63(7), 1240 LP – 1244.
<https://doi.org/10.1212/01.WNL.0000140706.52798.BE>
- Deco, G., Ponce-Alvarez, A., Hagmann, P., Romani, G. L., Mantini, D., & Corbetta, M. (2014). How local excitation-inhibition ratio impacts the whole brain dynamics. *Journal of Neuroscience*, 34(23), 7886–7898.
<https://doi.org/10.1523/JNEUROSCI.5068-13.2014>
- Del Tredici, K. (2002). Where does P.D pathology begin in the brain. *Journal of Neuropathology and Experimental Neurology*, 61(5), 413–426.
- DeLong, M., & Wichmann, T. (2009). Update on models of basal ganglia function and dysfunction. *Parkinsonism and Related Disorders*, 15(SUPPL. 3), S237–S240.
[https://doi.org/10.1016/S1353-8020\(09\)70822-3](https://doi.org/10.1016/S1353-8020(09)70822-3)
- Desikan, R. S., Ségonne, F., Fischl, B., Quinn, B. T., Dickerson, B. C., Blacker, D., Buckner, R. L., Dale, A. M., Maguire, R. P., Hyman, B. T., Albert, M. S., & Killiany, R. J. (2006). An automated labeling system for subdividing the human cerebral cortex on MRI scans into gyral based regions of interest. *NeuroImage*, 31(3), 968–980.
<https://doi.org/10.1016/j.neuroimage.2006.01.021>
- Donoghue, T., Haller, M., Peterson, E. J., Varma, P., Sebastian, P., Gao, R., Noto, T., Lara, A. H., Wallis, J. D., Knight, R. T., Shestyuk, A., & Voytek, B. (2020). Parameterizing neural power spectra into periodic and aperiodic components. *Nature Neuroscience*, 23(12), 1655–1665. <https://doi.org/10.1038/s41593-020-00744-x>
- Fearnley, J. M., & Lees, A. J. (1991). Ageing and parkinson's disease: Substantia nigra regional selectivity. *Brain*, 114(5), 2283–2301.
<https://doi.org/10.1093/brain/114.5.2283>
- Feingold, J., Gibson, D. J., Depasquale, B., & Graybiel, A. M. (2015). Bursts of beta oscillation differentiate postperformance activity in the striatum and motor cortex of monkeys performing movement tasks. *Proceedings of the National Academy of Sciences of the United States of America*, 112(44), 13687–13692.
<https://doi.org/10.1073/pnas.1517629112>
- Freeman, W. J., & Zhai, J. (2009). Simulated power spectral density (PSD) of background electrocorticogram (ECoG). *Cognitive Neurodynamics*, 3(1), 97–103.
<https://doi.org/10.1007/s11571-008-9064-y>
- Fries, P. (2005). A mechanism for cognitive dynamics: Neuronal communication through neuronal coherence. *Trends in Cognitive Sciences*, 9(10), 474–480.
<https://doi.org/10.1016/j.tics.2005.08.011>

- Fries, P. (2015). Communication Through Coherence (CTC 2.0). *Neuron*, 88(1), 220–235. <https://doi.org/10.1016/j.neuron.2015.09.034>.Rhythms
- Gao, R., Peterson, E. J., & Voytek, B. (2017). Inferring synaptic excitation/inhibition balance from field potentials. *NeuroImage*, 158(March), 70–78. <https://doi.org/10.1016/j.neuroimage.2017.06.078>
- George, J. S., Strunk, J., Mak-Mccully, R., Houser, M., Poizner, H., & Aron, A. R. (2013). Dopaminergic therapy in Parkinson's disease decreases cortical beta band coherence in the resting state and increases cortical beta band power during executive control. *NeuroImage: Clinical*, 3, 261–270. <https://doi.org/10.1016/j.nicl.2013.07.013>
- Gershman, S. J., & Uchida, N. (2019). Believing in dopamine. *Nature Reviews Neuroscience*, 20(11), 703–714. <https://doi.org/10.1038/s41583-019-0220-7>
- Gittis, A. H., Nelson, A. B., Thwin, M. T., Palop, J. J., & Kreitzer, A. C. (2010). Distinct roles of GABAergic interneurons in the regulation of striatal output pathways. *Journal of Neuroscience*, 30(6), 2223–2234. <https://doi.org/10.1523/JNEUROSCI.4870-09.2010>
- Gong, R., Wegscheider, M., Mühlberg, C., Gast, R., Fricke, C., Rumpf, J. J., Nikulin, V. V., Knösche, T. R., & Classen, J. (2021). Spatiotemporal features of β - γ phase-amplitude coupling in Parkinson's disease derived from scalp EEG. *Brain: A Journal of Neurology*, 144(2), 487–503. <https://doi.org/10.1093/brain/awaa400>
- Hammond, C., Bergman, H., & Brown, P. (2007). Pathological synchronization in Parkinson's disease: networks, models and treatments. *Trends in Neurosciences*, 30(7), 357–364. <https://doi.org/10.1016/j.tins.2007.05.004>
- Hanajima, R., Ugawa, Y., Terao, Y., Ogata, K., & Kanazawa, I. (1996). Ipsilateral cortico-cortical inhibition of the motor cortex in various neurological disorders. *Journal of the Neurological Sciences*, 140(1–2), 109–116. [https://doi.org/10.1016/0022-510X\(96\)00100-1](https://doi.org/10.1016/0022-510X(96)00100-1)
- He, B. J., Zempel, J. M., Snyder, A. Z., & Raichle, M. E. (2010). The temporal structures and functional significance of scale-free brain activity. *Neuron*, 66(3), 353–369. <https://doi.org/10.1016/j.neuron.2010.04.020>
- Heinzel, S., Berg, D., Gasser, T., Chen, H., & Yao, C. (2019). *Update of the MDS Research Criteria for Prodromal Parkinson 's Disease New Evidence and Revision of LRs*. 34(10), 1464–1470. <https://doi.org/10.1002/mds.27802>
- Hindle, J. V. (2010). Ageing, neurodegeneration and Parkinson's disease. *Age and Ageing*, 39(2), 156–161. <https://doi.org/10.1093/ageing/afp223>

- Hirschmann, J., Özkurt, T. E., Butz, M., Homburger, M., Elben, S., Hartmann, C. J., Vesper, J., Wojtecki, L., & Schnitzler, A. (2011). Distinct oscillatory STN-cortical loops revealed by simultaneous MEG and local field potential recordings in patients with Parkinson's disease. *NeuroImage*, 55(3), 1159–1168. <https://doi.org/10.1016/j.neuroimage.2010.11.063>
- Hirschmann, J., Özkurt, T. E., Butz, M., Homburger, M., Elben, S., Hartmann, C. J., Vesper, J., Wojtecki, L., & Schnitzler, A. (2013). Differential modulation of STN-cortical and cortico-muscular coherence by movement and levodopa in Parkinson's disease. *NeuroImage*, 68, 203–213. <https://doi.org/10.1016/j.neuroimage.2012.11.036>
- Holt, A. B., Kormann, E., Gulberti, A., Pötter-Nerger, M., McNamara, C. G., Cagnan, H., Baaske, M. K., Little, S., Köppen, J. A., Buhmann, C., Westphal, M., Gerloff, C., Engel, A. K., Brown, P., Hamel, W., Moll, C. K. E., & Sharott, A. (2019). Phase-dependent suppression of beta oscillations in parkinson's disease patients. *Journal of Neuroscience*, 39(6), 1119–1134. <https://doi.org/10.1523/JNEUROSCI.1913-18.2018>
- Huang, Y., Parra, L. C., & Haufe, S. (2016). The New York Head—A precise standardized volume conductor model for EEG source localization and tES targeting. *NeuroImage*, 140, 150–162. <https://doi.org/10.1016/j.neuroimage.2015.12.019>
- Hughes, A. J., Daniel, S. E., Kilford, L., & Lees, A. J. (1992). Accuracy of clinical diagnosis of idiopathic Parkinson's disease: A clinico-pathological study of 100 cases. *Journal of Neurology Neurosurgery and Psychiatry*, 55(3), 181–184. <https://doi.org/10.1136/jnnp.55.3.181>
- Hughes, Andrew J., Daniel, S. E., Ben-Shlomo, Y., & Lees, A. J. (2002). The accuracy of diagnosis of parkinsonian syndromes in a specialist movement disorder service. *Brain*, 125(4), 861–870. <https://doi.org/10.1093/brain/awf080>
- Iwai, A., Masliah, E., Yoshimoto, M., Ge, N., Flanagan, L., Rohan de Silva, H. A., Kittel, A., & Saitoh, T. (1995). The precursor protein of non-A β component of Alzheimer's disease amyloid is a presynaptic protein of the central nervous system. *Neuron*, 14(2), 467–475. [https://doi.org/10.1016/0896-6273\(95\)90302-X](https://doi.org/10.1016/0896-6273(95)90302-X)
- Jackson, N., Cole, S. R., Voytek, B., & Swann, N. C. (2019). Characteristics of waveform shape in Parkinson's disease detected with scalp electroencephalography. *ENeuro*, 6(3), 1–11. <https://doi.org/10.1523/ENEURO.0151-19.2019>
- Kaminski, M., & Blinowska, K. J. (2018). Is Graph Theoretical Analysis a Useful Tool for Quantification of Connectivity Obtained by Means of EEG/MEG Techniques?

- Kramer, M. A., Tort, A. B. L., & Kopell, N. J. (2008). Sharp edge artifacts and spurious coupling in EEG frequency comodulation measures. *Journal of Neuroscience Methods*, 170(2), 352–357. <https://doi.org/10.1016/j.jneumeth.2008.01.020>
- Kühn, A. A., Grosse, P., Holtz, K., Brown, P., Meyer, B. U., & Kupsch, A. (2004). Patterns of abnormal motor cortex excitability in atypical parkinsonian syndromes. *Clinical Neurophysiology*, 115(8), 1786–1795. <https://doi.org/10.1016/j.clinph.2004.03.020>
- Kühn, Andrea A., Doyle, L., Pogosyan, A., Yarrow, K., Kupsch, A., Schneider, G. H., Hariz, M. I., Trottenberg, T., & Brown, P. (2006). Modulation of beta oscillations in the subthalamic area during motor imagery in Parkinson's disease. *Brain*, 129(3), 695–706. <https://doi.org/10.1093/brain/awh715>
- Kühn, Andrea A., Trottenberg, T., Kivi, A., Kupsch, A., Schneider, G. H., & Brown, P. (2005). The relationship between local field potential and neuronal discharge in the subthalamic nucleus of patients with Parkinson's disease. *Experimental Neurology*, 194(1), 212–220. <https://doi.org/10.1016/j.expneurol.2005.02.010>
- Kühn, Andrea A., Tsui, A., Aziz, T., Ray, N., Brücke, C., Kupsch, A., Schneider, G. H., & Brown, P. (2009). Pathological synchronisation in the subthalamic nucleus of patients with Parkinson's disease relates to both bradykinesia and rigidity. *Experimental Neurology*, 215(2), 380–387. <https://doi.org/10.1016/j.expneurol.2008.11.008>
- Kühn, Andrea A., Williams, D., Kupsch, A., Limousin, P., Hariz, M., Schneider, G. H., Yarrow, K., & Brown, P. (2004). Event-related beta desynchronization in human subthalamic nucleus correlates with motor performance. *Brain*, 127(4), 735–746. <https://doi.org/10.1093/brain/awh106>
- Lalo, E., Thobois, S., Sharott, A., Polo, G., Mertens, P., Pogosyan, A., & Brown, P. (2008). Patterns of bidirectional communication between cortex and basal ganglia during movement in patients with Parkinson disease. *Journal of Neuroscience*, 28(12), 3008–3016. <https://doi.org/10.1523/JNEUROSCI.5295-07.2008>
- Lee, A. J., Wang, Y., Alcalay, R. N., Mejia-Santana, H., Saunders-Pullman, R., Bressman, S., Corvol, J. C., Brice, A., Lesage, S., Mangone, G., Tolosa, E., Pont-Sunyer, C., Vilas, D., Schüle, B., Kausar, F., Foroud, T., Berg, D., Brockmann, K., Goldwurm, S., ... Marder, K. (2017). Penetrance estimate of LRRK2 p.G2019S mutation in individuals of non-Ashkenazi Jewish ancestry. *Movement Disorders*, 32(10), 1432–1438. <https://doi.org/10.1002/mds.27059>

- Levy, R., Hutchison, W. D., Lozano, A. M., & Dostrovsky, J. O. (2000). High-frequency synchronization of neuronal activity in the subthalamic nucleus of Parkinsonian patients with limb tremor. *Journal of Neuroscience*, *20*(20), 7766–7775. <https://doi.org/10.1523/jneurosci.20-20-07766.2000>
- Lisman, J. E., & Jensen, O. (2013). The Theta-Gamma Neural Code. *Neuron*, *77*(6), 1002–1016. <https://doi.org/10.1016/j.neuron.2013.03.007>
- Little, S., Pogosyan, A., Kuhn, A. A., & Brown, P. (2012). Beta band stability over time correlates with Parkinsonian rigidity and bradykinesia. *Experimental Neurology*, *236*(2), 383–388. <https://doi.org/10.1016/j.expneurol.2012.04.024>
- Little, Simon, Tan, H., Anzak, A., Pogosyan, A., Kühn, A., & Brown, P. (2013). Bilateral functional connectivity of the basal ganglia in patients with Parkinson's disease and its modulation by dopaminergic treatment. *PLoS ONE*, *8*(12). <https://doi.org/10.1371/journal.pone.0082762>
- Litvak, V., Jha, A., Eusebio, A., Oostenveld, R., Foltynie, T., Limousin, P., Zrinzo, L., Hariz, M. I., Friston, K., & Brown, P. (2011). Resting oscillatory cortico-subthalamic connectivity in patients with Parkinson's disease. *Brain*, *134*(2), 359–374. <https://doi.org/10.1093/brain/awq332>
- Liu, R., Guo, X., Park, Y., Huang, X., Sinha, R., Freedman, N. D., Hollenbeck, A. R., Blair, A., & Chen, H. (2012). Caffeine intake, smoking, and risk of parkinson disease in men and women. *American Journal of Epidemiology*, *175*(11), 1200–1207. <https://doi.org/10.1093/aje/kwr451>
- Louis, E. D., & Bennett, D. A. (2007). Mild Parkinsonian signs: An overview of an emerging concept. *Movement Disorders*, *22*(12), 1681–1688. <https://doi.org/10.1002/mds.21433>
- Lozano-Soldevilla, D., Huurne, N., & Oostenveld, R. (2016). Neuronal oscillations with non-sinusoidal morphology produce spurious phase-to-amplitude coupling and directionality. *Frontiers in Computational Neuroscience*, *10*(AUG), 1–17. <https://doi.org/10.3389/fncom.2016.00087>
- MacDonald, A. A., Seergobin, K. N., Owen, A. M., Tamjeedi, R., Monchi, O., Ganjavi, H., & MacDonald, P. A. (2013). Differential Effects of Parkinson's Disease and Dopamine Replacement on Memory Encoding and Retrieval. *PLoS ONE*, *8*(9). <https://doi.org/10.1371/journal.pone.0074044>
- MacDonald, P. A., MacDonald, A. A., Seergobin, K. N., Tamjeedi, R., Ganjavi, H., Provost, J. S., & Monchi, O. (2011). The effect of dopamine therapy on ventral and dorsal striatum-mediated cognition in Parkinson's disease: Support from functional MRI. *Brain*, *134*(5), 1447–1463. <https://doi.org/10.1093/brain/awr075>

- Malekmohammadi, M., AuYong, N., Ricks-Oddie, J., Bordelon, Y., & Pouratian, N. (2018). Pallidal deep brain stimulation modulates excessive cortical high β phase amplitude coupling in Parkinson disease. *Brain Stimulation*, *11*(3), 607–617. <https://doi.org/10.1016/j.brs.2018.01.028>
- Malekmohammadi, M., Elias, W. J., & Pouratian, N. (2015). Human thalamus regulates cortical activity via spatially specific and structurally constrained phase-amplitude coupling. *Cerebral Cortex*, *25*(6), 1618–1628. <https://doi.org/10.1093/cercor/bht358>
- Manning, J. R., Jacobs, J., Fried, I., & Kahana, M. J. (2009). Broadband shifts in local field potential power spectra are correlated with single-neuron spiking in humans. *Journal of Neuroscience*, *29*(43), 13613–13620. <https://doi.org/10.1523/JNEUROSCI.2041-09.2009>
- Miller, A. M., Miocinovic, S., Swann, N. C., Rajagopalan, S. S., Darevsky, D. M., Gilron, R., de Hemptinne, C., Ostrem, J. L., & Starr, P. A. (2019). Effect of levodopa on electroencephalographic biomarkers of the parkinsonian state. *Journal of Neurophysiology*, *122*(1), 290–299. <https://doi.org/10.1152/jn.00141.2019>
- Miller, K. J., Sorensen, L. B., Ojemann, J. G., & Den Nijs, M. (2009). Power-law scaling in the brain surface electric potential. *PLoS Computational Biology*, *5*(12). <https://doi.org/10.1371/journal.pcbi.1000609>
- Molina, J. L., Voytek, B., Thomas, M. L., Joshi, Y. B., Bhakta, S. G., Talledo, J. A., Swerdlow, N. R., & Light, G. A. (2020). Memantine Effects on Electroencephalographic Measures of Putative Excitatory/Inhibitory Balance in Schizophrenia. *Biological Psychiatry: Cognitive Neuroscience and Neuroimaging*, *5*(6), 562–568. <https://doi.org/10.1016/j.bpsc.2020.02.004>
- Morens, D. M., Davis, J. W., Grandinetti, A., Ross, G. W., Popper, J. S., & White, L. R. (1996). Epidemiologic observations on Parkinson's disease. *Neurology*, *46*(4), 1044 LP – 1050. <https://doi.org/10.1212/WNL.46.4.1044>
- Müller, E. J., & Robinson, P. A. (2018). Suppression of parkinsonian beta oscillations by deep brain stimulation: Determination of effective protocols. *Frontiers in Computational Neuroscience*, *12*(December), 1–16. <https://doi.org/10.3389/fncom.2018.00098>
- Murthy, V. N., & Fetz, E. E. (1992). Coherent 25- To 35-Hz oscillations in the sensorimotor cortex of awake behaving monkeys. *Proceedings of the National Academy of Sciences of the United States of America*, *89*(12), 5670–5674. <https://doi.org/10.1073/pnas.89.12.5670>
- Neumann, W., Staub-bartelt, F., Horn, A., & Schanda, J. (2018). *Europe PMC Funders Group Long term correlation of subthalamic beta band activity with motor*

- impairment in patients with Parkinson ' s disease*. 128(11), 2286–2291. <https://doi.org/10.1016/j.clinph.2017.08.028>.Long
- Noyce, A. J., Bestwick, J. P., Silveira-Moriyama, L., Hawkes, C. H., Giovannoni, G., Lees, A. J., & Schrag, A. (2012). Meta-analysis of early nonmotor features and risk factors for Parkinson disease. *Annals of Neurology*, 72(6), 893–901. <https://doi.org/10.1002/ana.23687>
- O’Keeffe, A. B., Malekmohammadi, M., Sparks, H., & Pouratian, N. (2020). Synchrony drives motor cortex beta bursting, waveform dynamics, and phase-amplitude coupling in parkinson’s disease. *Journal of Neuroscience*, 40(30), 5833–5846. <https://doi.org/10.1523/JNEUROSCI.1996-19.2020>
- Oostenveld, R., Fries, P., Maris, E., & Schoffelen, J. M. (2011). FieldTrip: Open source software for advanced analysis of MEG, EEG, and invasive electrophysiological data. *Computational Intelligence and Neuroscience*, 2011. <https://doi.org/10.1155/2011/156869>
- Oran, Y., & Bar-Gad, I. (2018). Loss of balance between striatal feedforward inhibition and corticostriatal excitation leads to tremor. *Journal of Neuroscience*, 38(7), 1699–1710. <https://doi.org/10.1523/JNEUROSCI.2821-17.2018>
- Oswal, A., Beudel, M., Zrinzo, L., Limousin, P., Hariz, M., Foltynie, T., Litvak, V., & Brown, P. (2016). Deep brain stimulation modulates synchrony within spatially and spectrally distinct resting state networks in Parkinson’s disease. *Brain*, 139(5), 1482–1496. <https://doi.org/10.1093/brain/aww048>
- Oswal, A., Brown, P., & Litvak, V. (2013). Synchronized neural oscillations and the pathophysiology of Parkinson’s disease. *Current Opinion in Neurology*, 26(6), 662–670. <https://doi.org/10.1097/WCO.0000000000000034>
- Oswal, A., Cao, C., Yeh, C. H., Neumann, W. J., Gratwicke, J., Akram, H., Horn, A., Li, D., Zhan, S., Zhang, C., Wang, Q., Zrinzo, L., Foltynie, T., Limousin, P., Bogacz, R., Sun, B., Husain, M., Brown, P., & Litvak, V. (2021). Neural signatures of hyperdirect pathway activity in Parkinson’s disease. *Nature Communications*, 12(1), 1–14. <https://doi.org/10.1038/s41467-021-25366-0>
- Ozturk, M., Abosch, A., Francis, D., Wu, J., Jimenez-Shahed, J., & Ince, N. F. (2020). Distinct subthalamic coupling in the ON state describes motor performance in Parkinson’s disease. *Movement Disorders*, 35(1), 91–100. <https://doi.org/10.1002/mds.27800>
- Ozturk, M., Kaku, H., Jimenez-Shahed, J., Viswanathan, A., Sheth, S. A., Kumar, S., & Ince, N. F. (2020). Subthalamic Single Cell and Oscillatory Neural Dynamics of a

- Dyskinetic Medicated Patient With Parkinson's Disease. *Frontiers in Neuroscience*, 14(April), 1–8. <https://doi.org/10.3389/fnins.2020.00391>
- Pascual-Marqui, R. D. (2007). *Coherence and phase synchronization: generalization to pairs of multivariate time series, and removal of zero-lag contributions*. July, 1–12. <http://arxiv.org/abs/0706.1776>
- Pascual-Marqui, R. D., Lehmann, D., Koukkou, M., Kochi, K., Anderer, P., Saletu, B., Tanaka, H., Hirata, K., John, E. R., Prichep, L., Biscay-Lirio, R., & Kinoshita, T. (2011). Assessing interactions in the brain with exact low-resolution electromagnetic tomography. *Philosophical Transactions of the Royal Society A: Mathematical, Physical and Engineering Sciences*, 369(1952), 3768–3784. <https://doi.org/10.1098/rsta.2011.0081>
- Peterson, E. J., Rosen, B. Q., Campbell, A. M., Belger, A., & Voytek, B. (2017). 1/F Neural Noise Is a Better Predictor of Schizophrenia Than Neural Oscillations. *BioRxiv*. <https://doi.org/10.1101/113449>
- Pezzoli, G., & Cereda, E. (2013). Exposure to pesticides or solvents and risk of Parkinson disease. *Neurology*, 80(22), 2035–2041. <https://doi.org/10.1212/WNL.0b013e318294b3c8>
- Poewe, W., & Scherfler, C. (2003). Role of dopamine transporter imaging in investigation of parkinsonian syndromes in routine clinical practice. *Movement Disorders*, 18(SUPPL. 7), 16–21. <https://doi.org/10.1002/mds.10573>
- Pringsheim, T., Jette, N., Frolkis, A., & Steeves, T. D. L. (2014). The prevalence of Parkinson's disease: A systematic review and meta-analysis. *Movement Disorders*, 29(13), 1583–1590. <https://doi.org/10.1002/mds.25945>
- Ransmayr, G., Seppi, K., Donnemiller, E., Luginger, E., Marksteiner, J., Riccabona, G., Poewe, W., & Wenning, G. K. (2001). Striatal dopamine transporter function in dementia with Lewy bodies and Parkinson's disease. *European Journal of Nuclear Medicine*, 28(10), 1523–1528. <https://doi.org/10.1007/s002590100571>
- Ray, N. J., Jenkinson, N., Wang, S., Holland, P., Brittain, J. S., Joint, C., Stein, J. F., & Aziz, T. (2008). Local field potential beta activity in the subthalamic nucleus of patients with Parkinson's disease is associated with improvements in bradykinesia after dopamine and deep brain stimulation. *Experimental Neurology*, 213(1), 108–113. <https://doi.org/10.1016/j.expneurol.2008.05.008>
- Ridding, M. C., Rothwell, J. C., & Inzelberg, R. (1995). Changes in excitability of motor cortical circuitry in patients with parkinson's disease. *Annals of Neurology*, 37(2), 181–188. <https://doi.org/10.1002/ana.410370208>

- Robertson, M. M., Furlong, S., Voytek, B., Donoghue, T., Boettiger, C. A., & Sheridan, M. A. (2019). EEG power spectral slope differs by ADHD status and stimulant medication exposure in early childhood. *Journal of Neurophysiology*, *122*(6), 2427–2437. <https://doi.org/10.1152/jn.00388.2019>
- Rubinov, M., & Sporns, O. (2010). Complex network measures of brain connectivity: uses and interpretations. *NeuroImage* *52*, 1059–1069. doi: 10.1016/j.neuroimage.2009.10.003
- Saint-Cyr, J. A., Taylor, A. E., & Nicholson, K. (1995). Behavior and the basal ganglia. *Adv Neurol.*, *65*, 1-28. PMID: 7872134.
- Schwarz, J., Storch, A., Koch, W., Pogarell, O., Radau, P. E., & Tatsch, K. (2004). Loss of dopamine transporter binding in Parkinson's disease follows a single exponential rather than linear decline. *Journal of Nuclear Medicine*, *45*(10), 1694–1697.
- Sharma, A., Vidaurre, D., Vesper, J., Schnitzler, A., & Florin, E. (2021). Differential dopaminergic modulation of spontaneous cortico–subthalamic activity in parkinson's disease. *ELife*, *10*, 1–23. <https://doi.org/10.7554/eLife.66057>
- Sherman, M. A., Lee, S., Law, R., Haegens, S., Thorn, C. A., Hämäläinen, M. S., Moore, C. I., & Jones, S. R. (2016). Neural mechanisms of transient neocortical beta rhythms: Converging evidence from humans, computational modeling, monkeys, and mice. *Proceedings of the National Academy of Sciences of the United States of America*, *113*(33), E4885–E4894. <https://doi.org/10.1073/pnas.1604135113>
- Shi, X., Du, D., & Wang, Y. (2021). Interaction of Indirect and Hyperdirect Pathways on Synchrony and Tremor-Related Oscillation in the Basal Ganglia. *Neural Plasticity*, *2021*. <https://doi.org/10.1155/2021/6640105>
- Shimamoto, S. A., Ryapolova-Webb, E. S., Ostrem, J. L., Galifianakis, N. B., Miller, K. J., & Starr, P. A. (2013). Subthalamic nucleus neurons are synchronized to primary motor cortex local field potentials in Parkinson's disease. *Journal of Neuroscience*, *33*(17), 7220–7233. <https://doi.org/10.1523/JNEUROSCI.4676-12.2013>
- Silberstein, P., Pogosyan, A., Kühn, A. A., Hotton, G., Tisch, S., Kupsch, A., Dowsey-Limousin, P., Hariz, M. I., & Brown, P. (2005). Cortico-cortical coupling in Parkinson's disease and its modulation by therapy. *Brain*, *128*(6), 1277–1291. <https://doi.org/10.1093/brain/awh480>
- Sobesky, L., Goede, L., Odekerken, V. J. J., Wang, Q., Li, N., Neudorfer, C., Rajamani, N., Al-Fatly, B., Reich, M., Volkmann, J., de Bie, R. M. A., Kühn, A. A., & Horn, A. (2022). Subthalamic and pallidal deep brain stimulation: are we modulating the same network? *Brain*, *145*(1), 251–262. <https://doi.org/10.1093/brain/awab258>

- Speckmann, E. J., Elger, C. E., & Gorji, A. (2012). Neurophysiologic basis of EEG and DC potentials. *Niedermeyer's Electroencephalography*, 17-32.
- Stern, M. B., Lang, A., & Poewe, W. (2012). Toward a redefinition of Parkinson's disease. *Movement Disorders*, 27(1), 54–60. <https://doi.org/10.1002/mds.24051>
- Stoffers, D., Bosboom, J. L. W., Deijen, J. B., Wolters, E. C., Stam, C. J., & Berendse, H. W. (2008). Increased cortico-cortical functional connectivity in early-stage Parkinson's disease: An MEG study. *NeuroImage*, 41(2), 212–222. <https://doi.org/10.1016/j.neuroimage.2008.02.027>
- Swann, N. C., De Hemptinne, C., Aron, A. R., Ostrem, J. L., Knight, R. T., & Starr, P. A. (2015). Elevated synchrony in Parkinson disease detected with electroencephalography. *Annals of Neurology*, 78(5), 742–750. <https://doi.org/10.1002/ana.24507>
- Szczepanski, S. M., Crone, N. E., Kuperman, R. A., Augustine, K. I., Parvizi, J., & Knight, R. T. (2014). Dynamic Changes in Phase-Amplitude Coupling Facilitate Spatial Attention Control in Fronto-Parietal Cortex. *PLoS Biology*, 12(8). <https://doi.org/10.1371/journal.pbio.1001936>
- Tinkhauser, G., Pogosyan, A., Little, S., Beudel, M., Herz, D. M., Tan, H., & Brown, P. (2017). The modulatory effect of adaptive deep brain stimulation on beta bursts in Parkinson's disease. *Brain*, 140(4), 1053–1067. <https://doi.org/10.1093/brain/awx010>
- Tinkhauser, G., Pogosyan, A., Tan, H., Herz, D. M., Kühn, A. A., & Brown, P. (2017). Beta burst dynamics in Parkinson's disease off and on dopaminergic medication. *Brain*, 140(11), 2968–2981. <https://doi.org/10.1093/brain/awx252>
- Tinkhauser, G., Torrecillos, F., Duclos, Y., Tan, H., Pogosyan, A., Fischer, P., Carron, R., Welter, M. L., Karachi, C., Vandenberghe, W., Nuttin, B., Witjas, T., Régis, J., Azulay, J. P., Eusebio, A., & Brown, P. (2018). Beta burst coupling across the motor circuit in Parkinson's disease. *Neurobiology of Disease*, 117(June), 217–225. <https://doi.org/10.1016/j.nbd.2018.06.007>
- Tort, A. B. L., Kramer, M. A., Thorn, C., Gibson, D. J., Kubota, Y., Graybiel, A. M., & Kopell, N. J. (2008). Dynamic cross-frequency couplings of local field potential oscillations in rat striatum and hippocampus during performance of a T-maze task. *Proceedings of the National Academy of Sciences of the United States of America*, 105(51), 20517–20522. <https://doi.org/10.1073/pnas.0810524105>
- Trager, M. H., Koop, M. M., Velisar, A., Blumenfeld, Z., Nikolau, J. S., Quinn, E. J., Martin, T., & Bronte-Stewart, H. (2016). Subthalamic beta oscillations are attenuated after withdrawal of chronic high frequency neurostimulation in

- Parkinson's disease. *Neurobiology of Disease*, 96, 22–30. <https://doi.org/10.1016/j.nbd.2016.08.003>
- van Wijk, B. C. M., Beudel, M., Jha, A., Oswal, A., Foltynie, T., Hariz, M. I., Limousin, P., Zrinzo, L., Aziz, T. Z., Green, A. L., Brown, P., & Litvak, V. (2016). Subthalamic nucleus phase-amplitude coupling correlates with motor impairment in Parkinson's disease. *Clinical Neurophysiology*, 127(4), 2010–2019. <https://doi.org/10.1016/j.clinph.2016.01.015>
- Voon, V., Reynolds, B., Brezing, C., Gallea, C., Skaljic, M., Ekanayake, V., Fernandez, H., Potenza, M. N., Dolan, R. J., & Hallett, M. (2010). Impulsive choice and response in dopamine agonist-related impulse control behaviors. *Psychopharmacology*, 207(4), 645–659. <https://doi.org/10.1007/s00213-009-1697-y>
- Voytek, B., Kramer, M. A., Case, J., Lepage, K. Q., Tempesta, Z. R., Knight, R. T., & Gazzaley, A. (2015). Age-related changes in 1/f neural electrophysiological noise. *Journal of Neuroscience*, 35(38), 13257–13265. <https://doi.org/10.1523/JNEUROSCI.2332-14.2015>
- Wakabayashi, K., Tanji, K., Mori, F., & Takahashi, H. (2007). The Lewy body in Parkinson's disease: Molecules implicated in the formation and degradation of α -synuclein aggregates. *Neuropathology*, 27(5), 494–506. <https://doi.org/10.1111/j.1440-1789.2007.00803.x>
- Wakabayashi, K., Tanji, K., Odagiri, S., Miki, Y., Mori, F., & Takahashi, H. (2013). The Lewy body in Parkinson's disease and related neurodegenerative disorders. *Molecular Neurobiology*, 47(2), 495–508. <https://doi.org/10.1007/s12035-012-8280-y>
- Waschke, L., Wöstmann, M., & Obleser, J. (2017). States and traits of neural irregularity in the age-varying human brain. *Scientific Reports*, 7(1), 1–12. <https://doi.org/10.1038/s41598-017-17766-4>
- Weinberger, M., Mahant, N., Hutchison, W. D., Lozano, A. M., Moro, E., Hodaie, M., Lang, A. E., & Dostrovsky, J. O. (2006). Beta oscillatory activity in the subthalamic nucleus and its relation to dopaminergic response in Parkinson's disease. *Journal of Neurophysiology*, 96(6), 3248–3256. <https://doi.org/10.1152/jn.00697.2006>
- West, T. O., Berthouze, L., Halliday, D. M., Litvak, V., Sharott, A., Magill, P. J., & Farmer, S. F. (2018). Propagation of beta/gamma rhythms in the cortico-basal ganglia circuits of the parkinsonian rat. *Journal of Neurophysiology*, 119(5), 1608–1628. <https://doi.org/10.1152/jn.00629.2017>

- Wichmann, T., DeLong, M. R., Guridi, J., & Obeso, J. A. (2011). Milestones in research on the pathophysiology of Parkinson's disease. *Movement Disorders*, 26(6), 1032–1041. <https://doi.org/10.1002/mds.23695>
- Wingeier, B., Tcheng, T., Koop, M. M., Hill, B. C., Heit, G., & Bronte-Stewart, H. M. (2006). Intra-operative STN DBS attenuates the prominent beta rhythm in the STN in Parkinson's disease. *Experimental Neurology*, 197(1), 244–251. <https://doi.org/10.1016/j.expneurol.2005.09.016>
- Yau, Y., Zeighami, Y., Baker, T. E., Larcher, K., Vainik, U., Dadar, M., Fonov, V. S., Hagmann, P., Griffa, A., Mišić, B., Collins, D. L., & Dagher, A. (2018). Network connectivity determines cortical thinning in early Parkinson's disease progression. *Nature Communications*, 9(1), 1–10. <https://doi.org/10.1038/s41467-017-02416-0>
- Yin, Z., Zhu, G., Liu, Y., Zhao, B., Liu, D., Bai, Y., Zhang, Q., Shi, L., Feng, T., Yang, A., Liu, H., Meng, F., Neumann, W.-J., Kühn, A. A., Jiang, Y., & Zhang, J. (2022). Cortical phase-amplitude coupling is key to the occurrence and treatment of freezing of gait. *Brain*. <https://doi.org/10.1093/brain/awac121>
- Yoav Benjamini, & Yoel Hochberg. (1995). Controlling the False Discovery Rate: A Practical and Powerful Approach to Multiple Testing. *Journal of the Royal Statistical Society. Series B (Methodological)*, 57(1), 289–300.
- Zeighami, Y., Fereshtehnejad, S. M., Dadar, M., Collins, D. L., Postuma, R. B., Mišić, B., & Dagher, A. (2019). A clinical-anatomical signature of Parkinson's disease identified with partial least squares and magnetic resonance imaging. *NeuroImage*, 190(December), 69–78. <https://doi.org/10.1016/j.neuroimage.2017.12.050>
- Zhang, J., Idaji, M. J., Villringer, A., & Nikulin, V. V. (2021). Neuronal biomarkers of Parkinson's disease are present in healthy aging. *NeuroImage*, 243(August), 118512. <https://doi.org/10.1016/j.neuroimage.2021.118512>
- Zhang, J., Villringer, A., & Nikulin, V. V. (2022). Dopaminergic Modulation of Local Non-oscillatory Activity and Global-Network Properties in Parkinson's Disease: An EEG Study. *Frontiers in Aging Neuroscience*, 14(April), 1–18. <https://doi.org/10.3389/fnagi.2022.846017>
- Zhou, S., & Yu, Y. (2018). Synaptic E-I balance underlies efficient neural coding. *Frontiers in Neuroscience*, 12(FEB), 1–11. <https://doi.org/10.3389/fnins.2018.00046>
- Zhou, X., Ma, N., Song, B., Wu, Z., Liu, G., Liu, L., Yu, L., & Feng, J. (2021). Optimal Organization of Functional Connectivity Networks for Segregation and Integration With Large-Scale Critical Dynamics in Human Brains. *Frontiers in Computational Neuroscience*, 15(March), 1–17. <https://doi.org/10.3389/fncom.2021.641335>

Statutory Declaration

“I, *Juanli Zhang*, by personally signing this document in lieu of an oath, hereby affirm that I prepared the submitted dissertation on the topic *Non-invasive electrophysiological biomarkers of aging and Parkinson’s disease (Nicht-invasive elektrophysiologische Biomarker des Alterns und der Parkinson-Krankheit)*, independently and without the support of third parties, and that I used no other sources and aids than those stated.

All parts which are based on the publications or presentations of other authors, either in letter or in spirit, are specified as such in accordance with the citing guidelines. The sections on methodology (in particular regarding practical work, laboratory regulations, statistical processing) and results (in particular regarding figures, charts and tables) are exclusively my responsibility.

Furthermore, I declare that I have correctly marked all of the data, the analyses, and the conclusions generated from data obtained in collaboration with other persons, and that I have correctly marked my own contribution and the contributions of other persons (cf. declaration of contribution). I have correctly marked all texts or parts of texts that were generated in collaboration with other persons.

My contributions to any publications to this dissertation correspond to those stated in the below joint declaration made together with the supervisor. All publications created within the scope of the dissertation comply with the guidelines of the ICMJE (International Committee of Medical Journal Editors; <http://www.icmje.org>) on authorship. In addition, I declare that I shall comply with the regulations of Charité – Universitätsmedizin Berlin on ensuring good scientific practice.

I declare that I have not yet submitted this dissertation in identical or similar form to another Faculty.

The significance of this statutory declaration and the consequences of a false statutory declaration under criminal law (Sections 156, 161 of the German Criminal Code) are known to me.”

Date

Signature

Declaration of your own contribution to the publications

Juanli Zhang contributed the following to the below listed publications:

Publication 1: Zhang, J., Idaji, M. J., Villringer, A., & Nikulin, V. V.. Neuronal biomarkers of Parkinson's disease are present in healthy aging. *NeuroImage*, 2021.

Contribution in detail:

- Juanli Zhang developed the hypotheses in collaboration with the co-authors.
- She developed the pipeline independently to pre-process a large dataset (around 140 subjects in total) using EEGLab and custom-written scripts in Matlab.
- She independently implemented the analysis (for instance PAC, beta burst characteristics etc.) by writing the codes in Matlab.
- She independently performed all the statistical analyses by using FieldTrip and custom-written scripts in Matlab.
- She ran the source-reconstruction analysis with the collaboration with the co-authors.
- She independently carried out the visualization of all the methods and results with the feedback from the co-authors. All the figures were created by her.
- She interpreted the results, wrote the drafts of the manuscript which were revised by the co-authors.
- She was responsible for the submission and coordination processes. She addressed the extensive questions raised by the peer reviewers with the feedback from the co-authors. She performed all the additional analyses, and wrote all the drafts of response letter which were revised by the co-authors.

Publication 2: Zhang, J., Villringer, A., & Nikulin, V. V.. Dopaminergic Modulation of Local Non-oscillatory Activity and Global-Network Properties in Parkinson's Disease: An EEG Study. *Frontiers in Aging Neuroscience*, 2022

Contribution in detail:

- Juanli Zhang developed the central hypotheses independently and conceptualized the study with the feedback from her supervisors.
- She proactively searched for the appropriate open access datasets and accessed the data quality.
- She developed the pipeline independently to pre-process the data using EEGLab and custom-written scripts in Matlab.
- She implemented all the analysis by writing the scripts in Matlab.
- She performed all the statistical analyses by using FieldTrip and custom-written scripts in Matlab.
- She independently carried out the graphic representation of all the methods and results with the feedback from the co-authors. All the figures were created by her.
- She interpreted the findings, wrote all the drafts of the manuscript which were revised by the co-authors.
- She was responsible for the submission process and coordination with the journal editor's office. After receiving the comments from the peer reviewers, she wrote the response letter with the feedback from her supervisors.

Signature of doctoral candidate

Excerpt from Journal Summary List

Publication 1:

Journal Data Filtered By: **Selected JCR Year: 2020** Selected Editions: SCIE,SSCI
 Selected Categories: "**NEUROIMAGING**" Selected Category Scheme: WoS
Gesamtanzahl: 14 Journale

Rank	Full Journal Title	Total Cites	Journal Impact Factor	Eigenfactor Score
1	NEUROIMAGE	119,618	6.556	0.105820
2	Journal of NeuroInterventional Surgery	7,426	5.836	0.016070
3	HUMAN BRAIN MAPPING	27,538	5.038	0.035480
4	NeuroImage-Clinical	11,645	4.881	0.027860
5	Brain Imaging and Behavior	4,363	3.978	0.008050
6	AMERICAN JOURNAL OF NEURORADIOLOGY	27,423	3.825	0.024030
7	JOURNAL OF NEURORADIOLOGY	1,475	3.447	0.001920
8	NEURORADIOLOGY	6,702	2.804	0.005900
9	JOURNAL OF NEUROIMAGING	2,870	2.486	0.003940
10	PSYCHIATRY RESEARCH-NEUROIMAGING	6,308	2.376	0.005990
11	NEUROIMAGING CLINICS OF NORTH AMERICA	1,515	2.264	0.001340
12	STEREOTACTIC AND FUNCTIONAL NEUROSURGERY	2,298	1.875	0.001840
13	CLINICAL EEG AND NEUROSCIENCE	1,341	1.843	0.001370
14	KLINISCHE NEUROPHYSIOLOGIE	54	0.270	0.000020

Copyright © 2021 Clarivate Analytics

Publication 2:

Journal Data Filtered By: **Selected JCR Year: 2020** Selected Editions: SCIE,SSCI
 Selected Categories: **"NEUROSCIENCES"** Selected Category Scheme: WoS
Gesamtanzahl: 273 Journale

Rank	Full Journal Title	Total Cites	Journal Impact Factor	Eigenfactor Score
1	NATURE REVIEWS NEUROSCIENCE	49,897	34.870	0.048890
2	NATURE NEUROSCIENCE	73,709	24.884	0.128020
3	TRENDS IN COGNITIVE SCIENCES	33,482	20.229	0.036270
4	NEURON	111,115	17.173	0.175220
5	ACTA NEUROPATHOLOGICA	28,031	17.088	0.036970
6	MOLECULAR PSYCHIATRY	28,622	15.992	0.046220
7	Molecular Neurodegeneration	6,772	14.195	0.011650
8	TRENDS IN NEUROSCIENCES	22,858	13.837	0.019470
9	Nature Human Behaviour	5,549	13.663	0.023120
10	BRAIN	64,627	13.501	0.061550
11	BIOLOGICAL PSYCHIATRY	50,155	13.382	0.045540
12	JOURNAL OF PINEAL RESEARCH	12,492	13.007	0.008170
13	BEHAVIORAL AND BRAIN SCIENCES	11,610	12.579	0.007760
14	Annual Review of Neuroscience	14,699	12.449	0.010490
15	PROGRESS IN NEUROBIOLOGY	15,161	11.685	0.010300
16	SLEEP MEDICINE REVIEWS	11,218	11.609	0.014840
17	ANNALS OF NEUROLOGY	43,728	10.422	0.039960
18	NEUROSCIENCE AND BIOBEHAVIORAL REVIEWS	36,525	8.989	0.048970
19	Brain Stimulation	9,206	8.955	0.015960
20	npj Parkinsons Disease	1,093	8.651	0.003040
21	FRONTIERS IN NEUROENDOCRINOLOGY	5,338	8.606	0.005050

Rank	Full Journal Title	Total Cites	Journal Impact Factor	Eigenfactor Score
44	BRAIN PATHOLOGY	6,559	6.508	0.006220
45	Developmental Cognitive Neuroscience	4,477	6.464	0.011160
46	Annual Review of Vision Science	935	6.422	0.004560
47	Multiple Sclerosis Journal	15,551	6.312	0.016680
48	CEPHALALGIA	12,756	6.292	0.011940
49	Biological Psychiatry-Cognitive Neuroscience and Neuroimaging	2,193	6.204	0.007120
50	JOURNAL OF CEREBRAL BLOOD FLOW AND METABOLISM	22,732	6.200	0.019640
51	JOURNAL OF PSYCHIATRY & NEUROSCIENCE	4,100	6.186	0.004200
52	JOURNAL OF NEUROSCIENCE	186,015	6.167	0.130970
53	EUROPEAN JOURNAL OF NEUROLOGY	14,490	6.089	0.016730
54	NEUROBIOLOGY OF DISEASE	21,360	5.996	0.020680
55	Dialogues in Clinical Neuroscience	5,272	5.986	0.005200
56	SLEEP	28,688	5.849	0.023920
57	JOURNAL OF PAIN	13,655	5.820	0.014690
58	Frontiers in Aging Neuroscience	13,654	5.750	0.025540
59	CURRENT OPINION IN NEUROLOGY	6,723	5.710	0.008480
60	Frontiers in Molecular Neuroscience	10,570	5.639	0.022450
61	MOLECULAR NEUROBIOLOGY	20,795	5.590	0.033020
62	Journal of Parkinsons Disease	3,562	5.568	0.006390
63	Frontiers in Cellular Neuroscience	17,299	5.505	0.033870
64	Neurobiology of Stress	1,628	5.441	0.004280
65	Cognitive Computation	2,407	5.418	0.002870

Printing copies of the publications

Publication 1:

Zhang, J., Idaji, M. J., Villringer, A., & Nikulin, V. V. (2021). Neuronal biomarkers of Parkinson's disease are present in healthy aging. *NeuroImage*, 243(August), 118512.
<https://doi.org/10.1016/j.neuroimage.2021.118512>.



Neuronal biomarkers of Parkinson's disease are present in healthy aging

Juanli Zhang^{a,b,*}, Mina Jamshidi Idaji^{a,c,d}, Arno Villringer^{a,e}, Vadim V. Nikulin^{a,f,g,*}

^a Department of Neurology, Max Planck Institute for Human Cognitive and Brain Sciences, Leipzig, Germany

^b Department of Neurology, Charité – Universitätsmedizin Berlin, Berlin, Germany

^c Machine Learning Group, Technical University of Berlin, Berlin, Germany

^d International Max Planck Research School NeuroCom, Leipzig, Germany

^e Department of Cognitive Neurology, University Hospital Leipzig, Leipzig, Germany

^f Centre for Cognition and Decision Making, Institute for Cognitive Neuroscience, National Research University Higher School of Economics, Moscow, Russian Federation

^g Neuropsychology Group, Department of Neurology, Charité – Universitätsmedizin Berlin, Berlin, Germany



ARTICLE INFO

Keywords:

Resting state EEG

Healthy aging

Parkinson's disease

PAC

Beta burst

ABSTRACT

The prevalence of Parkinson's disease (PD) increases with aging and both processes share similar cellular mechanisms and alterations in the dopaminergic system. Yet it remains to be investigated whether aging can also demonstrate electrophysiological neuronal signatures typically associated with PD. Previous work has shown that phase-amplitude coupling (PAC) between the phase of beta oscillations and the amplitude of gamma oscillations as well as beta bursts features can serve as electrophysiological biomarkers for PD. Here we hypothesize that these metrics are also present in apparently healthy elderly subjects. Using resting state multichannel EEG measurements, we show that PAC between beta oscillation and broadband gamma activity (50–150 Hz) is elevated in a group of elderly (59–77 years) compared to young volunteers (20–35 years) without PD. Importantly, the increase of PAC is statistically significant even after ruling out confounds relating to changes in spectral power and non-sinusoidal shape of beta oscillation. Moreover, a trend for a higher percentage of longer beta bursts (> 0.2 s) along with the increase in their incidence rate is also observed for elderly subjects. Using inverse modeling, we further show that elevated PAC and longer beta bursts are most pronounced in the sensorimotor areas. Moreover, we show that PAC and longer beta bursts might reflect distinct mechanisms, since their spatial patterns only partially overlap and the correlation between them is weak. Taken together, our findings provide novel evidence that electrophysiological biomarkers of PD may already occur in apparently healthy elderly subjects. We hypothesize that PAC and beta bursts characteristics in aging might reflect a pre-clinical state of PD and suggest their predictive value to be tested in prospective longitudinal studies.

1. Introduction

Aging is associated with alterations in metabolism, neurotransmission, hormonal and immune dysregulation, and inflammation; thus leading to diverse neurocognitive impairments (Kim et al., 2017; Sibille, 2013; Zhuang et al., 2018). Healthy aging is accompanied by the loss of dopaminergic (DA) neurons (Rudow et al., 2008), and it is assumed that the clinical signs of Parkinson's disease in humans appear when the DA in the substantia nigra pars compacta (SNc) are degenerated by up to 60%–70% (Cheng et al., 2010; Darden, 2007). Although elderly people often demonstrate mild parkinsonian signs including rigidity, bradykinesia, tremor and problems with gait balance (Louis and Bennett, 2007), these signs do not meet the established clinical criteria for Parkinson's disease (PD) (Marsili et al., 2018). Yet, aging is the single most significant factor influencing the clinical presence and progression of PD (Hindle, 2010). A close association between ag-

ing and PD is further supported by the findings in non-human primates demonstrating that both processes have multiple similar biological features and share the directionality of alterations in the nigrostriatal DA system. This in turn leads to a hypothesis that aging is associated with biological changes (particularly in dopamine system) creating vulnerable conditions potentially serving as a foundation for PD (Collier et al., 2017).

Given a close relationship between PD and aging, it is tempting to speculate that this relation can also be reflected in electrophysiological brain signals. Interestingly, using invasive and non-invasive electrophysiological methods, several signatures of PD have been identified. But, to the best of our knowledge, it is not known whether similar changes are also present in apparently healthy elderly subjects compared to the young ones. The most pronounced electrophysiological signature of PD is represented by abnormally elevated beta oscillatory activity in the subthalamic nucleus (STN) (Alexandre Eusebio and Brown, 2009;

* Corresponding authors.

E-mail address: juanlizhang@cbs.mpg.de (J. Zhang).

<https://doi.org/10.1016/j.neuroimage.2021.118512>

Received 10 August 2021; Accepted 23 August 2021

Available online 26 August 2021.

1053-8119/© 2021 The Authors. Published by Elsevier Inc. This is an open access article under the CC BY-NC-ND license

(<http://creativecommons.org/licenses/by-nc-nd/4.0/>)

Brittain et al., 2014; Brown, 2003; Crowell et al., 2012; De Hemptinne et al., 2015; Hammond et al., 2007; Kühn et al., 2009; Little and Brown, 2014; Oswal et al., 2013; Weinberger et al., 2006). Beta power in the STN is correlated with bradykinesia (A. Eusebio et al., 2011; Chen et al., 2010; R. Levy et al., 2002) and is attenuated by levodopa (Kühn et al., 2009; Weinberger et al., 2006) and by deep brain stimulation (DBS) (Müller and Robinson, 2018; Ray et al., 2008; Wingeier et al., 2006). Moreover, a higher incidence of longer beta bursts in the STN has been shown to correlate positively with clinical impairment (Tinkhauser et al., 2017a, 2017b). At the level of the cortex, however, divergent studies demonstrated that either a decrease (Stoffers et al., 2007; Whitmer et al., 2012) or an increase (Melgari et al., 2014) in cortical beta power can occur during successful symptomatic therapy of PD. Notably, an alternative cortical biomarkers for PD is phase-amplitude coupling (PAC) between the phase of beta oscillations and the amplitude of broadband activity (also referred to here as “broadband gamma”) extending from 50 to 200 Hz (De Hemptinne et al., 2013, 2015). Increased cortical PAC observed in PD patients reflects a rather stereotypical neuronal recruitment pattern of sensorimotor areas and is hypothesized to promote rigidity and akinesia—cardinal symptoms of PD. Moreover, cortical beta-gamma PAC is considerably decreased during clinically effective DBS in the STN and by levodopa treatment (De Hemptinne et al., 2013; Swann et al., 2015). Non-invasive scalp-EEG analyses of cortical beta-gamma PAC (A. M. Miller et al., 2019; Swann et al., 2015) confirmed that PAC is indeed stronger in PD patients compared to age-matched healthy subjects. With respect to beta burst dynamics, a study by Tinkhauser et al. (2018) showed that longer beta bursts in the cortex coincide with longer burst in the STN showing further that episodes of elevated beta occur simultaneously in the basal ganglia and cortex thus limiting information coding capacity and leading to deterioration of movement performance. And more recently, a study using ECoG in M1 demonstrated a higher percentage of longer beta bursts in PD patients compared to the subjects without PD (O’Keefe et al., 2020). Taken together, these cortical features, namely PAC and beta burst dynamics, have been consistently reported in PD. Whether the two PD biomarkers are related to each other, so far, has been studied only in very few studies which suggested a close relationship between the two (Meidahl et al., 2019; O’Keefe et al., 2020). However, none of them investigated their relationship in a topographical manner. Yet, a different topographical pattern may indicate distinct underlined pathophysiology. Thus, investigating the presence and relationship of such biomarkers using multi-channel EEG might aid to better understanding the associated neurophysiological processes in PD and healthy aging.

Given the above-mentioned association between aging and PD, in the present study, we tested the hypothesis that electrophysiological signatures of PD at the cortical level, that is, PAC between the phase of beta oscillations and the amplitude of broadband gamma activity, as well as the incidence of longer beta bursts, is more pronounced in elderly compared to young subjects. Moreover, we expected that this effect would be most prominent in the sensorimotor areas of the cortex. We tested these hypotheses using the recently acquired LEMON dataset (Babayan et al., 2019) containing a large number of healthy young and old subjects with multichannel EEG.

2. Materials and methods

2.1. Subjects and task

The recruitment of the participants was carried out in two steps. First, participants were pre-screened by telephone with a semi-structured interview. Before the study, further individual screening was performed by a study physician who assessed for exclusion criteria such as diagnosis of hypertension, cardiovascular disease, history of neurological disorder or psychiatric disease, history of malignant disease etc. (Babayan et al., 2019). Participants were instructed to sit calmly and comfortably in a chair and the recording was conducted in a sound-

shielded room. The sessions consisted of 16 segments each lasting 60 s with each such segment related to interleaved eyes-closed (EC) or eyes-open (EO) condition. Therefore, each condition (EC or EO) lasted 8 min. In this study, only the data during eyes closed periods were included for further analysis. We included all the elderly subjects and selected an equally sized group of gender-matched young subjects. In total, there were 137 subjects: 71 young (age 20–35 years, mean age = 25.61, SD = 3.17, 24 females) and 66 old (age 59–77 years, mean age = 67.35, SD = 4.81, 31 females).

The Alertness subtest of the Test of Attentional Performance (TAP; orig. “Testbatterie zur Aufmerksamkeitsprüfung”; version 2.3; Zimmermann & Fimm, 2012) measures alertness and reaction speed. During this test, a cross appears on a screen at randomly varying intervals to which the subject should respond as quickly as possible by pressing a key. The mean reaction time over the trials is derived as a measure of intrinsic alertness for each subject, i.e. higher reaction time scores indicate a lower performance.

2.2. EEG recordings

62-channel EEG was acquired with BrainAmp MR-plus amplifiers using ActiCAP electrodes (both Brain Products, Germany). Electrode montage was based on the international standard 10–20 system with FCz being the reference during recording. Electrode impedance was kept below 5k Ω . Recordings were digitized at a sampling frequency of 2500 Hz and bandpass filtered between 0.015 Hz and 1 kHz.

2.3. Data analysis

2.3.1. Data pre-processing

In order to keep our data pre-processing comparable to previous EEG PD studies, we implemented it in an analogous manner to A. M. Miller et al. (2019) and Jackson et al. (2019). EEG data were analyzed with Matlab (The MathWorks Inc, Natick, Massachusetts, USA) using custom scripts and EEGLab toolbox (version 14.1.2; (Delorme and Makeig, 2004)) functions. At the first step, the data were down sampled to 512 Hz. A highpass filter at 1 Hz was then applied to remove low frequency drifts (two-way FIR filter, order = 1536, eegfilt.m from EEGLab). The continuous EEG data were then segmented into EC and EO conditions. Subsequently, independent component analysis (ICA – Infomax algorithm implemented in EEGLab) was used to remove physiological and non-physiological artifacts including cardiographic component, eye movements and blinks, muscle activity and line noise in the EC data. Next, the data were re-referenced to a common average. In the last stage, data were still examined visually for the presence of residual artifacts and segments contaminated by these events were marked and then excluded from the analysis. There was no difference between the groups in the length of the data (on average 444.36 s for elderly and 455.22 s for younger groups, respectively) included for further analysis (Wilcoxon rank sum test, $p = 0.2015$).

2.3.2. Spectral analysis

Power spectral density (PSD) was calculated using ‘*pwelch*’ function in MATLAB, with a Hamming window of 512 samples and a 50% overlap. The average PSD for beta band was obtained by averaging the spectral density in the beta frequency range (13–30 Hz). Individual beta peaks were detected using ‘*findpeaks*’ function in the frequency range 13–30 Hz.

2.3.3. Phase amplitude coupling (PAC)

PAC was calculated using the Kullback-Leibler-based modulation index method (Tort et al., 2008). Briefly, the modulation index (MI) quantifies the degree of deviation of the phase-modulated amplitude from the uniform distribution. The distribution of the normalized instantaneous amplitude envelope was computed for 18 phase bins, each covering 20 radians. A comparison of this distribution to the uniform distribution

was quantified with the Kullback-Leibler distance measure. The computed MI value is between 0 and 1 (0 for no coupling, and 1 for when the phase of the slower oscillation and the amplitude of the faster oscillation is fully coupled). MIs were calculated for phase-providing frequency across the 4–50 Hz range using a sliding window with a step size of 2 Hz and a bandwidth of 2 Hz, whilst the range for the amplitude-providing frequency varied from 4 to 170 Hz with a step size of 4 Hz. Since PAC measures require the filter for the amplitude extraction from faster frequency activity to have a bandwidth at least as great as the range of slower frequencies of interest, at each amplitude-providing frequency, we used a filter with a bandwidth as wide as that of the center-frequency of the phase-providing oscillation. The phase of the lower frequency and the amplitude of the higher frequency components were obtained using Hilbert transform after bandpass filtering using a two-way finite impulse response filter (FIR) (eegfilt.m with 'fir1' parameters from EEGLab, with the order of three cycles of lower cutoff frequency). To obtain meaningful values, we started the calculation between frequency pairs in which amplitude-providing frequency was always higher than the phase-providing one. The MIs across all the possible frequency pairs can be displayed as a phase-amplitude comodulogram.

A PAC value was derived for each channel and each subject as the mean of the MI values over the beta range (13–30 Hz) for phase-providing frequency and broadband gamma frequency range (50–150 Hz) for the amplitude-providing frequency. This approach has also been used in previous studies (A. M. Miller et al., 2019; Swann et al., 2015).

2.3.4. Non-sinusoidal waveform shape measure

In order to rule out the possibility that the statistical PAC could be due to the sharp edges of the waveforms (Kramer et al., 2008), non-sinusoidality of beta oscillation was quantified using sharpness and steepness ratios. The method proposed by (Cole et al., 2017) was used for this purpose. Below we elaborate on these calculations.

2.3.4.1. Sharpness ratio. First, we bandpass filtered (13–30 Hz, eegfilt.m from EEGLab, order = 118) the raw time series to obtain beta oscillations, for which we then identified rising and falling zero-crossing points. Then, in the raw signal, indices of maximum and minimum voltages between zero-crossings were found as the locations of peaks and troughs. Peak (trough) sharpness was defined as the mean voltage difference between the peak (trough) and neighboring three time points, which are ~6 ms before and after the peak (trough) (Cole et al., 2017). Finally, the sharpness ratio was calculated as the absolute value of the log-transform of the ratio of peak sharpness to trough sharpness.

2.3.4.2. Steepness ratio. The rise steepness was defined as the largest voltage rise between two subsequent data points (first derivative) in the time period between a trough and the peak after it. In the same manner, the decay steepness was calculated as the largest voltage drop between a peak and the trough following it. Similarly, steepness ratio was calculated as the absolute value of the log-transform of the ratio of rise steepness to decay steepness.

2.3.5. Beta bursts definition and characteristics

We referred to the methods proposed by Tinkhauser et al. (2017a) and Tinkhauser et al. (2017b) to estimate beta burst dynamics. First, we identified the mean beta peak frequency for each individual by averaging the peak frequencies over the channels. Then we detected the beta bursts in a frequency range of ± 5 Hz around the individual beta peak frequency (~15–25 Hz). Raw signal was bandpass filtered, and the amplitude envelope of the filtered data was extracted using Hilbert transform. A beta burst was defined as the time interval where the amplitude exceeds a certain threshold and stays above threshold for more than 100 ms (at least two cycles). We explored the region-specific differences of bursts characteristics with the threshold fixed at the 65th percentile of the amplitude. Moreover, to investigate the impact of the

burst thresholds, we included the analysis for a wide range of thresholds (percentiles 50, 55, 60, 65, 70, 75, 80, 85, and 90).

The histogram of the burst duration for each channel was investigated by binning the duration of the beta bursts into nine windows, namely 0.1–0.2 s, 0.2–0.3 s, 0.3–0.4 s, 0.4–0.5 s, 0.5–0.6 s, 0.6–0.7 s, 0.7–0.8 s, 0.8–0.9 s, and >0.9 s. Since total burst duration varies across channels and subjects, the histogram was normalized by the total number of beta bursts. Another feature of bursts, that is, incidence rate, was defined as the number of bursts per time unit (bursts/(second)). For the analysis across different threshold percentiles, we focused on two key features, namely mean burst duration and mean burst amplitude across all beta bursts.

2.3.6. Source space analysis

For the localization of neuronal sources we applied inverse modeling to project the EEG sensor recordings to cortical source level. After the EEG was preprocessed, EEG sensor signals were bandpass filtered within the frequency range of interest (eegfilt.m from EEGLab). We used the eLORETA algorithm (exact low resolution brain electromagnetic tomography, as implemented in the M/EEG Toolbox of Hamburg (METH, <https://www.nitrc.org/projects/meth/>) (Haufe and Ewald, 2016)) for inverse modeling and the New York head model with approximately 2000 vertices (Huang et al., 2016) to acquire the leadfield matrix. The cortical vertices were grouped into 96 regions of interest (ROIs) based on Harvard-Oxford atlas (Desikan et al., 2006). The time series estimated for each vertex was used for further analysis.

Specifically, for the PAC and beta band power analysis, we first estimated the metrics based on the time series from each vertex. Subsequently, we averaged the values across all the vertices within each ROI. To calculate PAC in a uniform way, we obtained the source reconstructed signal from beta band (13–30 Hz) and broadband gamma (50–150 Hz) to estimate the phase for lower frequency and amplitude for higher frequency components for each vertex, respectively. Then MI values were estimated for each vertex and further for each ROI from each subject. Beta power values were computed analogously by averaging PSD values over beta frequency range (13–30 Hz) for each vertex. Then, the ROI-based power value was estimated by averaging over the vertices within each ROI.

With respect to beta burst dynamics, we bandpass filtered data using the approach presented above for the sensor level (see Section 2.3.5.) and then projected the bandpass filtered sensor data to the cortical sources. Afterwards, singular value decomposition (SVD) was applied to the signals within each ROI in order to extract a representative ROI-based signal. Using SVD of the time series of all vertices within each ROI, the dominant time course of each ROI was extracted by preserving the first dominant SVD component. Thus, the 61-channel sensor level signal was transformed to 96-ROI signal at source level. Further analysis remained the same as for the sensor level.

2.3.7. Statistical tests

Statistical comparisons across groups were performed using a non-parametric Wilcoxon rank sum test between the old and young groups. To correct for multiple comparisons, false discovery rate (FDR) method was used according to Benjamini and Hochberg (1995) when multiple electrodes in sensor space, ROIs in source space, frequency bins and burst window bins were compared.

For the MI-comodulogram comparison between two groups at a single channel (C3), we performed frequency-frequency space cluster-based permutation procedure by using the 'Monte Carlo' method, as implemented in FieldTrip (Oostenveld et al., 2011). In brief, with 2000 permutations across the randomly shuffled labels for old and young groups, one can create the distribution of cluster statistics under the null hypothesis that there is no significant cluster. For each randomization, cluster level statistics (taking the sum of t values of all the frequency pair points within each cluster) were computed and the largest cluster statistic was

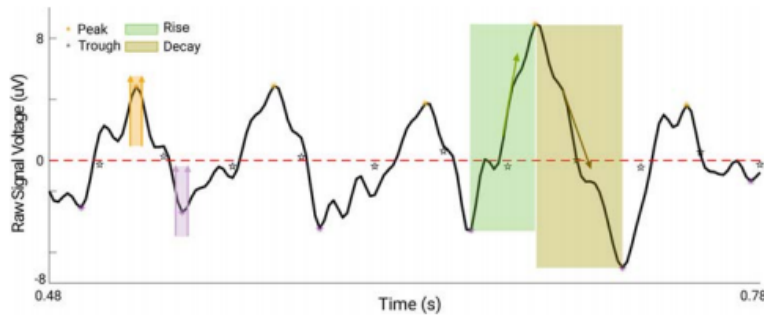


Fig. 1. Schematic illustration of the waveform shape estimation. Peaks and troughs in the raw signal that lie between the adjacent zero crossings identified from filtered beta band signal are color coded *: orange for peaks and purple for troughs. The light green area marks the rise period between a trough and subsequent peak to determine the rise steepness. Dark green area indicates the decay area where the decay steepness was estimated.

entered into the null distribution. Finally, the observed cluster in the empirical data was compared against the null distribution, and a p value below 0.05 (two tailed) was considered significant.

A correlation between different measures was performed using Spearman's approach. For the topographical correlation pattern, correlation strength was calculated for each channel or each ROI across the subjects, and then FDR was applied to correct for multiple comparisons across the channel/source space. The final correlation pattern was displayed as a head topography or on a standard reconstructed cortical surface model.

3. Results

3.1. PAC between beta band and broadband gamma activity is elevated with aging

3.1.1. PAC is elevated in sensorimotor areas in the elderly

To test the hypothesis that in the sensorimotor areas of the cortex PAC is elevated in the elderly, we first analyzed MI values from one of the electrodes typically attributed to the sensorimotor cortex (C3) (Swann et al., 2015). Fig. 2A shows mean comodulograms of MI at electrode C3 for each group. A prominent coupling can be observed between the phase of beta to low gamma and the amplitude of 50–150 Hz frequency range in the elderly (left panel) compared to the young group (right panel). Using cluster analysis, we examined the MI comodulograms for significant differences between the two groups. Fig. 2B shows a significant beta-gamma coupling group difference at electrode C3. The outlined cluster indicates a significant difference of PAC between the beta phase (13–30 Hz) and broadband gamma (50–150 Hz) frequency range, as well as PAC between low gamma phase frequency (30–50 Hz) and broadband gamma amplitude frequency. Further, we investigated at which phase providing frequencies the average PAC between the gamma amplitude and the phase from examined frequency differs between the two groups. This was done by computing PAC for the amplitude from 50 to 150 Hz for each phase-providing frequency window from 4 to 50 Hz (2 Hz width). The panel C of Fig. 2 depicts a significant PAC difference profile occurring starting from around 12 Hz extending up to low gamma range ($p < 0.05$, after FDR). Boxplots for PAC values from MIs averaged over 13–30 Hz for beta phase and 50–150 Hz for broadband gamma amplitude are presented in Fig. 2D. Although there was a considerable overlap between PAC values in two groups, the statistical analysis confirmed that the elderly group was characterized by significantly elevated PAC between beta oscillation and broadband gamma activity ($p = 0.0147$). Finally, we used normalized amplitude of broadband gamma (50–150 Hz) sorted according to the phase bins from beta band (see Section 2.3.3.) in order to see how it is modulated by the phase of beta oscillations (13–30 Hz). The upper panel E in Fig. 2 shows the mean of the normalized amplitude distribution at C3 in each group. Generally, broadband gamma amplitude is largely coupled to non-peak

phase of the beta oscillations by showing a strongest amplitude after (not at) $\pi/2$ radian in both groups. In addition, one can see elderly subjects showed a higher degree of modulation compared to young subjects. Circular bar plot in the bottom further confirms there is a certain age-dependent phase specificity: beta phase predominantly distributed within $\pi/6 \sim 2\pi/3$ when the highest amplitude occurred for both age groups.

Although we have found that the amplitude from broadband gamma range is coupled to the phase of beta and low gamma bands, further tests revealed that low-gamma phase driven PAC could be, to a very large extent, accounted for by simultaneous phase-phase coupling. This in turn indicates that low-gamma modulated PAC is likely to be driven by the sharpness of the low-gamma band waveform which is probably due to residuals of muscle activity (see supplemental analysis 1.1.). These results further justified our focus on beta-gamma PAC, which has previously been shown to be exaggerated in PD (de Hemptinne et al., 2013; Swann et al., 2015; Jackson et al., 2019; A. M. Miller et al., 2019).

3.1.2. PAC difference topography in aging demonstrates a left-hemisphere dominant pattern

To investigate the spatial pattern of PAC difference, we calculated the PAC values across all channels and performed comparisons (Wilcoxon rank sum test) between the two age groups using FDR-correction. Fig. 3A depicts the scalp topography of the difference between the two age groups. The comparison was conducted for the PAC values which were derived by averaging MI values over the beta range (13–30 Hz) for phase frequency and broadband gamma range (50–150 Hz) for amplitude frequency. Electrode labels are present only for the significant differences ($p < 0.05$, FDR corrected). The pattern has left-hemisphere dominant distribution over the centro-temporal areas and also extends to frontal areas. Moreover, we demonstrated the statistical PAC values using surrogate procedure are significant over sensorimotor areas within each group and the difference pattern based on the statistical PAC value are well overlapping with Fig. 3A obtained from raw PAC values (see details in Figure S7 in the supplemental material). At source space, we calculated the PAC value for each ROI and each subject (see Section 2.3.6.) and performed the comparison (Wilcoxon rank sum test) between groups (old vs. young) for all ROIs. Fig. 3B shows that PAC values are significantly increased in the elderly group. This result confirms the pattern which demonstrates left hemisphere dominance in PAC differences, with the most profound difference being localized in the left pre- and post-central gyri (extending to superior frontal and supramarginal gyri). Additionally, to rule out possible confounders which might contribute to age-related statistical PAC differences, we performed additional analyses on the power and non-sinusoidal waveform shape of beta oscillations (see supplemental analyses 1 and 2). These analyses confirmed further that the beta phase driven PAC difference between the two age groups is not likely to be driven by either beta band power or non-sinusoidality of beta waveform, although waveform

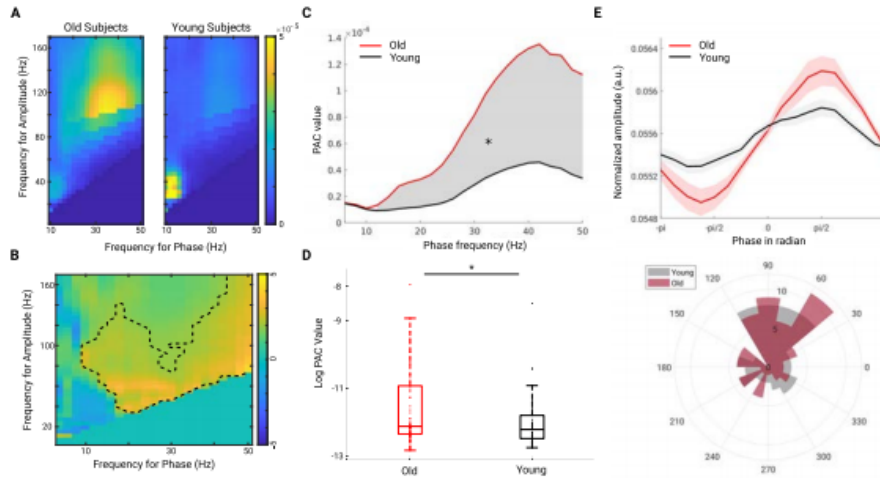


Fig. 2. PAC between beta, low-gamma band oscillations and broadband gamma activity is increased in the old compared to the young group at electrode C3. A. Mean comodulograms of modulation index across subjects in each group. Color bar indicates the PAC strength. B. The dashed black line shows the identified significant MI cluster of the difference-comodulogram (cluster-based permutation test, $p = 0.01$). Color bar represents the statistical value. C. Red and black lines show the mean of MI values across old and young subjects, respectively, within each phase-frequency window (estimated from broadband gamma amplitude frequency range (50–150 Hz)). Gray shaded areas show the phase frequencies which are coupled significantly stronger to the broadband gamma activity in elderly compared to young subjects. This is after FDR correction for multiple comparisons (across all the analyzed phase frequencies, $^*p < 0.05$). D. Boxplots of the averaged MI values over 13–30 Hz for beta phase and 50–150 Hz for broadband gamma amplitude for each age group. There is a significant difference between old and young groups (old vs. young) (two tailed Wilcoxon rank sum test, $^*p = 0.0147$) although one can also observe a considerable overlap between PAC values belonging to both groups. E. The upper panel shows the mean of the normalized broadband gamma amplitude according to the beta phase (from $-\pi$ to π). Red and black lines represent the mean of the normalized amplitude for the elderly and young group, respectively. Shaded areas indicate the standard error of the mean (SEM) across subjects within a group. Circular bar plot in the bottom shows the distribution of preferred beta phase at which the maximal coupling occurred across the subjects within the elderly (in red) and the young group (in gray). Beta phase predominantly distributed within $\pi/6 \sim 2^*\pi/3$ when the highest amplitude occurred for both age groups.

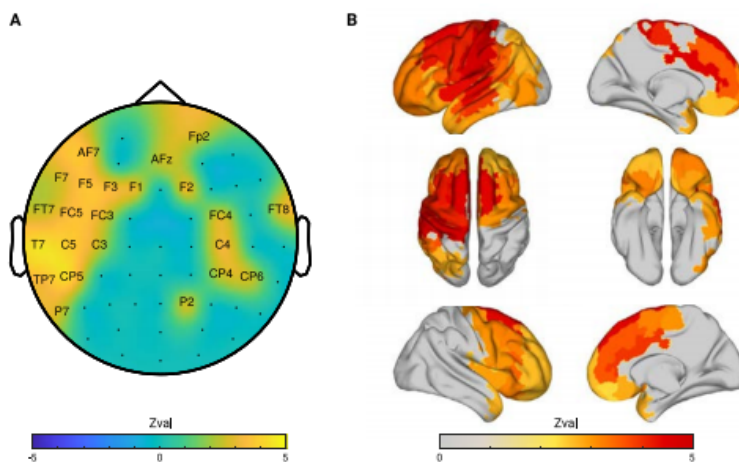


Fig. 3. Spatial topography of PAC difference between the two age groups (old vs. young). PAC values were calculated by averaging over beta range (13–30 Hz) for phase frequency and broadband gamma (50–150 Hz) range for amplitude frequency. A. Statistical comparisons (Wilcoxon rank sum test) were performed between the two age groups (old vs. young). The electrodes with labels show significant differences after FDR correction across all channels. B. Spatial difference pattern of PAC calculated in source space between the two age groups after FDR correction across ROIs. The topography demonstrated that the most significant difference occurred in the left precentral gyrus. Color bar indicates the test statistic. Positive values indicate stronger PAC values in the elderly group.

of the oscillation could represent another neural signatures characterizing aging (see supplemental discussion 1.).

3.1.3. Behavioral relevance of PAC shows differential pattern within two age groups

PAC has been shown to be associated closely to the severity of movement dysfunction in patients with PD. We were also interested to test

how PAC could relate to movement performance. However, in this open dataset, movement task was not specifically designed. Yet, to a certain degree a motor readiness can be assessed with the TAP-alertness task. This task measures cognitive alertness (alertness of Test of Attentional Performance, Zimmermann et al., 2012) which is an objective marker of the ability to maintain an alert state of response readiness, and it has been shown to decline with age (McAvinue et al., 2012). Here, the

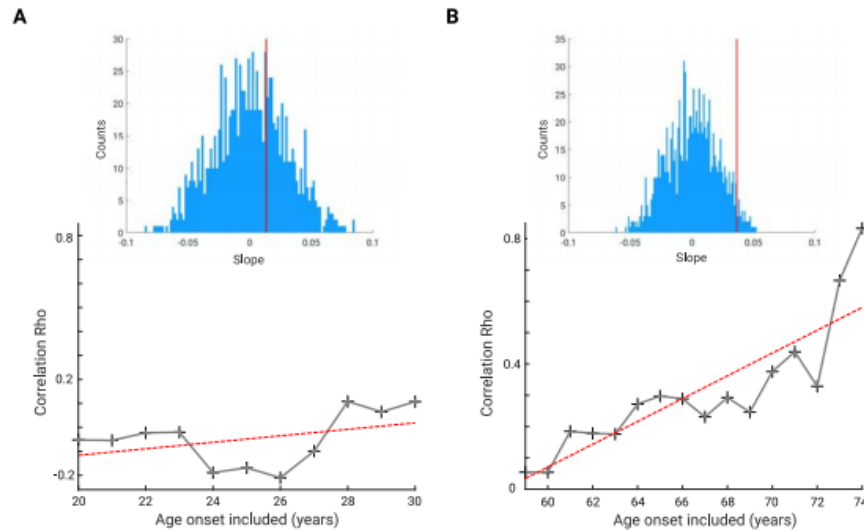


Fig. 4. Correlation between PAC and reaction time in subgroups with increasing age onset. **A.** Correlation between PAC and TAP-alertness reaction time in young group. X axis represents the age onset for which the subjects were included from for the subgroup. For instance, for the young subjects with age older than 26 (but still younger than 35), there is a negative but non-significant correlation between PAC and reaction time ($Rho = -0.2106$, $p = 0.2320$). The red dashed line shows the regression line for the correlation coefficients. The histogram shows the distribution of the slopes from permuted data (1000 times) while the vertical red line indicates the value where the observed actual slope (slope = 0.0135, $p = 0.3260$) is situated. **B.** The same analysis for the elderly group. There is a tendency for increasing correlation strengths with the age from which the subgroup starts. The red dashed line shows the regression line for the correlation coefficients within each subgroup while including older subjects from 59 years to 74 years old. The histogram shows the distribution of the slopes from randomized data (1000 times) while the vertical red line indicates where the regression slope obtained by the unpermuted data (slope = 0.0364, $p = 0.0320$) stands. P value is thus a fraction of slopes which are larger than the value corresponding to the red line.

mean reaction time for each subject was utilized to quantify the alertness where lower scores indicate better performance. To obtain a reliable measure of PAC from the sensorimotor areas for each subject, we took the mean of PAC values from left and right precentral gyri. First, we performed correlation analysis between PAC and the reaction time within each age group, and no significant results were observed either in the elderly group ($Rho = 0.0542$, $p = 0.6654$), or in the young group ($Rho = -0.0524$, $p = 0.6645$). We hypothesized that this might be due to the fact that the included elderly subjects were generally rather healthy (due to very strict exclusion criteria) and if we narrow down the aging group, the relationship probably would be more obvious. To test this hypothesis, we performed correlation analyses on the subgroups in which the inclusion criteria of age onset were increased stepwise, both for elderly and younger groups. In Fig. 4A, the strengths of correlations with increasing age onsets from 20 to 30 years in the young group are shown; all the correlations were not significant (sample size ≥ 7). Fig. 4B demonstrates the results of the same analysis for the elderly group (59 to 74 years old, sample size ≥ 8). We observed a trend for increased correlation strengths with increasing age.

To rule out the possibility that the observed tendency may result from a sub-sampling procedure itself (with age onset increasing, less samples are available), we further performed a permutation procedure to test the significance of the trend in correlation between PAC and reaction time in elderly participants. In brief, we randomized the elderly subjects and then performed all the steps as described above for the experimental data. Then, a linear regression line was fitted to the correlation coefficients and the slope of a linear regression was taken to build the null distribution. In total, the randomization was performed 1000 times, and a final p value was obtained for the observed regression slope compared to the null distribution obtained by permutations. As shown in the histograms of Fig. 4, the vertical red lines indicate the value of the

regression line for the younger group (slope = 0.0135, $p = 0.3260$) and the older group (slope = 0.0364, $p = 0.0320$), respectively. This demonstrates that the observed tendency to increase the positive association between PAC and reaction time occurred only for the group of elderly subjects while we controlled for the possible biasing effects associated with the sub-sampling procedure.

3.2. Properties of beta bursts are altered with aging

3.2.1. Aging is accompanied by a higher percentage of long burst events

Fig. 5A illustrates the change of relative percentage distribution of burst durations for two age groups with the 65th percentile threshold at representative channel CP3 (see Section 2.3.5.). Statistics (Wilcoxon rank sum test) showed that compared to the young group, elderly subjects showed a tendency for bursts with longer duration windows (0.2–0.5 s). The percentage of shorter beta bursts (0.1–0.2 s) was higher in young compared to elderly subjects ($*p = 0.0122$, after FDR). In contrast, across the nine burst duration windows, the percentage of relatively longer bursts in a given interval (0.2–0.3 s, 0.3–0.4 s, 0.4–0.5 s) was higher in the elderly group ($*p = 0.0132$, $*p = 0.0132$, $*p = 0.0184$, respectively, FDR corrected) compared to the young group. However, for the longer bursts lasting more than 0.5 s we did not observe any difference between the groups. Moreover, the relative number of the bursts in intervals (> 0.5 s) was much smaller compared to bursts lasting less than 0.5 s. These results showed that in the resting state EEG of the aged brain, beta rhythm commonly appears with a duration of around 2–6 cycles, with a few portions of bursts lasting ~ 10 cycles and rarely with a longer duration time (> 10 cycles). In order to investigate a spatial pattern of this effect, we categorized the windows into two categories, namely short windows (0.1–0.2 s) and long windows (0.2–0.5 s). Next, we compared the percentages of bursts with long windows

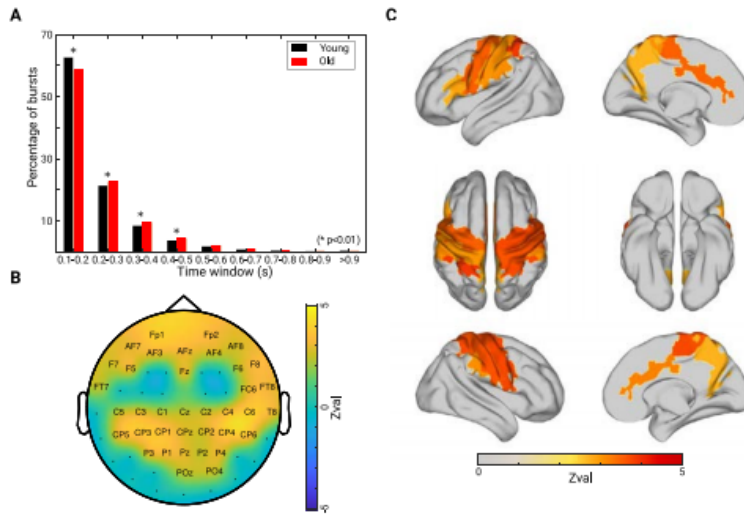


Fig. 5. Changes in burst duration distribution. A. The relative number of bursts in each bin is given as a percentage of the total number of bursts. The bar graph shows the mean of each age group across burst events with different bin duration at representative electrode CP3. For both groups, with increasing burst duration the percentage of bursts decreases. Elderly subjects had a lower percentage of short bursts (burst window: 0.1–0.2 s) ($p = 0.0122$, after FDR) and larger percentage of long bursts (burst window: 0.2–0.3, 0.3–0.4, 0.4–0.5 s) ($p = 0.0132, 0.0132, 0.0184$, respectively, after FDR) compared to young subjects. B. Scalp topography of differences (old vs. young) in percentages of long burst (0.2–0.5 s). Labeled electrodes are those showing significantly higher percentage of long bursts in elderly than in young subjects after FDR correction ($p < 0.05$). C. Spatial difference pattern in the percentage of long bursts (old vs. young) in source level. Positive values indicate larger values in the group with elderly subjects.

between the two groups for all channels. In Fig. 5B, we plotted the topographical pattern of the difference in relative number of beta bursts with long duration between two age groups. The cortical areas demonstrating strongest age-related beta burst differences are clustered over bilateral frontal and centro-parietal sites. Additionally, the analysis in source space further located the spatial difference pattern mostly in the bilateral sensorimotor cortices (Fig. 5C). To demonstrate how overall differences in burst duration and amplitude between two groups converge across various threshold percentiles for definition of beta burst event, we analyzed these two key parameters across a family of nine thresholds from the 50th to 90th percentiles (see supplemental analysis 3 and Figure S5). The analysis showed that generally the elderly subjects have longer beta burst events together with higher amplitude, regardless of the threshold definition. Additionally, we obtained similar results for this part of analysis with a different threshold for burst definition, i.e., 70th percentile (see Figure S8 in supplemental material).

3.2.2. Incidence rate of bursts with long duration is increased in elderly subjects

In addition, we investigated how often beta bursts occur with a given duration window. Burst incidence rate was calculated as the number of beta bursts per second. We compared the burst incidence rate for all windows across all channels. We found that there is no difference in incidence rate for shorter windows (0.1–0.2 s) between two groups, whereas for the longer windows (0.2–0.3 s, 0.3–0.4 s, 0.4–0.5 s) the incidence rates showed an increase in a region specific pattern in the elderly compared to the young group. The result for each window is shown in Fig. 6A. Specifically, for bursts with a duration 0.2–0.3 s, the frequency of bursts increased with most prominent changes occurring in fronto-central regions. The regions showing significant differences were more focally clustered for longer bursts (> 0.3 s). For the relatively longer 0.4–0.5 s window, the prominent difference was present in a small cluster of regions over centro-parietal sites. Furthermore, Fig. 6B shows a spatial difference pattern in source space. Burst incidence rate was averaged over all the bursts with long duration windows (0.2–0.5 s) and compared across all brain areas between the two groups (old vs. young). The pattern showed significant differences after FDR correction. With this analysis we further confirmed that the elderly subjects, compared to young subjects, were indeed characterized by more frequent long beta burst events, which occurred in multiple cortical regions but most

prominently in bilaterally pre- and post-central gyri. To show the distribution of the incidence of bursts for all channels and subjects in different groups regardless of window duration, we additionally obtained the mean burst incidence for each channel by averaging the burst incidence rate across the three above-mentioned windows, and then plotted a corresponding normalized histogram (see Fig. 6C). A trend was observed for the higher incidence rate in the elderly group in comparison to the young subjects.

3.3. Relationship between PAC and beta burst dynamics

Finally, to investigate whether PAC and bursts characteristics relate to the same neuro-physiological mechanism, we investigated a correlation between them topographically within each age group (PAC versus percentage of beta bursts with specific intervals showing the largest differences between the groups (short window of 0.1–0.2 s and mean of long windows of 0.2–0.5 s)), results are shown in Fig. 7. Spearman's correlations were performed for all channels and across all the subjects for young and old group, respectively. For the young group, there was no significant relationship between PAC and percentage of short bursts or long bursts. As shown in Fig. 7, the percentage of bursts with short (0.1–0.2 s, Fig. 7A) and long durations (0.2–0.5 s, Fig. 7B), were significantly related to PAC values only in a small cluster of electrodes primarily located in right frontal area in the elderly group. Specifically, PAC was positively correlated with the percentage of short bursts (Fig. 7A), and the opposite was observed for long bursts (Fig. 7B). Spatial correlation maps were distinct from those corresponding to PAC differences (Fig. 3) and beta burst differences (Fig. 5), thus suggesting that the PAC and beta bursts are likely to reflect distinct processes in healthy aging. In order to further localize the source of correlation map that we observed in sensor space, we performed correlation analysis similarly on metrics estimated from the signal reconstructed in the source space. Specifically, for each ROI, PAC and burst percentage (short and longer bursts) was estimated and then correlation analysis was performed across the subjects within the elderly group for all the ROIs. Before applying FDR correction, for the short bursts (0.1–0.2 s), strongest positive relations were observed in bilateral cingulate gyri, and left occipital pole. And analogously the strongest negative correlations were present in the bilateral cingulate gyri, left superior frontal gyrus and right insula cortex between longer burst (0.2–0.5 s) and PAC. After applying correction for multiple com-

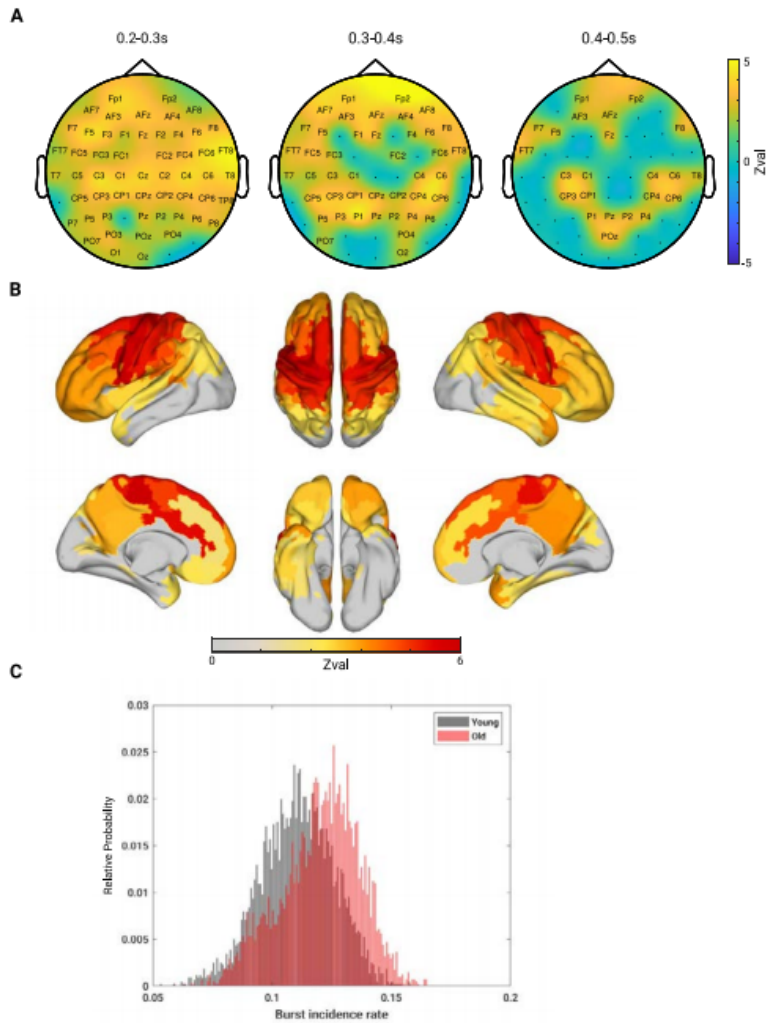


Fig. 6. Changes in incidence rate of longer duration windows (0.2–0.5 s) (old vs. young). A. Spatial topography of the difference in incidence rates of bursts with different durations. Electrodes with labels showed significant difference between the two groups (old vs. young) after FDR correction ($p < 0.05$). For bursts with a duration of 0.2–0.3 s, a significant increase was observed in many scalp sites but most prominently in fronto-central regions. For bursts with a duration between 0.4 and 0.5 s, the most prominent differences were found in centro-parietal areas. B. Spatial difference pattern (old vs. young) in burst incidence rate of long beta bursts (0.2–0.5 s) in source level. C. Normalized histogram of mean incidence rates of longer bursts (0.2–0.5 s) across all channels and subjects for the old (in red) and young (in black) group. Each count represents one channel from one subject. Color bar indicates the test statistic. Positive values indicate stronger bursting incidence in the elderly subjects.

parisons, none of the significance remained. The lack of significant relations between these two measures estimated in the source space may further support the idea that these two parameters might reflect different aspects of healthy aging.

4. Discussion

Despite previous clinical evidence in support of a close association between aging and PD, electrophysiological neuronal correlates of such an association have been rather elusive. Here, we showed that the electrophysiological biomarkers recently discovered for PD, are also present in apparently healthy elderly subjects. Specifically, we found the elevated PAC and more frequent beta bursts with longer duration being pronounced in the elderly group compared to the young one. Importantly, such differences were particularly manifested in sensorimotor areas. Furthermore, we found only a weak correlation between PAC

and beta bursts metrics, suggesting that these phenomena may reflect different aspects of healthy aging. Overall, our findings indicate that electrophysiological alterations detected in PD already exist in the apparently healthy aging brain and their further amplification may eventually manifest in clinical symptoms typically found in fully developed PD.

4.1. Topography of PAC changes in the healthy aging brain

PAC has been increasingly suggested to be a biomarker for pathology in PD, being a proxy for the locking of local spiking activity to beta oscillation within and across the basal ganglia-cortical network (De Hemptinne et al., 2015; Malekmohammadi et al., 2018; Swann et al., 2015; Weinberger et al., 2006). Although we were initially interested in testing the assumption that during apparently healthy aging an increase in PAC between beta band (13–30 Hz) and broadband gamma activity

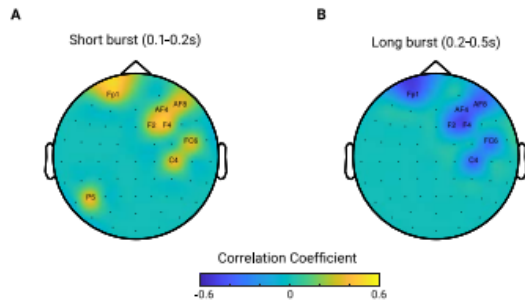


Fig. 7. Correlation maps between PAC values and percentage of burst with short and long durations. A. Correlation map between PAC and percentage of short bursts (0.1–0.2 s) within elderly group. B. Correlation between PAC values and long bursts (0.2–0.5 s) across all subjects within elderly group. The significance is indicated after applying FDR-correction across multiple comparisons for all the channels.

(50–150 Hz) could be observed over the sensorimotor cortex, as it has been repeatedly indicated in previous PD studies using ECoG or EEG (A. M. Miller et al., 2019; De Hemptinne et al., 2013; Jackson et al., 2019; Swann et al., 2015), we nonetheless investigated changes in PAC over the whole cortex. Given a premise that PAC in elderly subjects can resemble behavior of PAC in patients with PD, our results confirmed previous findings showing that PAC is primarily increased over the sensorimotor areas. This is in agreement with previous studies showing age-related alterations in cortical motor areas (Haug and Eggers, 1991; Ward and Frackowiak, 2003), as well as changes in the functioning of these areas (C. Clark and L. Taylor, 2012; Fathi et al., 2010; Heuninckx et al., 2005; Michely et al., 2018; Rowe et al., 2006). In addition, we also observed stronger differences over the left hemisphere. Such hemispheric asymmetry in PAC might relate to the stronger dopaminergic defect in the dominant compared to the non-dominant hemispheres defined by a subject's dominant hand, one of the major factors causing PD symptoms to emerge more often on the dominant hand-side (Shi et al., 2014). In our dataset, the majority of subjects are right-handed (129 out of 137).

Cortical broadband gamma is thought to reflect asynchronous spiking activity (K. J. Miller et al., 2009; Manning et al., 2009). Therefore, elevated coupling of beta and broadband gamma activity can represent a higher synchronization of local spiking activity to the phase of beta oscillation. Excessive PAC in the aging brain may reflect a physiological state in which the cortex is restricted to more rigid activity patterns, rendering it less able to respond dynamically to signals from higher order cortical regions. Such dynamic inflexibility is in line with previous studies, showing that aging is accompanied by decreased neuronal complexity estimated with fractal dimension using resting state measures of neuronal activity (Zappasodi et al., 2015). In addition, fMRI studies have also shown a lower level of spontaneous BOLD signal variability (another frequently used measure of neuronal complexity) in older subjects (Grady and Garrett, 2014; Kumral et al., 2020; Nomi et al., 2017).

4.2. Cortical beta bursts in the healthy aging brain

Beta oscillations are associated with prefrontal working memory (Lundqvist et al., 2011, 2018), stopping action and thought (Michelmann et al., 2016; Wessel and Aron, 2017), and most widely – to sensorimotor function (Baker, 2007; Espenhahn et al., 2019; Feingold et al., 2015; Gehringer et al., 2018; Pfurttscheller et al., 1996; Pollok et al., 2014). Age-related increase in beta band power over the bilateral sensorimotor cortices has been reported in previous studies

(Heinrichs-Graham and Wilson, 2016), consistent with that which we observed in our study (see supplemental analysis 1.2 and Figure S2). As beta power has been linked to the level of inhibitory GABAergic neural transmission, age related increase of beta power at baseline may suggest increased intracortical GABAergic inhibition (Rossiter et al., 2014).

Beta activity is characterized by short-lived burst events (Feingold et al., 2015; Murthy and Fetz, 1992; Sherman et al., 2016), instead of a continuous oscillatory pattern. Importantly, beta bursts have been investigated in the STN in PD studies which showed longer burst duration and increase of incidence rate in OFF compared to ON levodopa state (Tinkhauser et al., 2017b). Moreover, movement-associated reduced incidence rate and amplitude of bursts contributed to the pathological decrease of movement velocity (Lofredi et al., 2019) in PD patients. These distinct functional roles of transient beta events indicate the importance of episodic nature of beta bursts in flexible coordination of responses in tasks. In our study we extended previous findings to spontaneous resting state brain activity measured from scalp EEG, confirming the transient nature of cortical beta events. Furthermore, we demonstrated an age-related increase in the duration and occurrence of beta bursts in a region-specific pattern. Such re-distribution of burst duration to longer windows together with an increased occurrence of longer bursts may compromise the flexible coordination of brain dynamics, especially in motor processing, reflected in a central motor clustered spatial pattern.

The mechanistic origin of neocortical beta burst events was investigated in detail in the work of (Sherman et al., 2016). Their simulation results have shown that beta events could emerge from nearly synchronous bursts of excitatory synaptic drive targeting proximal and distal dendrites of pyramidal neurons in the cortex. Additionally, they suggested that the ventral medial/pallidal thalamus was particularly well suited for this distal drive. Importantly, the ventromedial (VM)/pallidal thalamus project dominantly and diffusely to the supragranular layers in the sensory and motor cortex as well as the prefrontal cortex, which is quite consistent with the spatial distribution in beta burst duration changes observed in our study (see Fig. 5B). This might lead to the assumption that thalamo-cortical loops of motor related pathway are a fundamental component in generation and age-related alteration in cortical beta burst dynamics. More frequent and longer beta bursts are probably due to the increased drive from the thalamus, which has been shown to be affected by age through complex changes in macrostructure, microstructure and neural connectivity (Fama and Sullivan, 2015). Meanwhile, cortical beta bursts could also be generated independently in the STN-GPe (external globus pallidus) network within the basal ganglia (Kumar et al., 2011) and propagate via thalamo-cortical loops to the cortex (McFarland and Haber, 2002).

In fact, a very recent study revealed a possible mechanism of propagation of beta bursts within the cortical-basal ganglia circuit in PD (Cagnan et al., 2019). The authors showed an association between cortical and basal ganglia beta bursts, when especially longer cortical beta bursts were associated with longer periods of increased beta amplitude in GPe following the burst onset. This is in line with a previous study showing that cortical beta changes preceded changes in sub-cortical regions, suggesting an important role for cortical feedback in maintaining pathological basal ganglia oscillations (De Hemptinne et al., 2013). Additionally, it has also been reported that the effective STN-DBS treatment not only modulates the local STN beta oscillations, but also attenuates the coherence between motor cortices and the STN (Oswal et al., 2016). These findings suggest that pathological coupling across nodes (cortical and sub-cortical) in the basal ganglia-thalamo-cortical (BGTC) network might play an important role in motor function impairment. Moreover, in the present study, we showed that cortical sensorimotor beta dynamics were also modulated due to physiological aging. This in turn indicates that cortical beta dynamics might serve as a proxy for the coordination of structures within the motor related network and underlying physiological and pathological changes.

4.3. Relationship between different measures of PAC and beta burst in healthy aging

Both PAC and beta bursts in the STN have previously been linked to symptom severity in PD. Dopamine replacement in PD patients suppresses both burst length (Cagnan et al., 2015; Tinkhauser et al., 2017b) and PAC (López-Azcárate et al., 2010; van Wijk et al., 2016). However, how these two different phenomena relate to each other remains rather elusive. To our best knowledge, one recent paper studied PAC during periods of beta bursting using macro and micro electrode recordings in the STN in PD patients (Meidahl et al., 2019). The authors provide converging evidence demonstrating that the coupling of spiking to the network beta oscillations is significantly higher during beta bursts and increases progressively with beta burst duration. Therefore, the authors suggested that PAC and beta bursts might reflect similar neurophysiology due to excessive synchronization. More recently, one study using ECoG at M1 demonstrated PAC was more pronounced during periods of beta burst than non-bursts in PD, but without showing significant difference between PD and non-PD groups during bursts (O’Keefe et al., 2020). In our resting EEG study, we also showed significantly elevated PAC and prolonged beta bursts with more frequent occurrence in healthy elderly compared to young subjects. We acknowledge that higher PAC is very likely to occur during episodes of beta bursts since a higher signal-to-noise ratio may play a critical role, which is, nevertheless, challenging to disentangle. However, by investigating an association between PAC and beta bursts features within each age group in a topographical manner with multichannel EEG, we found no spatial overlap between them, except for the focally distributing right frontal region (AF4, AF8, F2, F4) and several other isolated channels in the elderly group. In addition, by localizing the signal in the source space none of the cortical regions showed a significant correlation. We therefore suggest that in healthy aging, at the level of cortex PAC and beta burst dynamics may reflect rather different neurophysiological processes.

4.4. PD: accelerated aging phenomenon?

Aging and PD related brain alterations share similarities (G. Levy, 2007; Pang et al., 2019; Reeve et al., 2014). They can be manifested at the level of cellular mechanisms where dopamine cellular risk factors accumulate with age in a pattern which mimics the pattern of dopamine degeneration in PD based on the evidence from studies of non-human primates (Collier et al., 2011). Moreover, the evidence from midbrain dopamine neurons of aging non-human primates further supported the view that age-related changes in the dopamine system approach the biological threshold for parkinsonism (Collier et al., 2017).

Zeighami et al. (2019) used a data driven approach to investigate anatomical brain signatures of PD. In their first identified latent variable, age was the strongest contributor to brain atrophy. Further, in a longitudinal study, they showed that both healthy aging and PD were associated with cortical thinning over a one-year period, but with a more prominent alteration in PD patients than in healthy controls (Yau et al., 2018). This again demonstrates a similar directionality of alteration in aging and PD in terms of cortical anatomy. Age remains the largest risk factor for many diseases and in our study we showed that it can also be associated with electrophysiological biomarkers of PD. Importantly, our results demonstrated that not in all elderly subjects we observed increased PAC and longer beta bursts, which in turn indicates that other factors such as genes, life style, environment and other factors shape the corresponding neuronal processes and account for the individual variations.

Further, to address to what degree our estimated effects in healthy aging relate to the previously reported PD biomarkers, we compared them in rather a qualitative manner since factors such as the recording setup, data length and signal-processing steps could result in a different scale of the estimated metrics. With respect to the spectral and spatial overlap of PAC in healthy aging and PD, we refer here to

three previous studies in PD in which spatial distributions were provided offering a chance to have a general comparison. In the studies by Swann et al. (2015) and A. M. Miller et al. (2019), one could see a prominent PAC region over beta and further lower gamma phase frequency ranges (their Fig. 2A) and a slightly prominent cluster region over beta phase frequency (their Fig. 2A) in the PD Off-medication group, respectively. In a very recent paper, the authors also showed a pronounced PAC pattern over beta phase frequency in patients with PD compared to healthy controls (see their Fig. 2B) (Gong et al., 2021). However, since in all these studies there was no cluster-based permutation test or demonstration to which phase frequency the amplitude from broadband gamma was phase locked to, we may only draw the conclusion that the beta band phase modulating PAC in the current study, to a large extent, overlaps with the frequency range presented in previous studies. Regarding the spatial distribution, from the Fig. 5B from the first study (Swann et al., 2015) and Fig. 3B from the second one (A. M. Miller et al., 2019), together with what has been observed in the current study (Fig. 3A), one can see that the left central regions are consistently found in all three studies. In addition, in the study Gong et al. (2021) the authors averaged the data from the two hemispheres and the area with the largest differences was localized mainly in the sensorimotor region (premotor cortex (PMC) and primary motor cortex (M1)). Comparing the beta burst properties to that in the study by Tinkhauser et al. (2017b), we found that although in healthy aging a relatively larger percentage of longer bursts was observed, there was no difference in terms of the very long bursts, for instance bursts longer than 0.5 s. The other difference is that in the LFP of STN in PD during off medication, the percentage of bursts longer than 900 ms is abnormally high. The mean of the burst duration in PD off medication is thus higher than what we observed in healthy aging subjects and after the medication the mean duration dropped to less than 0.3 s which is comparable to the results from the healthy elderly participants in our study. In a recently published study using ECoG over motor cortices, the authors showed that in the motor cortex of patients with PD, a relative increase of beta burst duration was demonstrated in comparison to the patients with essential tremor (O’Keefe et al., 2020). Comparing our results to their Fig. 2B, we note that the mean duration of beta bursts in PD (around 0.2 s) is indeed more comparable to that from healthy elderly in the current study. Importantly, our findings regarding the burst features were well localized in the bilateral motor cortices (pre- and post- central gyri, see Fig. 5C and Fig. 6B). In conclusion, PAC features obtained in the present study largely overlap in frequency and spatial content in both aging and PD processes. Moreover, the effect of beta burst dynamics in healthy aging shows the same direction with that of PD during off state compared to the state after effective therapy (DBS or medication) or to the patients with essential tremor (instead of comparing to healthy controls), and it is commonly reported in the cortical motor region.

4.5. Potential non-invasive electrophysiological biomarker for detection of parkinsonian state

Early diagnosis of potential PD development is crucial for effective clinical intervention. Here, we provide evidence that the altered PAC and beta bursts are associated with aging in a manner similar to PD. Moreover, we conducted a correlation analysis between PAC and beta bursts across the whole scalp and cortical areas, and did not find a strong relationship between them. Therefore, we suggest that a combination of these two different metrics may lead to a more comprehensive estimation of age-related changes in the brain potentially culminating in the development of clinical symptoms typical for PD.

We have linked apparently healthy aging and PD by investigating electrophysiological signatures in a cross-sectional way. These non-invasive metrics might be helpful in estimating a proximity of neuronal dynamics relating to parkinsonian state. A recent study examined changes in cortical PAC in a progressive model of parkinsonism (Devergnas et al., 2019). Although the authors reported that cortical

PAC only reached significance when the animals became fully parkinsonian, their results showed a trend towards increased PAC in parallel with the development of parkinsonism. In the present study, although we did not find differences in TAP reaction times in elderly participants with high and low PAC values, a future prospective study may identify that participants with particularly strong PAC are more likely to develop parkinsonian symptoms. In this study, we observed in the elderly group, that there was a trend of increasing correspondence between PAC and age-related behavioral reaction times. Importantly, this relationship was not present in the young group. This may provide a hint regarding the functional relevance of the PAC increase in healthy aging, which might be related to a reduced readiness of the motor system to be engaged in the production of movements. Although we regard this as an interesting finding, we refrain from drawing a strong conclusion from it since these behavioral data are not a straightforward measure of movement performance.

Clearly, an objective set of criteria is needed to define a threshold for normal or abnormal brain aging. For this purpose, we suggest that longitudinal studies in which motor performance is specifically measured to be an indicative of potential parkinsonian state, measuring EEG over a long period, for instance 5–20 years, starting already in the middle age could provide additional information on the progression of PAC and beta burst dynamics in relation to possible development of parkinsonian symptoms. By combining both approaches, we may better identify a turning-point indicating a disruption of apparently healthy aging course, potentially relating to pathological aging process. Finally, applying interventions, such as medication or early non-invasive brain stimulation during sleep (Romanella et al., 2020), before healthy aging switches to a pathological trajectory might slow down or even restore pathological neural alterations relating to the development of PD.

5. Limitations

The first limitation of the study is that it was not based on the direct comparison of the EEG parameters obtained in cohorts of patients with PD and healthy subjects with aging. Besides, a comparison to the previous literature quantitatively is difficult since those studies have different settings such as cap electrodes density, postural condition, recording time length etc. Yet our main idea related to the effect of aging on EEG characteristics typically associated with PD. Certainly for further applicability of our findings to PD, patients should be recruited.

Furthermore, although we have performed a careful cleaning of the data based on ICA and removal of noisy segment via visual inspection, some residual artifacts might still be present. This is especially relevant for high gamma activity which lies in the frequency range of artifactual muscle activity. However, our source analysis has shown that the main differences in PAC between two groups of participants were over sensorimotor areas rather than over the temporal areas where one would expect the largest contribution from scalp muscles. Additionally, we provide further extensive discussion on the relevance of muscle activity for PAC effect (see supplemental discussion 2.). We would also like to note that due to the limitations of non-invasive recordings, we can't rule out completely the effect of residual muscle activity on the generation of PAC. Future studies, utilizing direct invasive measurement of cortical activity, should be more informative about such influence.

In our study, we applied standard head modeling and ROIs based analysis in the source space. More precise estimates could be obtained if the analysis is performed with individual head models. Yet, in our study we used a relatively large number of ROIs which at least partially negates a lack of spatial accuracy.

Conclusion

In this study, using resting state EEG, we found that apparently healthy aging is associated with the cortical neuronal signatures resembling those typically found in patients with PD. The differences in PAC

and in the burst characteristics of beta oscillations between elderly and young subjects exhibited distinct spatial patterns with a considerable presence over sensorimotor areas of the cortex. Aging related changes in PAC and beta burst dynamics share the directionality with that characterizing PD. Such a similarity may suggest that the electrophysiological signatures typically found in PD might already be detectable in the apparently healthy aging brain. Consequently we assume that further exaggeration of such neuronal changes may eventually result in the development of motor abnormalities typical for PD. Furthermore, once established and validated in other studies, the investigated metrics may have potential to serve as the biomarkers for the early detection of the gradually developing neuronal changes characterizing pre-parkinsonian state. Finally, our findings highlight the importance of adequate control for aging effects in PD studies via the inclusion of both patients and healthy controls.

Acknowledgments

We are grateful to Ruxue Gong for discussions on the data analysis. This work was supported in part by Deutsche Forschungsgemeinschaft (German Research Foundation) (Project ID: 424778381 TRR 295). JZ was supported by China Scholarship Council (CSC). VVN was supported in part by the Basic Research Program at the National Research University Higher School of Economics.

Data and code availability statement

EEG data are from a public dataset which was acquired by Babayan et al. (2019). The codes used for some key data analyses are publicly available via GitHub: <https://github.com/JuanliZhang/PAC>.

Supplementary materials

Supplementary material associated with this article can be found, in the online version, at doi:10.1016/j.neuroimage.2021.118512.

References

- Babayan, A., Erbey, M., Kumral, D., Reinelt, J.D., Reiter, A.M.F., Röbbig, J., Lina Schaare, H., Uhlig, M., Anwander, A., Bazin, P.L., Horstmann, A., Lampe, L., Nikulin, V.V., Okon-Singer, H., Preusser, S., Pampel, A., Rohr, C.S., Sacher, J., Thöne-Otto, A., ..., Villringer, A., 2019. Data descriptor: a mind-brain-body dataset of MRI, EEG, cognition, emotion, and peripheral physiology in young and old adults. *Sci. Data* 6, 1–21. doi:10.1038/sdata.2018.308.
- Baker, S.N., 2007. Oscillatory interactions between sensorimotor cortex and the periphery. *Curr. Opin. Neurobiol.* 17 (6), 649–655. doi:10.1016/j.conb.2008.01.007.
- Brittain, J.S., Sharott, A., Brown, P., 2014. The highs and lows of beta activity in cortico-basal ganglia loops. *Eur. J. Neurosci.* 39 (11), 1951–1959. doi:10.1111/ejn.12574.
- Brown, P., 2003. Oscillatory nature of human basal ganglia activity: relationship to the pathophysiology of parkinson's disease. *Mov. Disord.* 18 (4), 357–363. doi:10.1002/mds.10358.
- Clark, C., B., Taylor, L., J., 2012. Age-related changes in motor cortical properties and voluntary activation of skeletal muscle. *Curr. Aging Sci.* 4 (3), 192–199. doi:10.2174/1874609811104030192.
- Cagman, H., Duff, E.P., Brown, P., 2015. The relative phases of basal ganglia activities dynamically shape effective connectivity in Parkinson's disease. *Brain* 138 (6), 1667–1678. doi:10.1093/brain/awv093.
- Cagman, H., Mallet, N., Moll, C.K.E., Gulberti, A., Holt, A.B., Westphal, M., Gerloff, C., Engel, A.K., Hamel, W., Magill, P.J., Brown, P., Sharott, A., 2019. Temporal evolution of beta bursts in the parkinsonian cortical and basal ganglia network. *PNAS* 116 (32), 16095–16104. doi:10.1073/pnas.1819975116.
- Chen, C.C., Hsu, Y.T., Chan, H.L., Chiou, S.M., Tu, P.H., Lee, S.T., Tsai, C.H., Lu, C.S., Brown, P., 2010. Complexity of subthalamic 13–35Hz oscillatory activity directly correlates with clinical impairment in patients with Parkinson's disease. *Exp. Neurol.* 224 (1), 234–240. doi:10.1016/j.expneurol.2010.03.015.
- Cheng, H.C., Ulane, C.M., Burke, R.E., 2010. Clinical progression in Parkinson disease and the neurobiology of axons. *Ann. Neurol.* 67 (6), 715–725. doi:10.1002/ana.21995.
- Cole, S.R., van der Meij, R., Peterson, E.J., de Hemptinne, C., Starr, P.A., Voytek, B., 2017. Nonsinusoidal beta oscillations reflect cortical pathophysiology in parkinson's disease. *J. Neurosci.* 37 (18), 4830–4840. doi:10.1523/JNEUROSCI.2208-16.2017.
- Collier, T.J., Kanaan, N.M., Kordower, J.H., 2011. Ageing as a primary risk factor for Parkinson's disease: evidence from studies of non-human primates. *Nat. Rev. Neurosci.* 12 (6), 359–366. doi:10.1038/nrn3039.
- Collier, T.J., Kanaan, N.M., Kordower, J.H., 2017. Aging and Parkinson's disease: different sides of the same coin? *Mov. Disord.* 32 (7), 983–990. doi:10.1002/mds.27037.

- Crowell, A.L., Ryapolova-Webb, E.S., Ostrem, J.L., Galifianakis, N.B., Shimamoto, S., Lim, D.A., Starr, P.A., 2012. Oscillations in sensorimotor cortex in movement disorders: an electrocorticography study. *Brain* 135 (2), 615–630. doi:10.1093/brain/awr332.
- Darden, L., 2007. Mechanisms and models. *Cambridge Companion Philos. Biol.* 39, 139–159. doi:10.1017/CCOL9780521851282.008.
- De Hemptinne, C., Ryapolova-Webb, E.S., Air, E.L., Garcia, P.A., Miller, K.J., Ojemann, J.G., Ostrem, J.L., Galifianakis, N.B., Starr, P.A., 2013. Exaggerated phase-amplitude coupling in the primary motor cortex in Parkinson disease. *PNAS* 110 (12), 4780–4785. doi:10.1073/pnas.1214546110.
- De Hemptinne, C., Swann, N.C., Ostrem, J.L., Ryapolova-Webb, E.S., Luciano, S.M., Galifianakis, N.B., Starr, P.A., 2015. Therapeutic deep brain stimulation reduces cortical phase-amplitude coupling in Parkinson's disease. *Nat. Neurosci.* 18 (5), 779–786. doi:10.1038/nn.3997.
- Delorme, A., Makeig, S., 2004. EEGLAB: an open source toolbox for analysis of single-trial EEG dynamics including independent component analysis. *J. Neurosci. Methods* 134 (1), 9–21. doi:10.1016/j.jneumeth.2003.10.009.
- Desikan, R.S., Ségonne, F., Fischl, B., Quinn, B.T., Dickerson, B.C., Blacker, D., Buckner, R.L., Dale, A.M., Maguire, R.P., Hyman, B.T., Albert, M.S., Killiany, R.J., 2006. An automated labeling system for subdividing the human cerebral cortex on MRI scans into gyral based regions of interest. *Neuroimage* 31 (3), 968–980. doi:10.1016/j.neuroimage.2006.01.021.
- Devergnas, A., Caiola, M., Pittard, D., Wichmann, T., 2019. Cortical phase-amplitude coupling in a progressive model of Parkinsonism in nonhuman primates. *Cereb. Cortex* 29 (1), 167–177. doi:10.1093/cercor/bhx314.
- Espenhahn, S., van Wijk, B.C.M., Rosster, H.E., de Berker, A.O., Redman, N.D., Rondina, J., Diedrichsen, J., Ward, N.S., 2019. Cortical beta oscillations are associated with motor performance following visuomotor learning. *Neuroimage* 195 (February), 340–353. doi:10.1016/j.neuroimage.2019.03.079.
- Eusebio, A., Thevathasan, W., Doyle Gaynor, L., Pogosyan, A., Bye, E., Folyntic, T., Zrinzo, L., Ashkan, K., Aziz, T., Brown, P., 2011. Deep brain stimulation can suppress pathological synchronisation in parkinsonian patients. *J. Neurol., Neurosurg. Psychiatry* 82 (5), 569–573. doi:10.1136/jnnp.2010.217489.
- Eusebio, Alexandre, Brown, P., 2009. Synchronisation in the beta frequency-band - the bad boy of Parkinsonism or an innocent bystander? *Exp. Neurol.* 217 (1), 1–3. doi:10.1016/j.expneurol.2009.02.003.
- Fama, R., Sullivan, E.V., 2015. Thalamic structures and associated cognitive functions: relations with age and aging. *Neurosci. Biobehav. Rev.* 54, 29–37. doi:10.1016/j.neubiorev.2015.03.008.
- Fathi, D., Ueki, Y., Mima, T., Koganemaru, S., Nagamine, T., Tawfik, A., Fukuyama, H., 2010. Effects of aging on the human motor cortical plasticity studied by paired associative stimulation. *Clin. Neurophysiol.* 121 (1), 90–93. doi:10.1016/j.clinph.2009.07.048.
- Feingold, J., Gibson, D.J., Depasquale, B., Graybiel, A.M., 2015. Bursts of beta oscillation differentiate post performance activity in the striatum and motor cortex of monkeys performing movement tasks. *PNAS* 112 (44), 13687–13692. doi:10.1073/pnas.1517629112.
- Gehring, J.E., Arpin, D.J., Heinrichs-Graham, E., Wilson, T.W., Kurz, M.J., 2018. Neurophysiological changes in the visuomotor network after practicing a motor task. *J. Neurophysiol.* 120 (1), 239–249. doi:10.1152/jn.00020.2018.
- Gong, R., Wumpschneider, M., Mühlberg, C., Gast, R., Fricke, J.J., Nikulin, V.V., Knösche, T.R., Classen, J., 2021. Spatiotemporal features of β - γ phase-amplitude coupling in Parkinson's disease derived from scalp EEG. *Brain : J. Neurol.* 144 (2), 487–503. doi:10.1093/brain/awaa400.
- Grady, C.L., Garrett, D.D., 2014. Understanding variability in the BOLD signal and why it matters for aging. *Brain Imaging Behav.* 8 (2), 274–283. doi:10.1007/s11682-013-9253-0.
- Hammond, C., Bergman, H., Brown, P., 2007. Pathological synchronization in Parkinson's disease: networks, models and treatments. *Trends Neurosci.* 30 (7), 357–364. doi:10.1016/j.tins.2007.05.004.
- Haufe, S., Ewald, A., 2016. A Simulation Framework for Benchmarking EEG-Based Brain Connectivity Estimation Methodologies. *Brain Topography*.
- Haug, H., Eggers, R., 1991. Morphometry of the human cortex cerebri and corpus striatum during aging. *Neurobiol. Aging* 12 (4), 336–338. doi:10.1016/0197-4580(91)90013-A.
- Heinrichs-Graham, E., Wilson, T.W., 2016. Is an absolute level of cortical beta suppression required for proper movement? Magnetoencephalographic evidence from healthy aging. *Neuroimage* 134, 514–521. doi:10.1016/j.neuroimage.2016.04.032.
- Heuninckx, S., Wenderoth, N., Debaere, F., Peeters, R., Swinnen, S.P., 2005. Neural basis of aging: the penetration of cognition into action control. *J. Neurosci.* 25 (29), 6787–6796. doi:10.1523/JNEUROSCI.1263-05.2005.
- Hindle, J.V., 2010. Ageing, neurodegeneration and Parkinson's disease. *Age Ageing* 39 (2), 156–161. doi:10.1093/ageing/afp223.
- Huang, Y., Parra, L.C., Haufe, S., 2016. The New York Head—a precise standardized volume conductor model for EEG source localization and tES targeting. *Neuroimage* 140, 150–162. doi:10.1016/j.neuroimage.2015.12.019.
- Jackson, N., Cole, S.R., Voytek, B., Swann, N.C., 2019. Characteristics of waveform shape in Parkinson's disease detected with scalp electroencephalography. *ENeuro* 6 (3), 1–11. doi:10.1523/ENEURO.0151-19.2019.
- Kim, S., Myers, L., Wyckoff, J., Cherry, K.E., Jazwinski, S.M., 2017. The frailty index outperforms DNA methylation age and its derivatives as an indicator of biological age. *Geroscience* 39 (1), 83–92. doi:10.1007/s11357-017-9960-3.
- Kramer, M.A., Tort, A.B.L., Kopell, N.J., 2008. Sharp edge artifacts and spurious coupling in EEG frequency comodulation measures. *J. Neurosci. Methods* 170 (2), 352–357. doi:10.1016/j.jneumeth.2008.01.020.
- Kühn, A.A., Tsui, A., Aziz, T., Ray, N., Brücke, C., Kupsch, A., Schneider, G.H., Brown, P., 2009. Pathological synchronisation in the subthalamic nucleus of patients with Parkinson's disease relates to both bradykinesia and rigidity. *Exp. Neurol.* 215 (2), 380–387. doi:10.1016/j.expneurol.2008.11.008.
- Kumar, A., Cardanobile, S., Rotter, S., Aertsen, A., 2011. The role of inhibition in generating and controlling Parkinson's disease oscillations in the basal ganglia. *Front. Syst. Neurosci.* 5 (OCTOBER 2011), 1–14. doi:10.3389/fnsys.2011.00086.
- Kumral, D., Şansal, F., Cesnaite, E., Mahjoory, K., Al, E., Gaebler, M., Nikulin, V.V., Villringer, A., 2020. BOLD and EEG signal variability at rest differently relate to aging in the human brain. *Neuroimage* 207. doi:10.1016/j.neuroimage.2019.116373.
- Levy, G., 2007. The relationship of Parkinson disease with aging. *Arch. Neurol.* 64 (9), 1242–1246. doi:10.1001/archneur.64.9.1242.
- Levy, R., Hutchison, W.D., Lozano, A.M., Dostrovsky, J.O., 2002. Synchronized neuronal discharge in the basal ganglia of Parkinsonian patients is limited to oscillatory activity. *J. Neurosci.* 22 (7), 2855–2861. doi:10.1523/jneurosci.22-07-02855.2002.
- Little, S., Brown, P., 2014. The functional role of beta oscillations in Parkinson's disease. *Parkinson. Relat. Disord.* 20 (SUPPL.1), S44–S48. doi:10.1016/S1353-8020(13)70013-0.
- Lofredi, R., Tan, H., Neumann, W.J., Yeh, C.H., Schneider, G.H., Kühn, A.A., Brown, P., 2019. Beta bursts during continuous movements accompany the velocity decrease in Parkinson's disease patients. *Neurobiol. Dis.* 127 (March), 462–471. doi:10.1016/j.nbd.2019.03.013.
- López-Azcárate, J., Tainta, M., Rodríguez-Oroz, M.C., Valencia, M., González, R., Gurruti, J., Iriarte, J., Obeso, J.A., Artieda, J., Alegre, M., 2010. Coupling between beta and high-frequency activity in the human subthalamic nucleus may be a pathophysiological mechanism in Parkinson's disease. *J. Neurosci.* 30 (19), 6667–6677. doi:10.1523/JNEUROSCI.5459-09.2010.
- Louis, E.D., Bennett, D.A., 2007. Mild Parkinsonian signs: an overview of an emerging concept. *Mov. Disord.* 22 (12), 1681–1688. doi:10.1002/mds.21433.
- Lundqvist, M., Herman, P., Lansner, A., 2011. Theta and gamma power increases and alpha/beta power decreases with memory load in an attractor network model. *J. Cogn. Neurosci.* 23 (10), 3008–3020. doi:10.1162/jocn.2010.00029.
- Lundqvist, M., Herman, P., Warden, M.R., Brincat, S.L., Miller, E.K., 2018. Gamma and beta bursts during working memory readout suggest roles in its volitional control. *Nat. Commun.* 9 (1), 1–12. doi:10.1038/s41467-017-02791-8.
- Malekmohammadi, M., AuYong, N., Ricks-Oddie, J., Bordelon, Y., Pouratian, N., 2018. Pallidal deep brain stimulation modulates excessive cortical high β phase amplitude coupling in Parkinson disease. *Brain Stimul.* 11 (3), 607–617. doi:10.1016/j.brs.2018.01.028.
- Manning, J.R., Jacobs, J., Fried, I., Kahana, M.J., 2009. Broadband shifts in local field potential power spectra are correlated with single-neuron spiking in humans. *J. Neurosci.* 29 (43), 13613–13620. doi:10.1523/JNEUROSCI.2041-09.2009.
- Marsili, L., Rizzo, G., Colosimo, C., 2018. Diagnostic criteria for Parkinson's disease: from James Parkinson to the concept of prodromal disease. *Front. Neurol.* 9 (MAR), 1–10. doi:10.3389/fneur.2018.00156.
- McAvinue, L.P., Habekost, T., Johnson, K.A., Kyllingsbæk, S., Vangkilde, S., Bundesen, C., Robertson, I.H., 2012. Sustained attention, attentional selectivity, and attentional capacity across the lifespan. *Attention, Percept. Psychophys.* 74 (8), 1570–1582. doi:10.3758/s13414-012-0352-6.
- McFarland, N.R., Haber, S.N., 2002. Thalamic relay nuclei of the basal ganglia form both reciprocal and nonreciprocal cortical connections, linking multiple frontal cortical areas. *J. Neurosci.* 22 (18), 8117–8132. doi:10.1523/jneurosci.22-18-08117.2002.
- Meidahl, A.C., Moll, C.K.E., van Wijk, B.C.M., Gulberti, A., Tinkhauer, G., Westphal, M., Engel, A.K., Hamel, W., Brown, P., Sharott, A., 2019. Synchronised spiking activity underlies phase amplitude coupling in the subthalamic nucleus of Parkinson's disease patients. *Neurobiol. Dis.* 127, 101–113. doi:10.1016/j.nbd.2019.02.005.
- Melgari, J.M., Curcio, G., Mastroianni, F., Salomone, G., Trotta, L., Tombini, M., Biase, L.D., Scarscia, F., Fini, R., Fabrizio, E., Rossini, P.M., Vernieri, F., 2014. Alpha and beta EEG power reflects L-dopa acute administration in parkinsonian patients. *Front. Aging Neurosci.* 6 (OCT), 1–7. doi:10.3389/fnagi.2014.00302.
- Michelmann, S., Bowman, H., Hanslmayr, S., 2016. The temporal signature of memories: identification of a general mechanism for dynamic memory replay in humans. *PLoS Biol.* 14 (8), 1–27. doi:10.1371/journal.pbio.1002528.
- Michely, J., Volz, L.J., Hoffstaedter, F., Tittgemeyer, M., Eickhoff, S.B., Fink, G.R., Grekes, C., 2018. Network connectivity of motor control in the ageing brain. *Neuroimage: Clin.* 18 (February), 443–455. doi:10.1016/j.nicl.2018.02.001.
- Miller, A.M., Miciocovic, S., Swann, N.C., Rajagopalan, S.S., Daresky, D.M., Gilron, R., de Hemptinne, C., Ostrem, J.L., Starr, P.A., 2019. Effect of levodopa on electroencephalographic biomarkers of the parkinsonian state. *J. Neurophysiol.* 122 (1), 290–299. doi:10.1152/jn.00141.2019.
- Miller, K.J., Sorensen, L.B., Ojemann, J.G., Den Nijs, M., 2009. Power-law scaling in the brain surface electric potential. *PLoS Comput. Biol.* 5 (12), doi:10.1371/journal.pcbi.1000609.
- Müller, E.J., Robinson, P.A., 2018. Suppression of parkinsonian beta oscillations by deep brain stimulation: determination of effective protocols. *Front. Comput. Neurosci.* 12 (December), 1–16. doi:10.3389/fncom.2018.00098.
- Murthy, V.N., Fetz, E.E., 1992. Coherent 25- to 35-Hz oscillations in the sensorimotor cortex of awake behaving monkeys. *PNAS* 89 (12), 5670–5674. doi:10.1073/pnas.89.12.5670.
- Nomi, J.S., Bolt, T.S., Chiemeka Erie, C.E., Uddin, L.Q., Heller, A.S., 2017. Moment-to-moment BOLD signal variability reflects regional changes in neural flexibility across the lifespan. *J. Neurosci.* 37 (22), 5539–5548. doi:10.1523/JNEUROSCI.3408-16.2017.
- O'Keefe, A.B., Malekmohammadi, M., Sparks, H., Pouratian, N., 2020. Synchrony drives motor cortex beta bursting, waveform dynamics, and phase-amplitude cou-

- pling in parkinson's disease. *J. Neurosci.* 40 (30), 5833–5846. doi:10.1523/JNEUROSCI.1996-19.2020.
- Oostenveld, R., Fries, P., Maris, E., Schoffelen, J.M., 2011. FieldTrip: open source software for advanced analysis of MEG, EEG, and invasive electrophysiological data. *Comput. Intell. Neurosci.* 2011. doi:10.1155/2011/156869.
- Oswal, A., Beudel, M., Zrinzo, L., Limousin, P., Hariz, M., Foltynie, T., Litvak, V., Brown, P., 2016. Deep brain stimulation modulates synchrony within spatially and spectrally distinct resting state networks in Parkinson's disease. *Brain* 139 (5), 1482–1496. doi:10.1093/brain/aww048.
- Oswal, A., Brown, P., Litvak, V., 2013. Synchronized neural oscillations and the pathophysiology of Parkinson's disease. *Curr. Opin. Neurol.* 26 (6), 662–670. doi:10.1097/WCO.0b000000000000034.
- Pang, S.Y.Y., Ho, P.W.L., Liu, H.F., Leung, C.T., Li, L., Chang, E.E.S., Ramsden, D.B., Ho, S.L., 2019. The interplay of aging, genetics and environmental factors in the pathogenesis of Parkinson's disease. *Transl. Neurodegener.* 8 (1), 1–11. doi:10.1186/s40035-019-0165-9.
- Pfurtscheller, G., Stancák, A., Neuper, C., 1996. Post-movement beta synchronization. A correlate of an idling motor area? *Electroencephalogr. Clin. Neurophysiol.* 98 (4), 281–293. doi:10.1016/0013-4694(95)00258-8.
- Pollok, B., Latz, D., Krause, V., Butz, M., Schnitzler, A., 2014. Changes of motor-cortical oscillations associated with motor learning. *Neuroscience* 275, 47–53. doi:10.1016/j.neuroscience.2014.06.008.
- Ray, N.J., Jenkinson, N., Wang, S., Holland, P., Brittain, J.S., Joint, C., Stein, J.F., Aziz, T., 2008. Local field potential beta activity in the subthalamic nucleus of patients with Parkinson's disease is associated with improvements in bradykinesia after dopamine and deep brain stimulation. *Exp. Neurol.* 213 (1), 108–113. doi:10.1016/j.expneurol.2008.05.008.
- Reeve, A., Simcox, E., Turnbull, D., 2014. Ageing and Parkinson's disease: why is advancing age the biggest risk factor? *Ageing Res. Rev.* 14 (1), 19–30. doi:10.1016/j.arr.2014.01.004.
- Romanella, S.M., Roe, D., Pacioret, R., Cappon, D., Ruffini, G., Menardi, A., Rossi, A., Rossi, S., Santarnecchi, E., 2020. Sleep, noninvasive brain stimulation, and the aging brain: challenges and opportunities. *Ageing Res. Rev.* 61. doi:10.1016/j.arr.2020.101067, (August 2019).
- Rossiter, H.E., Davis, E.M., Clark, E.V., Boudrias, M.H., Ward, N.S., 2014. Beta oscillations reflect changes in motor cortex inhibition in healthy ageing. *Neuroimage* 91, 360–365. doi:10.1016/j.neuroimage.2014.01.012.
- Rowe, J.B., Siebner, H., Filipovic, S.R., Cordivari, C., Gerschlagner, W., Rothwell, J., Frackowiak, R., 2006. Aging is associated with contrasting changes in local and distant cortical connectivity in the human motor system. *Neuroimage* 32 (2), 747–760. doi:10.1016/j.neuroimage.2006.03.061.
- Rudow, G., O'Brien, R., Savonenko, A.V., Resnick, S.M., Zonderman, A.B., Pletnikova, O., Marsh, L., Dawson, T.M., Crain, B.J., West, M.J., Troncoso, J.C., 2008. Morphometry of the human substantia nigra in ageing and Parkinson's disease. *Acta Neuropathol. (Berl)* 115 (4), 461–470. doi:10.1007/s00401-008-0352-8.
- Sherman, M.A., Lee, S., Law, R., Haegens, S., Thorn, C.A., Hämmäläinen, M.S., Moore, C.J., Jones, S.R., 2016. Neural mechanisms of transient neocortical beta rhythms: converging evidence from humans, computational modeling, monkeys, and mice. *PNAS* 113 (33), E4885–E4894. doi:10.1073/pnas.1604135113.
- Shi, J., Liu, J., Qu, Q., 2014. Handedness and dominant side of symptoms in Parkinson's disease. *Med. Clin. (Barc)* 142 (4), 141–144. doi:10.1016/j.medcli.2012.11.028.
- Sibille, E., 2013. Molecular aging of the brain, neuroplasticity, and vulnerability to depression and other brain-related disorders. *Dialogues Clin. Neurosci.* 15 (1), 53–65.
- Stoffers, D., Bosboom, J.L.W., Deijen, J.B., Wolters, E.C., Berendse, H.W., Stam, C.J., 2007. Slowing of oscillatory brain activity is a stable characteristic of Parkinson's disease without dementia. *Brain* 130 (7), 1847–1860. doi:10.1093/brain/awm034.
- Swann, N.C., De Hemptinne, C., Aron, A.R., Ostrem, J.L., Knight, R.T., Starr, P.A., 2015. Elevated synchrony in Parkinson disease detected with electroencephalography. *Ann. Neurol.* 78 (5), 742–750. doi:10.1002/ana.24507.
- Tinkhauser, G., Pogoyan, A., Little, S., Beudel, M., Herz, D.M., Tan, H., Brown, P., 2017a. The modulatory effect of adaptive deep brain stimulation on beta bursts in Parkinson's disease. *Brain* 140 (4), 1053–1067. doi:10.1093/brain/aww010.
- Tinkhauser, G., Pogoyan, A., Tan, H., Herz, D.M., Kühn, A.A., Brown, P., 2017b. Beta burst dynamics in Parkinson's disease off and on dopaminergic medication. *Brain* 140 (11), 2968–2981. doi:10.1093/brain/aww252.
- Tinkhauser, G., Torrecillos, F., Ducloux, Y., Tan, H., Pogoyan, A., Fischer, P., Caron, R., Welter, M.L., Karachi, C., Vandenberghe, W., Nuttin, B., Witjas, T., Régis, J., Azulay, J.P., Eusebio, A., Brown, P., 2018. Beta burst coupling across the motor circuit in Parkinson's disease. *Neurobiol. Dis.* 117 (June), 217–225. doi:10.1016/j.nbd.2018.06.007.
- Tort, A.B.L., Kramer, M.A., Thorn, C., Gibson, D.J., Kubota, Y., Graybiel, A.M., Kopell, N.J., 2008. Dynamic cross-frequency couplings of local field potential oscillations in rat striatum and hippocampus during performance of a T-maze task. *PNAS* 105 (51), 20517–20522. doi:10.1073/pnas.0810524105.
- van Wijk, B.C.M., Beudel, M., Jha, A., Oswal, A., Foltynie, T., Hariz, M.I., Limousin, P., Zrinzo, L., Aziz, T.Z., Green, A.L., Brown, P., Litvak, V., 2016. Subthalamic nucleus phase-amplitude coupling correlates with motor impairment in Parkinson's disease. *Clin. Neurophysiol.* 127 (4), 2010–2019. doi:10.1016/j.clinph.2016.01.015.
- Ward, N.S., Frackowiak, R.S.J., 2003. Age-related changes in the neural correlates of motor performance. *Brain* 126 (4), 873–888. doi:10.1093/brain/awg071.
- Weinberger, M., Mahant, N., Hutchison, W.D., Lozano, A.M., Moro, E., Hodajic, M., Lang, A.E., Dostrovsky, J.O., 2006. Beta oscillatory activity in the subthalamic nucleus and its relation to dopaminergic response in Parkinson's disease. *J. Neurophysiol.* 96 (6), 3248–3256. doi:10.1152/jn.00697.2006.
- Wessel, J.R., Aron, A.R., 2017. On the globality of motor suppression: unexpected events and their influence on behavior and cognition. *Neuron* 93 (2), 259–280. doi:10.1016/j.neuron.2016.12.013.
- Whitmer, D., de Solages, C., Hill, B., Yu, H., Henderson, J.M., Bronte-Stewart, H., 2012. High frequency deep brain stimulation attenuates subthalamic and cortical rhythms in Parkinson's disease. *Front. Hum. Neurosci.* 6 (JUNE 2012), 1–18. doi:10.3389/fnhum.2012.00155.
- Wingeier, B., Tchong, T., Koop, M.M., Hill, B.C., Heit, G., Bronte-Stewart, H.M., 2006. Intra-operative STN DBS attenuates the prominent beta rhythm in the STN in Parkinson's disease. *Exp. Neurol.* 197 (1), 244–251. doi:10.1016/j.expneurol.2005.09.016.
- Yau, Y., Zeighami, Y., Baker, T.E., Larcher, K., Vainik, U., Dadar, M., Fonov, V.S., Haggmann, P., Griffa, A., Mišić, B., Collins, D.L., Dagher, A., 2018. Network connectivity determines cortical thinning in early Parkinson's disease progression. *Nat. Commun.* 9 (1), 1–10. doi:10.1038/s41467-017-02416-0.
- Benjamini, Yoav, Hochberg, Yoav, 1995. Controlling the false discovery rate: a practical and powerful approach to multiple testing. *J. R. Stat. Soc. Ser. B (Methodol.)* 57 (1), 289–300.
- Zappasodi, F., Marzetti, L., Olejarczyk, E., Tecchio, F., Pizzella, V., 2015. Age-related changes in electroencephalographic signal complexity. *PLoS ONE* 10 (11), 1–13. doi:10.1371/journal.pone.0141995.
- Zeighami, Y., Feresthtehnejad, S.M., Dadar, M., Collins, D.L., Postuma, R.B., Mišić, B., Dagher, A., 2019. A clinical-anatomical signature of Parkinson's disease identified with partial least squares and magnetic resonance imaging. *Neuroimage* 190 (December), 69–78. doi:10.1016/j.neuroimage.2017.12.050.
- Zhuang, F.J., Chen, Y., He, W.B., Cai, Z.Y., 2018. Prevalence of white matter hyperintensities increases with age. *Neural Regen. Res.* 13 (12), 2141–2146. doi:10.4103/1673-5374.241465.

Publication 2:

Zhang, J., Villringer, A., & Nikulin, V. V. (2022). Dopaminergic Modulation of Local Non-oscillatory Activity and Global-Network Properties in Parkinson's Disease: An EEG Study. *Frontiers in Aging Neuroscience*, 14(April), 1–18.

<https://doi.org/10.3389/fnagi.2022.846017>.



Dopaminergic Modulation of Local Non-oscillatory Activity and Global-Network Properties in Parkinson's Disease: An EEG Study

Juanli Zhang^{1,2*}, Arno Villringer^{1,3} and Vadim V. Nikulin^{1,4*}

OPEN ACCESS

Edited by:
Aneta Kielar,

University of Arizona, United States

Reviewed by:

Eugenia Fatima Hesse Rizzi,
Universidad de San Andrés, Argentina
Shivakumar Viswanathan,
Institute of Neuroscience
and Medicine, Julich Research
Center, Helmholtz Association
of German Research Centres (HZ),
Germany

***Correspondence:**

Juanli Zhang
juanlizhang@cbs.mpg.de
Vadim V. Nikulin
nikulin@cbs.mpg.de

Specialty section:

This article was submitted to
Parkinson's Disease
and Aging-related Movement
Disorders,
a section of the journal
Frontiers in Aging Neuroscience

Received: 30 December 2021

Accepted: 31 March 2022

Published: 29 April 2022

Citation:

Zhang J, Villringer A and
Nikulin VV (2022) Dopaminergic
Modulation of Local Non-oscillatory
Activity and Global-Network
Properties in Parkinson's Disease: An
EEG Study.
Front. Aging Neurosci. 14:846017.
doi: 10.3389/fnagi.2022.846017

¹ Department of Neurology, Max Planck Institute for Human Cognitive and Brain Sciences, Leipzig, Germany, ² Department of Neurology, Charité – Universitätsmedizin Berlin, Berlin, Germany, ³ Department of Cognitive Neurology, University Hospital Leipzig, Leipzig, Germany, ⁴ Neurophysics Group, Department of Neurology, Charité – Universitätsmedizin Berlin, Berlin, Germany

Dopaminergic medication for Parkinson's disease (PD) modulates neuronal oscillations and functional connectivity (FC) across the basal ganglia-thalamic-cortical circuit. However, the non-oscillatory component of the neuronal activity, potentially indicating a state of excitation/inhibition balance, has not yet been investigated and previous studies have shown inconsistent changes of cortico-cortical connectivity as a response to dopaminergic medication. To further elucidate changes of regional non-oscillatory component of the neuronal power spectra, FC, and to determine which aspects of network organization obtained with graph theory respond to dopaminergic medication, we analyzed a resting-state electroencephalography (EEG) dataset including 15 PD patients during OFF and ON medication conditions. We found that the spectral slope, typically used to quantify the broadband non-oscillatory component of power spectra, steepened particularly in the left central region in the ON compared to OFF condition. In addition, using lagged coherence as a FC measure, we found that the FC in the beta frequency range between centro-parietal and frontal regions was enhanced in the ON compared to the OFF condition. After applying graph theory analysis, we observed that at the lower level of topology the node degree was increased, particularly in the centro-parietal area. Yet, results showed no significant difference in global topological organization between the two conditions: either in global efficiency or clustering coefficient for measuring global and local integration, respectively. Interestingly, we found a close association between local/global spectral slope and functional network global efficiency in the OFF condition, suggesting a crucial role of local non-oscillatory dynamics in forming the functional global integration which characterizes PD. These results provide further evidence and a more complete picture for the engagement of multiple cortical regions at various levels in response to dopaminergic medication in PD.

Keywords: Parkinson's disease, dopaminergic medication, spectral slope, functional connectivity, graph theory

INTRODUCTION

Parkinson's disease (PD) is the second most common neural degenerative disorder characterized by massive degeneration of dopaminergic neurons in the nigrostriatal dopamine system (Olanow et al., 2009). It has been increasingly recognized that PD is accompanied by functional disturbances both at subcortical and cortical levels (Braak et al., 2003; Boon et al., 2019). Clinically, dopamine loss is managed *via* dopaminergic therapy (DT). The dopaminergic system has been shown to have considerable and widespread modulatory influences on many brain structures including the cortex (Steiner and Kitai, 2001). While dopamine replacement therapy is efficient for improving the motor symptoms, the neural mechanisms of dopaminergic medication are not yet fully understood (Schapira, 2005).

In PD, it has been repeatedly reported that it is characterized by abnormal oscillatory synchrony in the basal ganglia-thalamus-cortical (BGTC) network in the beta frequency band (13–30 Hz) that could be modulated by dopaminergic medications and deep brain stimulation (DBS) (Brown, 2003; Wingeier et al., 2006; Kühn et al., 2009; De Hemptinne et al., 2015; Müller and Robinson, 2018). In the frequency domain, electrophysiological brain signals typically consist of a power-law $1/f$ component and periodic oscillatory activities. While a majority of studies have so far been dedicated to the oscillatory activity, increasing evidence shows that non-oscillatory (aperiodic) activity also provides information about the intricate neuronal dynamics unfolding at different temporal scales (He et al., 2010; Voytek et al., 2015). A broadband aperiodic component of the spectrum is often represented by the slope of the fitted line in log-log space (known as spectral slope). The changes in spectral slope have been associated with neural development, healthy aging, and performance in working memory tasks (Voytek et al., 2015; Donoghue et al., 2020). In addition, previous studies have reported that it is altered in different pathologies, such as schizophrenia (Peterson et al., 2017; Molina et al., 2020) and ADHD (attention deficit/hyperactivity disorder) (Robertson et al., 2019). Importantly, it has also been demonstrated that the spectral slope is a potential indicator of the local excitation/inhibition balance (Gao et al., 2017; Colombo et al., 2019). In addition, TMS (transcranial magnetic stimulation) studies, which can directly probe the changes in excitation and inhibition, have shown that PD is accompanied by changes in cortical excitability (Ridding et al., 1995; Hanajima et al., 1996; Cantello, 2002). Thus, it would be important to test whether and how this measure is altered in PD, in particular with dopaminergic medication.

While regional changes could provide comprehensive understanding of the underlying local circuitry, the brain rather functions as a distributed network. Functional connectivity (FC) analysis allows us to understand how distinct regions interact, and graph-theory based approach enables a macroscopic perspective of brain connections on the regional and whole-brain network level. Many previous studies showed that network architecture is related to brain function or dysfunction (Bassett and Bullmore, 2009; Bullmore and Sporns, 2009). Using resting state fMRI (functional magnetic resonance imaging), it has

been intensively investigated how dopaminergic medication modulates brain FC in the BGTC network (Tahmasian et al., 2015). The most consistent finding across different rs-fMRI studies revealed decreased connectivity within the posterior putamen in PD (Tessitore et al., 2019), and that its cortical projections are modulated by dopaminergic medication (Herz et al., 2014). To date, few fMRI studies have adopted graph theoretical approach in PD, and the reported findings have been inconsistent. Specifically, compared to healthy controls, PD patients showed lower global efficiency (GE) (Sang et al., 2015), while no abnormalities in topographical property at the global level were observed in PD (Berman et al., 2016; Hou et al., 2018; Ruan et al., 2020). Both increase (Sang et al., 2015) and decrease (Hou et al., 2018) in nodal centrality have been observed in PD compared to healthy controls. In addition, it was found that levodopa administration significantly decreased local efficiency of the network (Berman et al., 2016), and conversely resulted in an increase in eigenvector centrality of cerebellum and brainstem in PD (Jech et al., 2013).

As for the EEG/MEG (electro- and magnetoencephalography) studies, compared to healthy controls, increased cortico-cortical FC in PD has been found primarily in alpha and beta frequency ranges, and cortico-cortical coherence was linked to the severity of the clinical symptoms (Silberstein et al., 2005; Stoffers et al., 2007, 2008; Bosboom et al., 2009; George et al., 2013; Miller et al., 2019). Dopaminergic medication induced changes in cortical synchronization have also been investigated by computing pairwise coherence across the entire montage using multi-channel EEG/MEG. However, both reduction of FC after dopamine medication (Silberstein et al., 2005; George et al., 2013; Heinrichs-Graham et al., 2014) and the absence of connectivity modulation were previously reported (Miller et al., 2019). Very recently, using advanced modeling analysis, in response to dopaminergic medication, increased cortico-cortical synchronization in beta band has been detected by taking into account the contribution from other sub-networks (Sharma et al., 2021). To capture the changes across the whole cortex, through the application of graph theoretical measures in EEG/MEG, previous studies have demonstrated abnormalities in topographical organizations of functional network in PD compared to healthy controls, suggesting that the interactions between cortical areas become abnormal and contribute to PD symptoms at various stages (Utianski et al., 2016). Furthermore, the alterations in network attributes were linked to both motor and cognitive dysfunctions (Olde Dubbelink et al., 2014; Boon et al., 2017). However, how the topological organization of the cortical functional network changes after dopaminergic administration remains rather elusive. To address this issue, we applied graph theory-based network analysis to investigate further changes in cortical connectivity in patients with PD after the administration of dopaminergic medication. Besides, previous studies have suggested a close link between the local excitation/inhibition balance and information transmission locally and globally (Deco et al., 2014), and the network's organizational structure (Zhou et al., 2021). Therefore, we asked whether and how the spectral slope, as a proxy of the local E/I ratio, would relate to the network-wise activity in the context of PD.

To further characterize the regional and functional network changes due to dopaminergic medication, we address the following questions. Regarding local properties: (1) How does the aperiodic property of the electrophysiological brain signal change in response to dopaminergic medication administration? With respect to cross-area interactions: (2) What is the effect of dopaminergic medication on functional connectivity? (3) Does dopaminergic medication induce alterations in the lower and/or higher level of the network architectures? (4) Do local changes in non-oscillatory component of neural activity influence functional network topology/organization? To answer these questions, we analyzed a publicly available dataset including EEG data of PD patients from ON and OFF dopaminergic medication conditions (George et al., 2013; Rockhill et al., 2020).

MATERIALS AND METHODS

Participants

The data analyzed in this study is open-source data (George et al., 2013; Swann et al., 2015; Jackson et al., 2019). This dataset includes resting state EEG data with a duration of around 3 min. Data were collected from 15 PD patients (8 female, average age = 63.2 ± 8.2 years, mild to moderate disease with average disease duration of 4.5 ± 3.5 years) during OFF and ON dopaminergic medication sessions. All participants were right-handed and provided written consent in accordance with the Institutional Review Board of the University of California, San Diego and the Declaration of Helsinki. For more information you may refer to George et al. (2013).

Data Collection

EEG of patients with PD were recorded on two different days for ON and OFF medication sessions which were counterbalanced across subjects. For the OFF medication session, patients were requested to withdraw from their medication at least 12 h prior to the EEG recording. For the ON medication session, subjects took their medication as usual. A 32-channel EEG cap with BioSemi ActiveTwo system was used to acquire the EEG data with a sampling rate of 512 Hz. Two additional electrodes were placed over the left and right mastoids used for reference. During the EEG recording, participants were instructed to sit comfortably and fixate on a cross presented on the screen. Each recording session lasted at least 3 min. In addition, participants completed a few clinical assessments which were previously reported in George et al. (2013). In this study, we did not link the clinical scores of patients to the EEG measures as the authors of the original paper mentioned some uncertainty about these scores. Yet, to assure these two conditions represent two distinct parkinsonian states, we examined the change in the motor section of unified Parkinson's disease rating scale (UPDRS III) scores between the two conditions. Statistical analysis showed that there was a significant reduction of the clinical scores in ON condition (mean \pm SD: 32.67 ± 10.42) compared to that in OFF condition (mean \pm SD: 39.27 ± 9.71). Note, that in this dataset a healthy control group was also included. However, we focused on the comparison of data between ON and OFF conditions which is

also a standard study setup for differential parkinsonian states induced by medication in PD (Tinkhauser et al., 2017; Sharma et al., 2021).

Data Pre-processing

EEG data were analyzed using EEGLAB (version 14.1.2; Delorme and Makeig, 2004) and FieldTrip toolboxes, together with customized scripts in Matlab (The MathWorks Inc., Natick, MA, United States). First, a high-pass filter at 1 Hz was applied to remove low frequency drifts (two-way FIR filter, order = 1,536, eegfilt.m from EEGLab). Subsequently, independent component analysis (ICA – infomax algorithm implemented in EEGLab) was used to remove artifactual sources of cardiographic components, eye movements and blinks, and muscle activity in the data. Further, channels with inadequate quality were rejected by visually inspecting whether their spectra demonstrated residual EMG at higher frequency ranges [on average 5.4 ± 3.1 for OFF and 5.2 ± 2.8 for ON, no difference between conditions ($p = 0.6606$)]. Bad channels were interpolated with neighboring electrodes using a method of spherical splines (EEGLab function "eeg_interp"). Next, data were examined visually for the presence of residual artifacts and segments contaminated by gross artifacts and these events were marked and then excluded from further analysis [on average 172.5 ± 22.7 s in OFF and 165.5 ± 33.6 s in the ON condition remained, no difference in the number of rejected data points ($p = 0.3591$)]. Subsequently, data were re-referenced to the common average.

DATA ANALYSIS

Power Spectral Density

Power spectral density (PSD) was calculated using the function "pwelch" in MATLAB, with a Hamming window of 512 samples (i.e., 1 s) and a 50% overlap. Beta band power was estimated as the averaged PSD in the beta frequency range (13–30 Hz). In addition, in line with a previous study (Donoghue et al., 2020), we utilized another way of estimating the oscillatory beta power by accounting for the overall spectral slope. For this purpose, we subtracted the spectral slope (measured by a fitted line in a log-log space) and estimated the beta power on the residuals of the PSD.

Power Spectral Density Slope

To reduce contamination from high frequency non-neuronal noise, we estimated the slope of the PSD in a frequency range of 2–45 Hz. A three-step robust regression method was used to estimate the slope based on the computed PSD. This method was proposed and applied by Colombo et al. (2019). First, a least-squares linear line was fitted to the raw PSD using the function "robustfit" in MATLAB in the log frequency-log PSD space. Second, frequency points with larger than 1 median absolute deviations of the PSD residuals were identified as oscillatory peaks. Continuous frequency bins surrounding these peak frequencies were considered as the base of the oscillatory peaks and were also excluded for the further step. Last, a second least-squares fit was performed on the rest of the frequency ranges. We took the slope (with the sign) of the second fitted

line as the final spectral slope of the PSD. Thus, a more negative slope demonstrates a steeper decay, while a less negative slope represents a flatter one. One advantage of this method is that it considers the potential bias resulting from linearly spaced frequency bins being estimated with a logarithmic scale. Therefore, before the regression procedure, the PSD curve was up-sampled with logarithmically distributed frequency bins. For more details, please refer to the study by Colombo et al. (2019).

Functional Network Analysis

A network is constructed by a collection of nodes and links between pairs of nodes. In this study, we defined each node as a brain region approximately represented by each channel, while links represent the connectivity between pairs of channels. FC between the brain areas was determined by computing the lagged coherence which accounts for the volume conduction issue. Each network can be represented by a symmetrical 32×32 adjacency matrix.

Functional Connectivity

Functional connectivity measure was quantified by the lagged coherence between all the channel pairs in a frequency range of 1–35 Hz with resolution of 1 Hz. This metric quantifies the strength of phase coupling between two signals by eliminating the effects of volume conduction (Pascual-Marqui, 2007; Pascual-Marqui et al., 2011), and it has been shown to be even more suitable than phase lag index for the application of connectivity estimation when using EEG and MEG (Hindriks, 2021). Its value ranges between [0, 1]: “0” stands for no coupling, and “1” represents perfect coupling. This measure has been utilized in earlier EEG studies (Milz et al., 2014; Vecchio et al., 2021). FC in an oscillatory frequency band was acquired by averaging the FC values over the respective frequency range (for instance beta band FC was obtained by averaging the FC values over 13–30 and 8–12 Hz for the alpha band). To investigate whether medication could result in changes in FC in oscillatory frequency band across the whole brain (neighboring areas and remote regions), we applied a seed-based connectivity comparison approach. This means that the connectivity was calculated between a given electrode (seed) and all other electrodes for each subject. Then, whole-head connectivity was compared between conditions using a cluster-based permutation test to account for multiple comparisons.

Network Measure

We estimated the brain network metrics based on the scalp sensor-based EEG connectivity matrix. Although often performed in source space, due to a small number of channels (Lantz et al., 2003) we did it rather in sensor space similar to previous studies (Stam et al., 2007; Zeng et al., 2015; Chai et al., 2019; Sun et al., 2019; Mitsis et al., 2020; Smith et al., 2021). In the discussion, we mention and discuss limitations associated with the estimation of graph metrics in sensor space.

Node Degree

Node degree estimates the number of edges connected to each node. To estimate the importance of each node (each

channel in our case), node degree centrality weighted by edge importance (the connection is stronger, edge weights are larger) was utilized for this purpose. Specifically, we used the function “Centrality” implemented in Matlab for this measure (parameter “importance” specified by edge weights).

Graph Theory Based Complex Network Measures

Overall Functional Connectivity. For each individual FC matrix, the overall FC was obtained by averaging all the connectivity values across all the pairs of the connection in a matrix.

Proportional Thresholding. Proportional thresholding is a commonly applied approach to remove connections with lower strength and to obtain a sparse connectivity matrix for computing the network properties based on graph theory. Here, we applied a proportional threshold to keep a consistent density of the connections across individuals (Bassett and Bullmore, 2009; van den Heuvel et al., 2017). If a proportional threshold (PT%) is applied to a functional network, all the strongest PT% of the connections are preserved and set to 1; the other connections are set to 0. As suggested by Rubinov and Sporns (2010), networks should be ideally characterized and show consistent patterns across a broad range of thresholds. These threshold values are often determined differently across studies. Therefore, in this study we examined a wide range of thresholds ranging from 36 to 4% (resulting in networks with around 20–200 links) in steps of 2%, similar to a previous study (van den Heuvel et al., 2017). To show how the network looks like, in **Figure 1**, we plotted the grand mean networks within each group at differential thresholding values (20, 10, and 2%).

Graph Metrics. Various measures characterize a network's structure. Two fundamental ones are included here: clustering coefficient (CC) and global efficiency (GE). These two basic graph metrics were computed as implemented in the Brain Connectivity Toolbox (Rubinov and Sporns, 2010). Clustering coefficient is a commonly used measure to quantify the functional network segregation. It is defined as the fraction of triangles (ratio of the present and total possible number of connected triangles) around an individual node and is equivalent to the fraction of a node's neighbors that are neighbors of each other (Watts and Strogatz, 1998). The clustering coefficient of a network CC is the average clustering coefficient across all the nodes in the network. It reflects the prevalence of clustered connectivity around individual nodes (Rubinov and Sporns, 2010): the larger the CC, the greater the degree of functional segregation.

The other metric, GE, was used to quantify the functional network integration. This is based on a basis measure – shortest characteristic path length. Paths are sequences of distinct nodes and links, with shortest paths between two nodes defined as the path with the fewest edges in a network (the sum of the number of its constituent edges is minimized). GE for a network, obtained by the average inverse shortest path length between all the pairs, is a measure of functional network integration: the larger the GE, the greater the degree of global integration. All these measures

were computed with an open source Matlab toolbox (Rubinov and Sporns, 2010).¹

Statistical Tests

Non-parametric Wilcoxon signed rank test was performed for the comparisons of measures in PD OFF and ON states. Spearman's correlation coefficients were calculated to estimate the relations between different measures. We applied the false discovery rate (FDR) procedure (Benjamini and Hochberg, 1995) to correct for multiple tests (correlation calculation) across channels. Significance is reported when FDR-corrected p -values are below 0.05.

To account for multiple comparisons of metrics across all channels, we performed a channel space cluster-based permutation test using the "Monte Carlo" method, as implemented in FieldTrip (Oostenveld et al., 2011). At sample level (each channel in this case), a dependent t -test was utilized to estimate the effect. A total of 1,000 randomizations were performed across groups (ON and OFF conditions) and for each permutation. Additionally, the single sample t -values are thresholded at the 95th quantile, and cluster-level statistics (sum of t -values within each cluster) were computed and the largest cluster statistic was taken to build a null distribution. We then compared the observed cluster-level statistic from the empirical data against the null distribution derived from the permutation procedure. p -Values below 0.05 (two-tailed) were considered significant. A positive or negative cluster demonstrates a significant difference between two conditions (OFF > ON) or (OFF < ON).

RESULTS

Spatial Specificity and Effects of Medication on Spectral Slope

The grand mean of PSD averaged from all channels across subjects in each group is shown in Figure 2A. One can observe that the PSD decay in PD OFF was shallower compared to the PSD decay in PD in the ON condition. The spectral slope was computed for each channel and each subject. Figure 2B shows the topography of the grand mean of the spectral slope across all subjects within each group (upper panel for OFF and lower panel for ON condition). As shown in Figure 2B, for both groups, spectral slopes were more negative (steeper slopes) along the fronto-central-parietal midline of the brain and flatter in the other regions. In general, the ON condition was characterized by a more negative slope than that in the OFF condition.

We investigated the difference between the two conditions for all channels. As described in section "Materials and Methods," we applied a non-parametric cluster-based permutation test to correct for multiple comparisons in the channel space. When comparing slope values in PD OFF with those of PD ON, a significant positive cluster ($p = 0.0220$) indicated an increased slope (flatter) in PD OFF. This difference

demonstrated a lateralized pattern covering mostly left central region (Figure 2C).

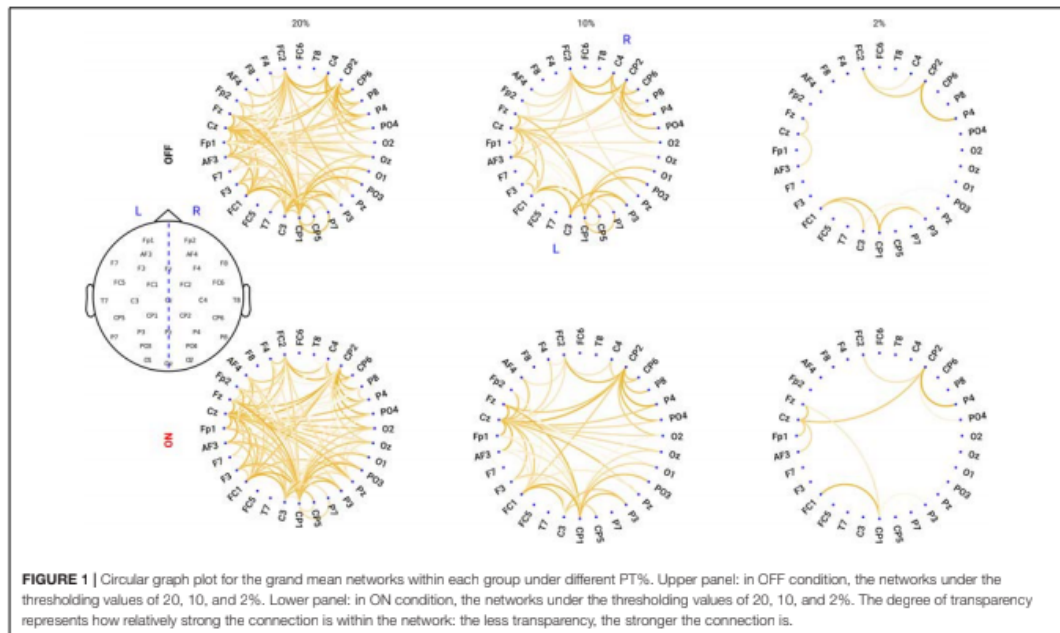
No Beta Power Difference Between Conditions Before and After Correcting for the Slope Effect

Previous studies have demonstrated inconsistent changes in cortical beta power: an increase of beta power after dopaminergic medication (Melgari et al., 2014) and insignificant cortical beta power changes after DT in PD (George et al., 2013; Miller et al., 2019). Since we showed that the background slope was significantly modulated by dopaminergic medication (significantly steepened by the medication), we assumed that insignificant beta power reports might partly be attributed to the overall broadband slope changes. To test this assumption, we first applied a traditional approach to estimate the beta band power on the raw PSD. We computed the mean PSD value in the beta frequency range (13–30 Hz) for each channel and each subject in each group. Cluster-based permutation tests in channel space showed no significant difference in beta power between conditions (Figure 3A). Next, to address whether this finding might be due to a flattened background spectral slope (as observed in the PD OFF vs. ON comparison) on the top of which oscillations were present, we used a second approach controlling for the spectral slope to estimate beta-oscillation power for each channel and subject. Figure 3B shows the grand mean of the residuals of the PSD across all channels after accounting for spectral slope. By averaging the PSD values in the same frequency range of 13–30 Hz, beta band power for each channel and each subject was re-calculated. Cluster-based permutation tests identified two non-significant negative clusters (OFF-ON) ($p = 0.0739, 0.0939$), mainly localized in bilateral centro-parietal regions (CP5, CP1 and C4, CP6, Figure 3C). This demonstrates that even after accounting for the background slope effect, there were no significant beta power changes between the two medication conditions.

Functional Connectivity in Beta Band Is Increased After Medication

First, we predominantly focused on the sensorimotor seed-based connectivity changes, which typically include C3 and C4 electrodes (Swann et al., 2015; Miller et al., 2019). The upper panel of Figure 4A depicts the FC between C3 and one of the representative channels from the parietal region (Pz) along a wide frequency range (1–35 Hz). One can observe clear peaks around the alpha and beta frequency bands for both the ON and OFF conditions. Next, we averaged the connectivity values in the beta frequency range (13–30 Hz) as a measure of beta band FC. As described above, C3 seed-based beta band connectivity was compared between medication conditions. A negative cluster localized in the parieto-occipital region (OFF < ON, $p = 0.007$) was identified as shown in the upper panel of Figure 4B, demonstrating a lower connectivity between C3 and parieto-occipital regions in the OFF compared to the ON conditions. However, there was no significant difference in the comparison of C4 seed-based connectivity between conditions.

¹<http://www.brain-connectivity-toolbox.net>

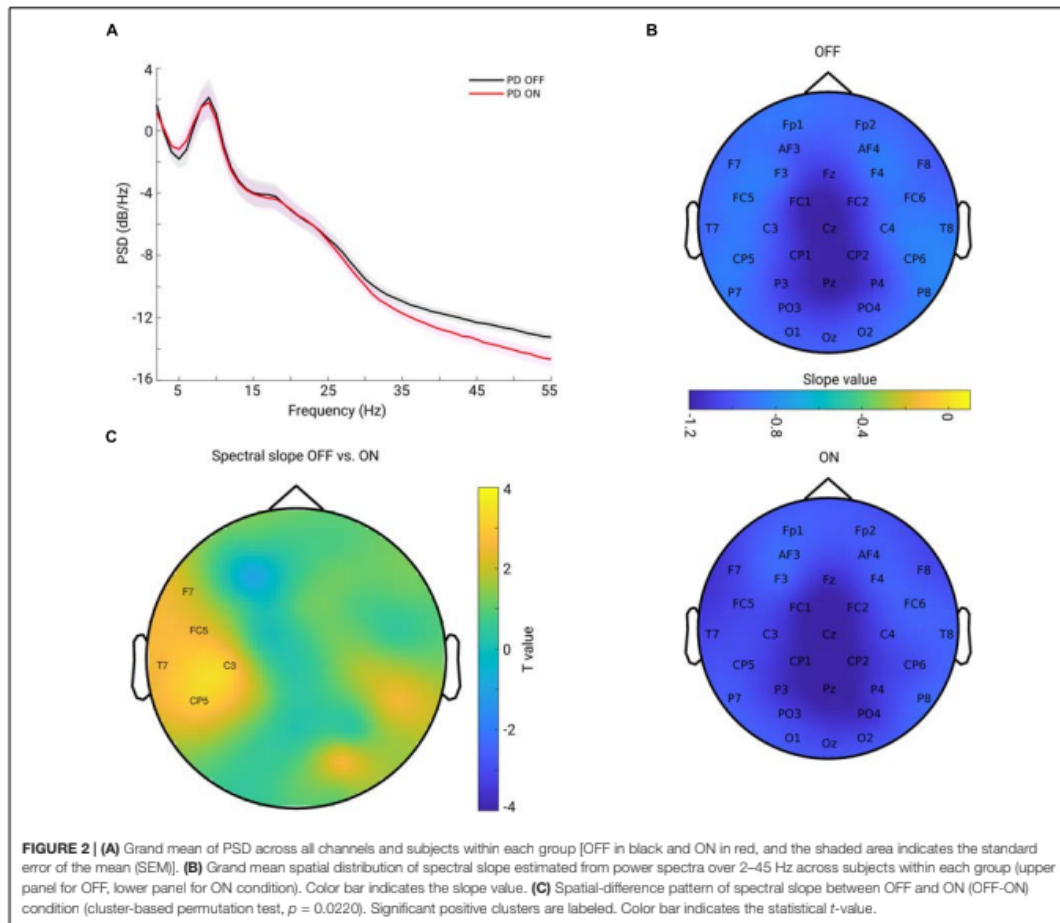


Furthermore, to investigate whether the frontal region showed altered synchronization with other regions, we chose one of the representative channels in the frontal area [Fz, which is typically within the cluster of electrodes near the supplementary motor area (Casarotto et al., 2019)] and performed the same analysis as for electrode C3. As shown in the lower panel of **Figure 4A**, there were obvious peaks in the broad oscillatory frequency range (alpha and beta) for both conditions. The lower panel of **Figure 4B** shows the topographical pattern for the comparison between OFF and ON conditions, and a significant negative cluster ($p = 0.0250$) localized primarily in the parietal region. This demonstrated that the synchronization between Fz and parietal regions in the beta band was significantly enhanced in the ON compared to OFF condition in PD. Finally, we performed the same analysis for the other channels to demonstrate whole-head comparisons in a head-in-head plot (**Figure 4C**). As in C3 and Fz seed-based connectivity comparisons, the other channels in seed-based connectivity also showed significant increase in ON compared to OFF conditions. Significant clusters ($p < 0.05$) are marked by warm color. In general, the topographies showed significant alterations in synchronization between frontal, central, and parieto-occipital regions. To show that these connectivity effects are not mainly driven by the power of the beta oscillation itself, we also examined the PSD and connectivity profiles and found that in the beta band the peaks of the connectivity between the two channels do not coincide with the peaks of the power from either of the relevant channels (see **Supplementary Figure 1**). Therefore, we conclude that the connectivity effect estimated from the

lagged coherence is not driven by the power and rather reflects phase-driven interaction. In addition, due to presence of peaks of the FC in the alpha band, we used the same approach to explore the FC changes in alpha band (8–12 Hz). Yet, there was no significant cluster detected for all the possible seeds when comparing the two conditions. Due to our predominant interest in the beta frequency range and pronounced effects observed in this frequency band, in the rest of the study we focus on the measures from the beta band.

Node Degree in Centro-Parietal Region in Beta Band Is Increased After Medication

Next, we tested whether the local level of a network feature, namely the node degree, was modulated by the medication effect. For this purpose, we calculated the node degree (from the connectivity in the beta band) for each channel and each subject. **Figure 5A** shows the topographical maps of the grand mean of the node degree across subjects within each group. As can be seen from **Figure 5A**, both groups showed a spatial specificity regarding the degree distribution (left for OFF and right for ON conditions): a higher level of the node degree in central areas than in other regions. This demonstrates that the central region might, in general, interact more with other regions in the whole brain network. Next, we compared the node degree between conditions for all channels using a cluster-based permutation test. **Figure 5B** shows the spatial difference pattern – a significant negative cluster was detected ($p = 0.0140$, OFF vs. ON, shown by labels)

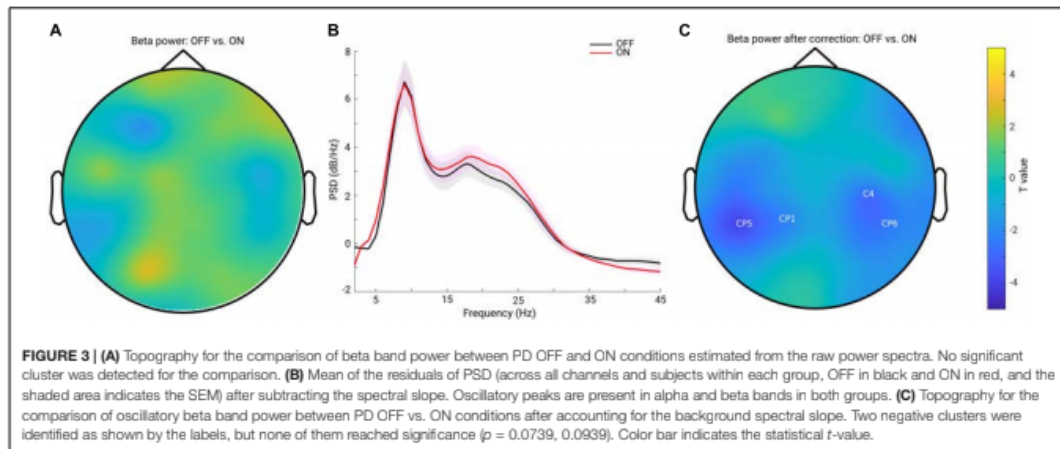


mainly in the centro-parietal region, suggesting that medication modulated the node degree of the beta band functional network in a way that the connectivity of the centro-parietal region became more pronounced in the whole network. Thus, this analysis further confirmed our findings obtained from seed-based connectivity analyses, revealing that synchronization was up-regulated by medication specifically between the centro-parietal region and other regions.

No Significant Change in the Global Network Topology: Either in Network Segregation or Network Integration Measure

To answer the question whether the global network structure is modulated by medication, we estimated the two fundamental features of a network: the GE for measuring functional network

integration and the CC for measuring network functional segregation. We report the comparison results for both of the measures across a wide range of proportional thresholding values (36–4%, with a step of 2%) between the two conditions. Since it has been shown that differences in overall FC could have predictable consequences for between-group differences in network topology (van den Heuvel et al., 2017), we here first checked whether in our data there could be a possible bias for the comparison. However, no significant difference in overall FC between condition comparisons was found (Wilcoxon signed rank test, two-tailed, $p = 0.1514$). Thus, the overall FC is probably not a significant bias in the comparisons we performed as shown below. As seen in **Figure 6A**, across the whole range of thresholding (36–4%), the mean GE across subjects in the OFF condition (in black) almost overlapped with that from the ON condition (in red). As for clustering coefficient, the grand mean of CC in the OFF condition (black line) showed higher values



than those in the ON condition (red line) across all thresholding values (Figure 6B). However, the statistical comparison did not indicate a significant difference in GE ($p > 0.05$, p -values shown in dashed orange line, right y -axis), or in CC between the two conditions ($p > 0.05$, p -values shown in dashed orange line, right y -axis). Thus, controlling for the overall FC values and across a wide range of thresholding values, we were not able to demonstrate a significant impact of medication on global network configuration.

Spectral Slope (Local and Global) Predicts the Network Global Efficiency in OFF Medication

Next, we asked how the spectral slope, as a proxy of measuring local E/I balance, would relate to the brain functional network; thus, we investigated a possible relationship between spectral slope and network topology. First, we averaged the spectral slope across all channels to represent an overall slope (referred to as global slope) for each subject. Spearman's correlation was performed between global slope and network metrics (GE and CC) derived under an exemplary thresholding value at 20% in both groups. As shown in the scatter plot in Figure 7A, GE negatively correlated with global slope ($Rho = -0.7643$, $p < 0.001$) in the OFF condition. In contrast, no such association was observed in the ON condition ($Rho = -0.1036$, $p = 0.7144$). Next, we performed a correlation analysis for the channel-wise slope (referred to as local slope) and network GE in the OFF condition. This analysis revealed a significant negative relationship between local slope values and network GE as shown in the topographical map (channels demonstrating significance are highlighted by label, FDR-corrected) in Figure 7B, and this relationship was most pronounced in the left centro-parietal area. There was no significant relationship between local slopes and GE in the ON condition. In addition, we examined if the relationship we observed at the 20% thresholding could be obtained regardless of the specific thresholding value. We performed the correlation

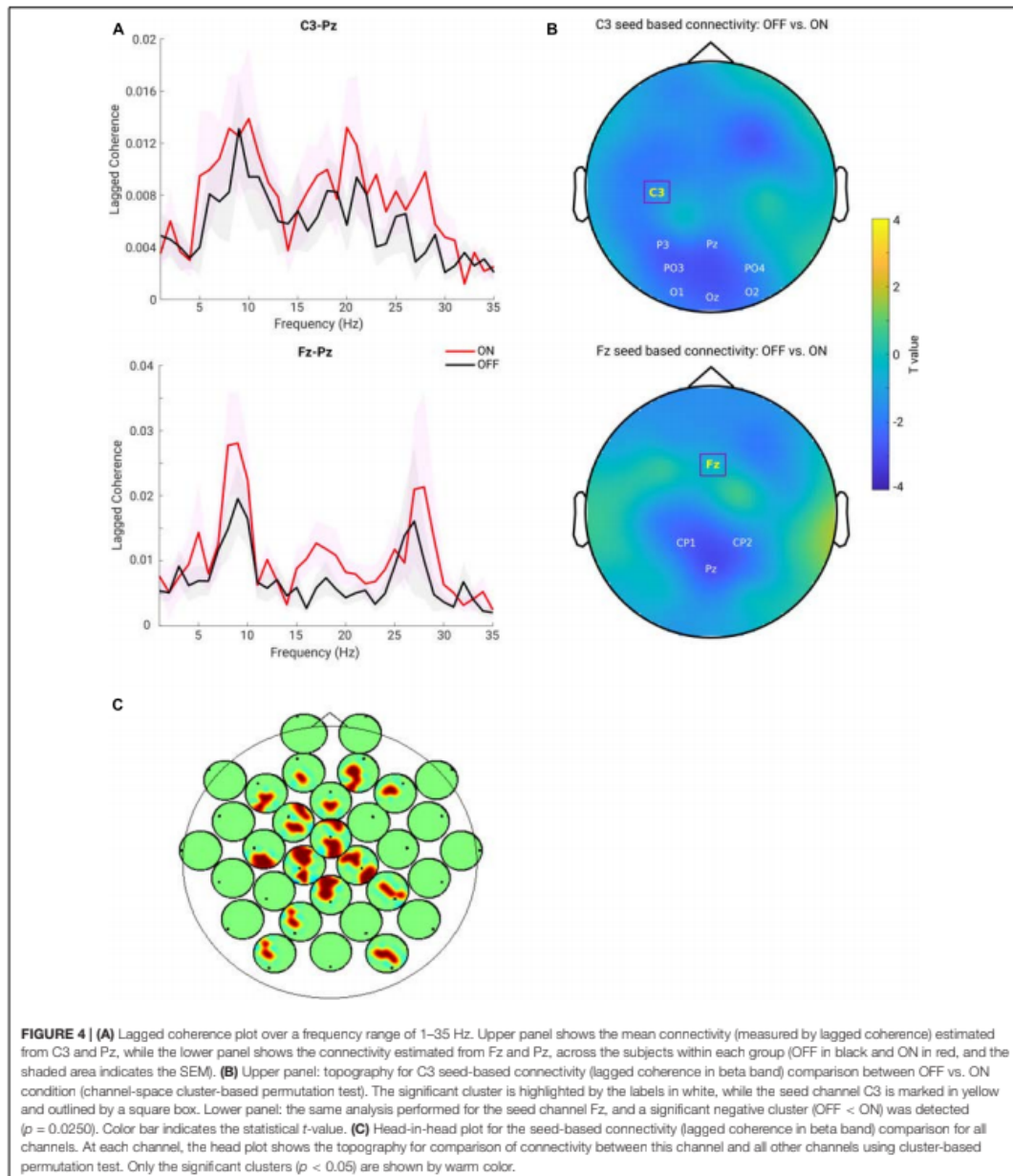
analyses between global slope and network GE across the whole range of thresholding values (36–4% with a step of 2%) in the OFF group. As shown in Figure 7C, almost across all PT%, the negative association between global slope and network GE was present consistently ($p < 0.05$, p -values shown in dashed orange line, right y -axis), except under an extreme thresholding value of 4%. The spatial correlation pattern between local slope and network GE was also examined under the same range of thresholding values, and consistently negative relations between local slope from the centro-parietal region and network GE were observed (see Supplementary Figure 4). These results showed that global slope negatively correlated with network GE across a wide range of thresholding values, and a further topographical correlation map between local slope and network GE demonstrated a region-specific pattern.

Control for the Discontinuity in the Data

To assure that the estimation of the metrics is not affected by signal discontinuity introduced by removing the artifacts, we additionally performed the main analyses respecting the cutting borders. Consistently, we obtained very similar results with respect to spectral slope and lagged coherence. The differences between the two medication conditions remained unchanged. A detailed report can be found in Supplementary Figures 2, 3.

DISCUSSION

In this study, we investigated local and global changes induced by dopaminergic medication in a cohort of PD patients using non-oscillatory spectral slope measure and connectivity analysis in resting state EEG. Locally, we estimated the slope of the non-oscillatory wideband background activity and showed that the left central region had a significantly decreased (steeper) spectral slope during the ON compared to OFF medication state. In addition, in ON compared to OFF, we observed an increase in the FC in the beta band, mainly between centro-parietal and



frontal regions. Further, graph theory-based analysis showed an enhanced node centrality in particular in the centro-parietal regions but no significant alteration in the complex level of network topology (GE or CC). Lastly, we found a strong negative

relationship between spectral slope (locally and globally) and network's GE in the OFF condition, where a flatter slope was associated with a smaller degree of GE of the functional network. These findings provide further evidence for the engagement of

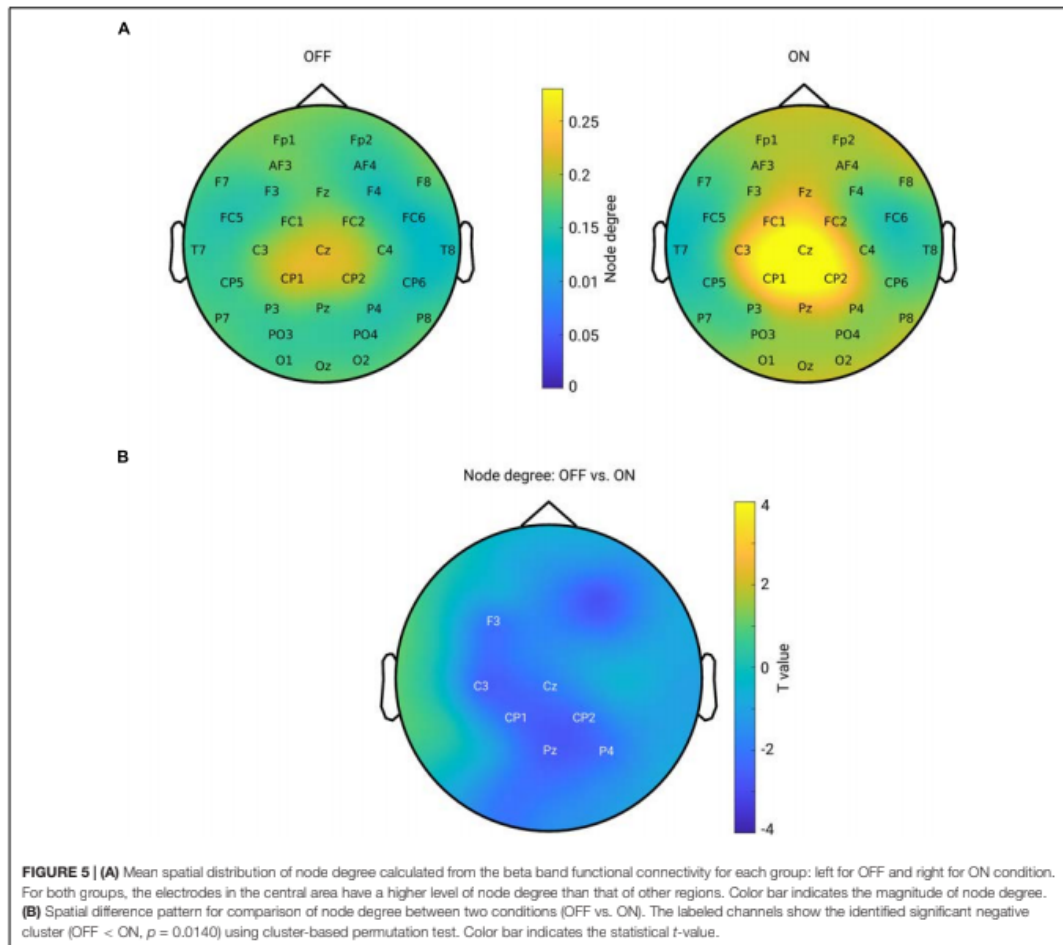


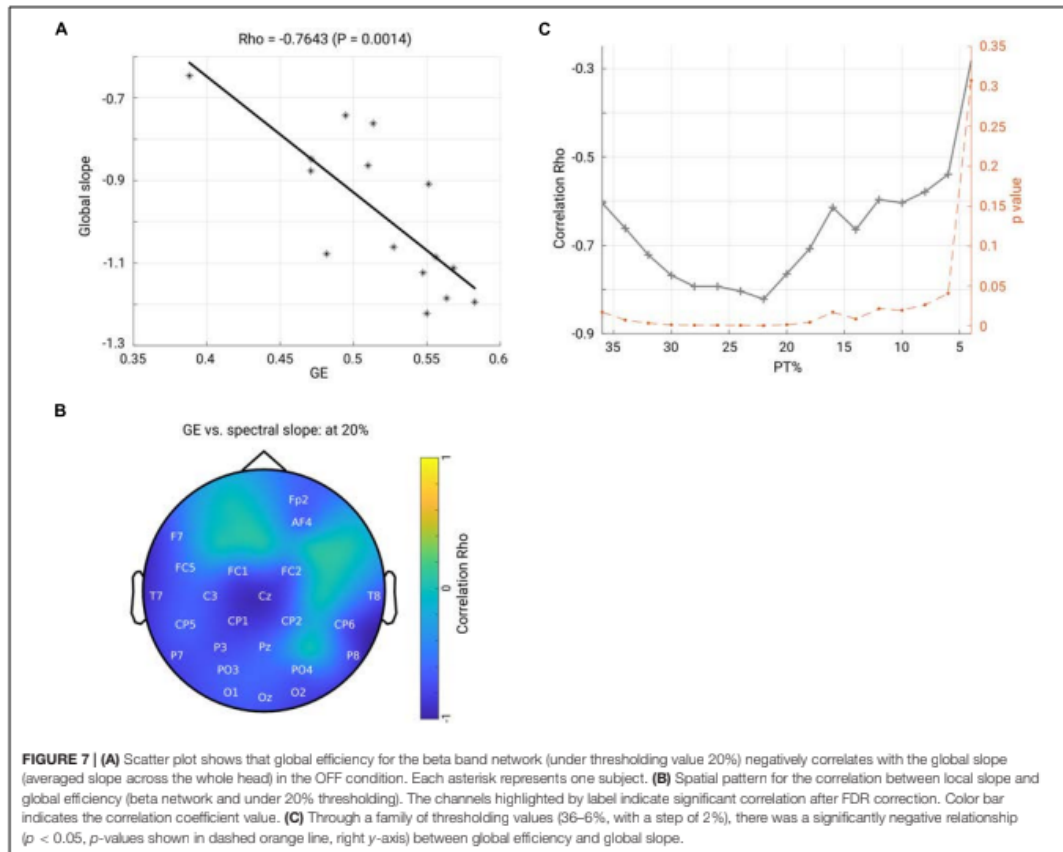
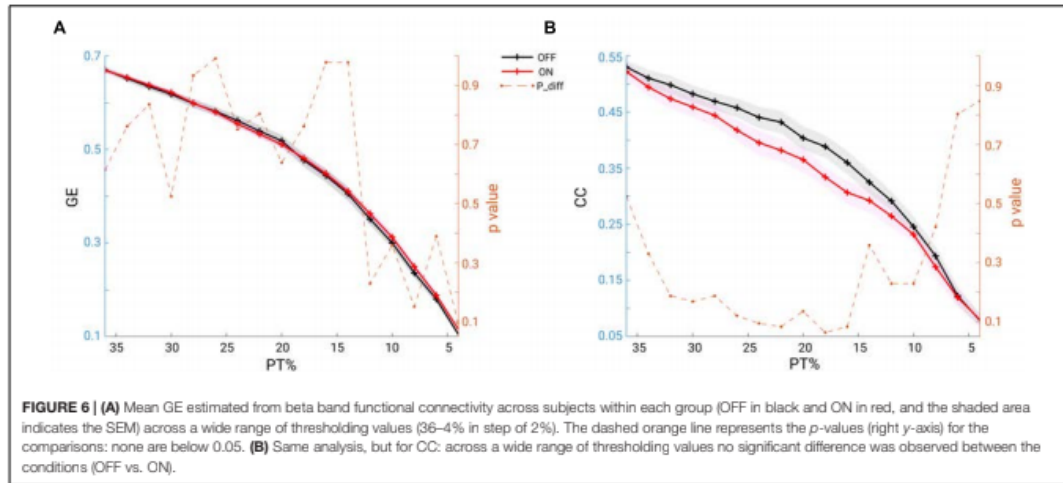
FIGURE 5 | (A) Mean spatial distribution of node degree calculated from the beta band functional connectivity for each group: left for OFF and right for ON condition. For both groups, the electrodes in the central area have a higher level of node degree than that of other regions. Color bar indicates the magnitude of node degree. **(B)** Spatial difference pattern for comparison of node degree between two conditions (OFF vs. ON). The labeled channels show the identified significant negative cluster (OFF < ON, $p = 0.0140$) using cluster-based permutation test. Color bar indicates the statistical t-value.

multiple cortical regions in response to dopaminergic medication in PD, which in turn may indicate that the therapeutic efficacy of dopaminergic medication may relate to both regional and global changes in cortical activity.

Non-oscillatory Background Spectral Slope

Using multi-channel resting state EEG, we observed that patients with PD in the medication OFF condition had an increased (flatter) spectral slope compared to medication ON condition. This effect was found to be spatially specific to the left central region. The spectral slope, a metric to quantify this background power spectrum, has been reported to be altered in the first year of development, healthy aging and in mental disorder such as schizophrenia (Peterson et al., 2017; Donoghue et al., 2020;

Molina et al., 2020; Schaworonkow and Voytek, 2021), and could also predict the dynamic behavioral outcome in working memory tasks (Voytek et al., 2015; Donoghue et al., 2020). In our study, we observed that the spectral slope steepened in ON compared to OFF conditions. Given that previous studies demonstrated that healthy aging is accompanied by flattening of the spectral slope (Voytek et al., 2015; Cesnaite et al., 2021) and that neural electrophysiological biomarkers associated with PD are already present in the apparently healthy aging brain (Zhang et al., 2021), one can speculate that PD might be accompanied by a flattening of the power spectra and that dopaminergic medication might reverse this flattening effect. The effect was found most pronounced in the left central area (strongest at C3 electrode in the detected cluster), which might indicate a modification over the sensorimotor area by the medication. The broadband spectral slope underlying the dopamine medication modulation effect



in patients with PD may thus potentially serve as a biomarker sensitive to dopamine replacement therapy. At the same time, even though we carefully cleaned the data and removed artifacts which might contribute to the estimation of spectral slope, we could not completely rule out this confounder. However, we would like to emphasize that this is unlikely to drive the effect of spectral slope we observed, otherwise one would expect a spatial pattern which shows strongest difference over the frontal or temporal areas (which cover large muscle groups and prone to be contaminated by the muscle activity). Additionally, as we mentioned before, the spectral slope has been shown to index the E/I balance, and we will discuss the implication of this finding below (see section "Spectral Slope and Network Global Efficiency: Local E/I Balance and Global Network").

Power of Beta Oscillation

Previous studies have demonstrated an increase in cortical beta-band power in PD compared to healthy controls and alleviated beta band synchrony after medication administration (Stanzione et al., 1996) and attenuation by DBS (Whitmer et al., 2012). On the other hand, other studies have also reported an opposite effect—an increase of beta band power after dopaminergic medication (Melgari et al., 2014). In addition, some studies demonstrated that dopaminergic medication did not have any effect on cortical beta power (Stoffers et al., 2007; George et al., 2013; Swann et al., 2015; Miller et al., 2019). Importantly, all previous PD studies on this topic have only considered total power of beta without separating it into oscillatory and 1/f aperiodic components. In the present study, we tested the impact of the removal of the aperiodic part of the spectrum on the estimation of oscillatory power. We found that a conventional approach to estimate oscillatory power based on the raw PSD resulted in a non-significant difference in beta band in the PD OFF compared to ON state. After accounting for the spectral slope changes, a marginal increase of beta power was detected in the centro-parietal regions in the comparison between the ON and OFF conditions, yet this difference failed to reach significance. Our data thus suggests that even though the beta-band power estimation by the conventional approach might be partly affected by the background wideband PSD spectra, correcting the effect still does not yield a clear and statistically significant difference between the ON and OFF conditions. Thus, in line with some previous studies (George et al., 2013; Swann et al., 2015; Miller et al., 2019), we further confirm that with and without considering the background slope effect, there was no difference in beta power between the medication conditions. In addition, we discuss a possible relation of our findings to prior studies which were based on the same dataset. The only intersecting aspect across all these prior studies and ours is the investigation of beta-band power change during resting state. Consistently with what have been reported by George et al. (2013) and Swann et al. (2015), our study demonstrated there was no beta power change between the two medication states. Importantly, in our study, we have examined a possible bias from the overall PSD slope effect and showed that even when considering it there was no spectral power change in beta frequency range between the two conditions. Yet, we suggest

that future studies should take into account the effect of the aperiodic spectral component for the comprehensive evaluation of oscillatory power changes in PD.

Functional Connectivity

We observed a significant increase in FC of beta oscillations in the ON compared to OFF condition, in particular between the centro-parietal regions with frontal regions. Previous studies have demonstrated a presence of beta-band coherence between STN (subthalamic nucleus) and multiple cortical regions, including sensorimotor (Hirschmann et al., 2011, 2013; Litvak et al., 2011), parietal and frontal areas (Litvak et al., 2011) in the OFF medication condition in patients with PD. Dopaminergic medication can also alter the beta-band connectivity between STN and cortical regions (Stoffers et al., 2008; Litvak et al., 2011; Hirschmann et al., 2013; van Wijk et al., 2016). As for the cortico-cortical connectivity, dopaminergic medication administration was shown to either reduce interactions between cortical areas (Silberstein et al., 2005; George et al., 2013; Pollok et al., 2013; Heinrichs-Graham et al., 2014) or not to produce any significant changes (Miller et al., 2019). In a very recent study using combined STN-LFP (local field potential) and MEG recordings, the authors discovered differential effects of dopaminergic medication in different levels of networks (Sharma et al., 2021). Specifically, in the cortico-cortical network, sensorimotor-cortical connectivity across multiple regions was enhanced in the beta band during the ON medication state. Therefore, our observations of the enhancement of such a coherent fronto-parietal motor network in the ON condition is consistent with this recent report. Such enhancement of FC is partially in agreement with another study which employed simultaneous fMRI/EEG recordings and showed that a higher dose of dopaminergic medication increased FC between motor areas and the default mode network in fMRI, whereas EEG connectivity remained unaffected (Evangelisti et al., 2019). In general, the dopaminergic effect over the cortico-cortical motor network might relate to the motor decision-making associated network, which has been shown to involve cortical fronto-parietal regions (Siegel et al., 2015), or it might relate to the default-mode network changes associated with non-motor symptoms in PD as suggested by other fMRI studies (Gao and Wu, 2016). Notably, a recent EEG study in PD using source localization demonstrated the presence of strong phase-amplitude coupling between the phase of beta and the amplitude of broadband gamma oscillations in a variety of cortical regions (including sensorimotor, somatosensory, and prefrontal areas) involved in motor and executive control (Gong et al., 2021). In line with this study, our findings of increased connectivity between centroparietal-frontal regions after dopaminergic medication further emphasize the importance of cortico-cortical connections in PD. These electrophysiological findings are consistent with previous fMRI studies suggesting a critical role of motor circuitry in PD in response to dopamine administration (Shen et al., 2020).

Global and Local Network Organization

Using graph theory, we demonstrated that in the ON condition, there was a significant increase in node degree in centro-parietal

regions implying that these regions became more influential in the communication within the network. However, the network topology does not seem to undergo a major re-configuration as we did not identify significant changes in GE or CC in the brain network. This seems consistent with findings of previous studies in which PD patients were compared to healthy controls and no differences in topographical properties were found at the global level either in fMRI (Ruan et al., 2020) or in EEG in all frequency bands (Hassan et al., 2017). Another previous study also investigated the topographical structure of functional network using graph analysis based on MEG of patients with PD (Olde Dubbelink et al., 2013). Compared to healthy controls, their longitudinal study revealed a tendency toward a more random brain functional organization which was associated with lower local integration in multiple frequency bands and lower GE in the upper alpha band. However, another study using EEG found an increase in local integration and a decrease in GE across all the frequency bands in PD compared to healthy subjects (Utianski et al., 2016). In the present study, we explored the alterations in a functional spectral network using graph metrics and showed that dopaminergic medication intake did not significantly alter the brain network organization but did exert a significant enhancement in node degree of some particular regions within the network. The absence of significant changes in global integration and segregation of the functional network might suggest that dopaminergic medication does not re-configure the network at a global organizational level. Instead, these observations appear to imply that the brain network as a whole does not respond to medication at the complex (global integration and segregation) but rather at the low-level network topology (local node). It would be interesting for future studies to test whether this relates to the clinical improvement of symptoms and whether it is possible to significantly alter the network organization through different therapeutic interventions based on brain stimulation.

Spectral Slope and Network Global Efficiency: Local E/I Balance and Global Network

A steeper spectral slope after dopaminergic medication intake was evident in PD. As proposed by previous computational work, the scaling property of the power spectrum of the membrane potentials and EEG could be due to the frequency attenuation of the extracellular medium itself (Bédard et al., 2006), or the intrinsic low-pass filtering effect of the electrical properties of the neural dendrites (Lindén et al., 2010; Einevoll et al., 2013). Alternatively, steepening of the slope could be a consequence of dampened activity propagation (Freeman and Zhai, 2009). More recently, by applying a realistic computational model, it has been demonstrated that stronger inhibitory activity results in steeper spectral decay compared to a situation with a stronger excitatory drive and thus the spectral slope value can be linked to the local excitation/inhibition ratio (Gao et al., 2017). Importantly, this spectral slope derived from ECoG recording dynamically reflects the effects of anesthesia induced by propofol. Furthermore, other pharmacological studies on resting state EEG confirmed further

that spectral slope can differentiate the states of wakefulness compared to a reduction or a complete loss of consciousness induced in the anesthesia (Colombo et al., 2019). Even though an exact generative mechanism of the 1/f shaped arrhythmic brain activity is still unclear (He, 2014), these recent prior work from simulations and experiments with the recordings across different spatial scales have indicated that the spectral slope could be a sensitive marker of the E/I dynamics. Following the E/I balance hypothesis of the spectral slope, a steeper slope after medication, observed in this study, may indicate that dopamine induced a state characterized by stronger inhibition over excitation. This line of interpretation agrees with previous TMS studies reporting a reduction of intracortical inhibition at rest in PD OFF medication (Ridding et al., 1995; Hanajima et al., 1996; Cantello, 2002) and an enhancement of evoked inhibitory activity (reflected in late TMS-evoked activity and beta TMS-evoked oscillations) after dopaminergic medication intake (Casula et al., 2017).

In addition, we found a close relationship between broadband non-oscillatory background activity measured by the spectral slope and the beta-band GE of the functional network. Global network efficiency represents the ability of integration of activity of widely distributed regions within a network, impacting information transmission and communication (Bullmore and Sporns, 2012). Notably, a previous simulation work demonstrated that synaptic E/I balance is crucial for efficient neural coding (Zhou and Yu, 2018), and the local E/I ratio plays a role in information transmission at large scale brain level (Deco et al., 2014). This theory concurs with our findings: the local and global spectral slope, reflecting the local and global tune of E/I balance, is closely associated with the functional network global integration property. The negative relationship between them implies that more excitation over inhibition corresponds to a lower level of functional network integration. Consistently, a recent study from both fMRI recording and simulation data showed that the local E/I ratio could have a significant impact on the organization of whole brain functional networks: GE of the functional network is an inverted-U shaped function of local E/I ratio and the more deviation from the balanced E/I state (in either direction), the lower GE of the whole functional network (Zhou et al., 2021). Our observation about the relationship between local and global slopes with the global network integration property can potentially be explained by this model: in OFF medication, an imbalanced E/I state (indexed by flatter slope) deviating from balanced E/I ratio exerts a monotonous negative relation with functional network GE. A presence of a negative relation between the spectral slope and GE might indicate that the network in PD OFF state resides within the left part of the inverted-U shaped function [GE vs. E/I ratio, refer to the Figure 8A of the study (Zhou et al., 2021)] where a monotonous correlation can be expected. Such a close association did not hold for the medication ON group. We assume that the medication moves the network back closer to a more balanced state, reflected in a steeper spectral slope (steepening of the flattened slope in OFF state); thus, functional network organization was no longer closely related to the E/I, since in a close-to balanced E/I state the GE would rather remain

stable (i.e., it reaches a maximum at the optimal E/I state). Our data did not show a difference in the network's GE property and in contrast did demonstrate a difference in E/I dynamics (reflected by the spectral slope) between the two conditions, thus actually providing a possibility which allows us to more specifically identify a position of the network in the OFF state. One intriguing explanation would be that GE changes rather slowly for quickly changing E/I ratio; therefore, the network in OFF condition stays relatively close to the one in ON condition along the GE axis, and along the E/I axis the networks from two conditions stay further apart.

The spatial distribution of local slope and GE demonstrated a specific pattern where the slope from the centro-parietal regions showed strongest relations with the GE of the brain network. In line with previous fMRI studies demonstrating that the nodal property of the parietal cortex is closely associated with motor outcome and decreased with progressing disease stage (Hoehn and Yahr stage) in PD (Sang et al., 2015; Fang et al., 2017; Suo et al., 2017), we assume that centro-parietal regions play an important role in orchestrating the whole global network organization. This is congruent with the finding that the connectivity patterns in these cortical regions are also affected by dopaminergic medication, as discussed above.

LIMITATIONS

The first limitation of this study is that due to a rather low density of electrodes, we performed all connectivity analysis in sensor space. Thus, we refrain from making any conclusions about the specific structure of the networks (e.g., small-world and scale-free networks) as is also suggested in a critical study on the application of graph measures in EEG/MEG (Kaminski and Blinowska, 2018). It should also be noted that even if the analysis were to be conducted in source space, the volume conduction issue may still be present. Importantly, we applied a connectivity measure that is specifically used to overcome the volume conduction issue. Moreover, we were able to show that our findings remained consistent for a wide range of thresholds for the networks' properties.

Another limitation of our study is that clinical measures were not available and therefore, we could not associate EEG measures with the severity of clinical symptoms. We acknowledge this and suggest that future studies could include such a design so that the link between EEG parameters and clinical phenotypes can be explored. Future work should test whether and how local and global EEG parameters relate to clinical symptoms.

Lastly, due to the lack of EEG comparison with the healthy control group and the possibility to link the observed effects to differential components of the clinical symptoms in PD, we are rather restricted in our interpretation of the neuronal effects due to dopaminergic modulation. In particular, significant modulation of the spectral slopes and connectivity in some specific regions might potentially indicate a successful improvement associated with particular motor aspects (for

instance bradykinesia), while non-significant changes might indicate the absence of such modulation for other motor components such as internal motor control as shown in a recent study (Michely et al., 2015). Alternatively, the absence of neuronal changes in some regions might imply a co-existence of possible non-dopaminergic alterations (for instance serotonergic dysfunction) that could also become present in the course of PD and are not modulated by dopaminergic medication (Politis and Niccolini, 2015).

CONCLUSION

Using multi-channel resting EEG recordings in PD patients, we showed differential effects of dopaminergic medication on local non-oscillatory components and connectivity parameters. Both from the local-level and brain-network perspective, the centro-parietal area was identified as the region where significant alterations in non-oscillatory wideband activity, measured by spectral slope and node centrality within the spectral functional network in the beta band, occurred. However, the network's global topologies, namely global integration (measured by GE) and global segregation (measured by CC) remained unaffected by the dopaminergic medication. Furthermore, during the OFF state, a close association between the spectral slopes (local and global) and network global integration was observed. These findings align with the theory that local E/I balance impacts global network structure, which might in turn demonstrate a crucial role of local non-oscillatory dynamics in forming the functional global integration in PD.

DATA AVAILABILITY STATEMENT

Publicly available datasets were analyzed in this study. This data can be found here: <https://openneuro.org/datasets/ds002778>.

ETHICS STATEMENT

The studies involving human participants were reviewed and approved by the Institutional Review Board Protocol at the University of California, San Diego. The patients/participants provided their written informed consent to participate in this study.

AUTHOR CONTRIBUTIONS

JZ: conceptualization, methodology, software, formal analysis, data curation, writing—original draft, writing—review and editing, visualization, and project administration. AV: writing—review and editing, and supervision. VN: conceptualization, methodology, writing—original draft, writing—review and editing, project administration, and supervision. All authors contributed to the article and approved the submitted version.

FUNDING

This work was supported by Deutsche Forschungsgemeinschaft (German Research Foundation) (Project ID: 424778381 TRR 295).

ACKNOWLEDGMENTS

We thank Tilman Stephani for valuable discussions on the manuscript.

SUPPLEMENTARY MATERIAL

The Supplementary Material for this article can be found online at: <https://www.frontiersin.org/articles/10.3389/fnagi.2022.846017/full#supplementary-material>

Supplementary Figure 1 | Normalized PSDs and connectivity profiles in OFF and ON conditions. In the upper panel: in OFF state, blue lines show the PSD profiles and black lines show the connectivity (left for C3-Pz and right for Fz-Pz). In the lower panel: in ON state, blue lines show the PSD profiles and red lines show the connectivity (left for C3-Pz and right for Fz-Pz).

Supplementary Figure 2 | Spectral slope effect remains the same after taking care of the cutting borders. **(A)** Left panel: grand mean PSD plot in PD ON

condition before and after respecting the cutting borders (original PSD estimation in magenta and PSD estimation with taking care of the cutting borders in light blue). Two lines almost completely overlap across all the frequencies. Right panel: histograms of the estimated spectral slope values across all the channels and all the subjects within PD ON group with original approach in magenta and new approach (considering the borders) in light blue. **(B)** Topographical pattern of the comparison of the spectral slope between two conditions based on the estimations considering the cutting borders (OFF vs. ON, $p = 0.0240$). This topography is consistent with the **Figure 2C** of the main manuscript.

Supplementary Figure 3 | Functional connectivity effects remain unchanged after taking care of the borders introduced by removing the artifactual segments. **(A)** Left panel: averaged functional connectivity between Fz-Pz channels in PD OFF condition before and after considering the cutting borders (original and new estimation in magenta and light blue color, respectively). Two approaches give rise to very similar estimation values. Right panel: same analysis but in the PD ON condition. **(B)** Topographical pattern of the comparison of the Fz-seed based functional connectivity between two conditions (OFF vs. ON, $p = 0.028$). The significant cluster is highlighted by the labels in white, while the seed channel Fz is marked in yellow outlined by a square box. This spatial difference pattern is very consistent with the lower panel of **Figure 4B** of the main manuscript.

Supplementary Figure 4 | Spatial patterns for the correlation between local slope and global efficiency (beta network and under a variety of thresholding values). Significant channels are shown in labels ($p < 0.05$) after FDR correction. Color bar indicates the correlation coefficient value. The spatial specificity over the centro-parietal region is generally consistent across a family of thresholding values (36–18%). At the PT% of 14%, a significant negative relationship is still present. For the higher PT% values, no significant correlation remains after multiple testing correction.

REFERENCES

- Bassett, D. S., and Bullmore, E. T. (2009). Human brain networks in health and disease. *Curr. Opin. Neurol.* 22, 340–347. doi: 10.1097/WCO.0b013e32832d93dd
- Bédard, C., Kröger, H., and Destexhe, A. (2006). Does the 1/f frequency scaling of brain signals reflect self-organized critical states? *Phys. Rev. Lett.* 97:118102. doi: 10.1103/PhysRevLett.97.118102
- Benjamini, Y., and Hochberg, Y. (1995). Controlling the false discovery rate: a practical and powerful approach to multiple testing. *J. R. Stat. Soc. Lond. B Methodol.* 57, 289–300.
- Berman, B. D., Smucny, J., Wylie, K. P., Shelton, E., Kronberg, E., Leehey, M., et al. (2016). Levodopa modulates small-world architecture of functional brain networks in Parkinson's disease. *Mov. Disord.* 31, 1676–1684. doi: 10.1002/mds.26713
- Boon, L. I., Geraedts, V. J., Hillebrand, A., Tannemaat, M. R., Contarino, M. F., Stam, C. J., et al. (2019). A systematic review of MEG-based studies in Parkinson's disease: the motor system and beyond. *Hum. Brain Mapping.* 40, 2827–2848. doi: 10.1002/hbm.24562
- Boon, L. I., Hillebrand, A., Olde Dubbelink, K. T. E., Stam, C. J., and Berendse, H. W. (2017). Changes in resting-state directed connectivity in cortico-subcortical networks correlate with cognitive function in Parkinson's disease. *Clin. Neurophysiol.* 128, 1319–1326. doi: 10.1016/j.clinph.2017.04.024
- Bosboom, J. L. W., Stoffers, D., Wolters, E. C., Stam, C. J., and Berendse, H. W. (2009). MEG resting state functional connectivity in Parkinson's disease related dementia. *J. Neural Trans.* 116, 193–202. doi: 10.1007/s00702-008-0132-6
- Braak, H., Del Tredici, K., Rüb, U., De Vos, R. A. I., Jansen Steur, E. N. H., and Braak, E. (2003). Staging of brain pathology related to sporadic Parkinson's disease. *Neurobiol. Aging* 24, 197–211. doi: 10.1016/S0197-4580(02)00065-9
- Brown, P. (2003). Oscillatory nature of human basal ganglia activity: relationship to the pathophysiology of parkinson's disease. *Mov. Disord.* 18, 357–363. doi: 10.1002/mds.10358
- Bullmore, E., and Sporns, O. (2009). Complex brain networks: graph theoretical analysis of structural and functional systems. *Nat. Rev. Neurosci.* 10, 186–198. doi: 10.1038/nrn2575
- Bullmore, E., and Sporns, O. (2012). The economy of brain network organization. *Nat. Rev. Neurosci.* 13, 336–349. doi: 10.1038/nrn3214
- Cantello, R. (2002). Applications of transcranial magnetic stimulation in movement disorders. *J. Clin. Neurophysiol.* 19, 272–293. doi: 10.1097/00004691-200208000-00003
- Casarotto, S., Turco, F., Comanducci, A., Perretti, A., Marotta, G., Pezzoli, G., et al. (2019). Excitability of the supplementary motor area in Parkinson's disease depends on subcortical damage. *Brain Stimul.* 12, 152–160. doi: 10.1016/j.brs.2018.10.011
- Casula, E. P., Stampanoni Bassi, M., Pellicciari, M. C., Ponzio, V., Veniero, D., Peppe, A., et al. (2017). Subthalamic stimulation and levodopa modulate cortical reactivity in Parkinson's patients. *Park. Relat. Disord.* 34, 31–37. doi: 10.1016/j.parkreldis.2016.10.009
- Cesnaite, E., Steinfath, P., Idaji, M. J., Stephani, T., Haufe, S., Sander, C., et al. (2021). Alterations in rhythmic and non-rhythmic resting-state EEG activity and their link to cognition in older age. *bioRxiv* [Preprint] 1–34. doi: 10.1101/2021.08.26.457768
- Chai, M. T., Amin, H. U., Izhar, L. I., Saad, M. N. M., Abdul Rahman, M., Malik, A. S., et al. (2019). Exploring EEG effective connectivity network in estimating influence of color on emotion and memory. *Front. Neuroinform.* 13:66. doi: 10.3389/fninf.2019.00066
- Colombo, M. A., Napolitani, M., Boly, M., Gosseries, O., Casarotto, S., Rosanova, M., et al. (2019). The spectral exponent of the resting EEG indexes the presence of consciousness during unresponsiveness induced by propofol, xenon, and ketamine. *NeuroImage* 189, 631–644. doi: 10.1016/j.neuroimage.2019.01.024
- De Hemptinne, C., Swann, N. C., Ostrem, J. L., Ryapolova-Webb, E. S., San Luciano, M., Galifianakis, N. B., et al. (2015). Therapeutic deep brain stimulation reduces cortical phase-amplitude coupling in Parkinson's disease. *Nat. Neurosci.* 18, 779–786. doi: 10.1038/nn.3997
- Deco, G., Ponce-Alvarez, A., Hagmann, P., Romani, G. L., Mantini, D., and Corbetta, M. (2014). How local excitation-inhibition ratio impacts the whole brain dynamics. *J. Neurosci.* 34, 7886–7898. doi: 10.1523/JNEUROSCI.5068-13.2014
- Delorme, A., and Makeig, S. (2004). EEGLAB: an open source toolbox for analysis of single-trial EEG dynamics including independent component analysis. *J. Neurosci. Methods* 134, 9–21. doi: 10.1016/j.jneumeth.2003.10.009

- Donoghue, T., Haller, M., Peterson, E. J., Varma, P., Sebastian, P., Gao, R., et al. (2020). Parameterizing neural power spectra into periodic and aperiodic components. *Nat. Neurosci.* 23, 1655–1665. doi: 10.1038/s41593-020-00744-x
- Einevoll, G. T., Kayser, C., Logothetis, N. K., and Panzeri, S. (2013). Modelling and analysis of local field potentials for studying the function of cortical circuits. *Nat. Rev. Neurosci.* 14, 770–785. doi: 10.1038/nrn3599
- Evangelisti, S., Pittau, F., Testa, C., Rizzo, G., Gramagna, L. L., Ferri, L., et al. (2019). L-dopa modulation of brain connectivity in Parkinson's disease patients: a pilot EEG-fMRI study. *Front. Neurosci.* 13:611. doi: 10.3389/fnins.2019.00611
- Fang, J., Chen, H., Cao, Z., Jiang, Y., Ma, L., Ma, H., et al. (2017). Impaired brain network architecture in newly diagnosed Parkinson's disease based on graph theoretical analysis. *Neurosci. Lett.* 657, 151–158. doi: 10.1016/j.neulet.2017.08.002
- Freeman, W. J., and Zhai, J. (2009). Simulated power spectral density (PSD) of background electrocorticogram (ECoG). *Cogn. Neurodyn.* 3, 97–103. doi: 10.1007/s11571-008-9064-y
- Gao, L. L., and Wu, T. (2016). The study of brain functional connectivity in Parkinson's disease. *Transl. Neurodegener.* 5:18. doi: 10.1186/s40035-016-0066-0
- Gao, R., Peterson, E. J., and Voytek, B. (2017). Inferring synaptic excitation/inhibition balance from field potentials. *NeuroImage* 158, 70–78. doi: 10.1016/j.neuroimage.2017.06.078
- George, J. S., Strunk, J., Mak-McCully, R., Houser, M., Poizner, H., and Aron, A. R. (2013). Dopaminergic therapy in Parkinson's disease decreases cortical beta band coherence in the resting state and increases cortical beta band power during executive control. *NeuroImage Clin.* 3, 261–270. doi: 10.1016/j.nicl.2013.07.013
- Gong, R., Wegscheider, M., Mühlberg, C., Gast, R., Fricke, C., Rumpf, J. J., et al. (2021). Spatiotemporal features of β - γ phase-amplitude coupling in Parkinson's disease derived from scalp EEG. *Brain* 144, 487–503. doi: 10.1093/brain/awaa400
- Hanajima, R., Ugawa, Y., Terao, Y., Ogata, K., and Kanazawa, I. (1996). Ipsilateral cortico-cortical inhibition of the motor cortex in various neurological disorders. *J. Neurol. Sci.* 140, 109–116. doi: 10.1016/0022-510X(96)00100-1
- Hassan, M., Chaton, L., Benquet, P., Delval, A., Leroy, C., Plomhause, L., et al. (2017). Functional connectivity disruptions correlate with cognitive phenotypes in Parkinson's disease. *NeuroImage Clin.* 14, 591–591. doi: 10.1016/j.nicl.2017.03.002
- He, B. J. (2014). Scale-free brain activity: past, present, and future. *Trends Cogn. Sci.* 18, 480–487. doi: 10.1016/j.tics.2014.04.003
- He, B. J., Zempel, J. M., Snyder, A. Z., and Raichle, M. E. (2010). The temporal structures and functional significance of scale-free brain activity. *Neuron* 66, 353–369. doi: 10.1016/j.neuron.2010.04.020
- Heinrichs-Graham, E., Kurz, M. J., Becker, K. M., Santamaria, P. M., Gendelman, H. E., and Wilson, T. W. (2014). Hypersynchrony despite pathologically reduced beta oscillations in patients with Parkinson's disease: a pharmacomagnetoencephalography study. *J. Neurophysiol.* 112, 1739–1747. doi: 10.1152/jn.00383.2014
- Herz, D. M., Eickhoff, S. B., Løkkegaard, A., and Siebner, H. R. (2014). Functional neuroimaging of motor control in parkinson's disease: a meta-analysis. *Hum. Brain Mapp.* 35, 3227–3237. doi: 10.1002/hbm.22397
- Hindriks, R. (2021). Relation between the phase-lag index and lagged coherence for assessing interactions in EEG and MEG data. *NeuroImage Rep.* 1:100007. doi: 10.1016/j.ynrp.2021.100007
- Hirschmann, J., Özkurt, T. E., Butz, M., Homburger, M., Elben, S., Hartmann, C. J., et al. (2011). Distinct oscillatory STN-cortical loops revealed by simultaneous MEG and local field potential recordings in patients with Parkinson's disease. *NeuroImage* 55, 1159–1168. doi: 10.1016/j.neuroimage.2010.11.063
- Hirschmann, J., Özkurt, T. E., Butz, M., Homburger, M., Elben, S., Hartmann, C. J., et al. (2013). Differential modulation of STN-cortical and cortico-muscular coherence by movement and levodopa in Parkinson's disease. *NeuroImage* 68, 203–213. doi: 10.1016/j.neuroimage.2012.11.036
- Hou, Y., Wei, Q., Ou, R., Yang, J., Song, W., Gong, Q., et al. (2018). Impaired topographic organization in cognitively unimpaired drug-naïve patients with rigidity-dominant Parkinson's disease. *Park. Relat. Disord.* 56, 52–57. doi: 10.1016/j.parkrel.2018.06.021
- Jackson, N., Cole, S. R., Voytek, B., and Swann, N. C. (2019). Characteristics of waveform shape in Parkinson's disease detected with scalp electroencephalography. *eNeuro* 6:ENEURO.0151-19.2019. doi: 10.1523/ENEURO.0151-19.2019
- Jech, R., Mueller, K., Schroeter, M. L., and Růžička, E. (2013). Levodopa increases functional connectivity in the cerebellum and brainstem in Parkinson's disease. *Brain* 136:e234. doi: 10.1093/brain/awt015
- Kaminski, M., and Blinowska, K. J. (2018). Is graph theoretical analysis a useful tool for quantification of connectivity obtained by means of EEG/MEG Techniques? *Front. Neural Circ.* 12:76. doi: 10.3389/fncir.2018.00076
- Kühn, A. A., Tsui, A., Aziz, T., Ray, N., Brücke, C., Kupsch, A., et al. (2009). Pathological synchronisation in the subthalamic nucleus of patients with Parkinson's disease relates to both bradykinesia and rigidity. *Exp. Neurol.* 215, 380–387. doi: 10.1016/j.expneurol.2008.11.008
- Lantz, G., Grave de Peralta, R., Spinelli, L., Seeck, M., and Michel, C. M. (2003). Epileptic source localization with high density EEG: how many electrodes are needed? *Clin. Neurophysiol.* 114, 63–69. doi: 10.1016/S1388-2457(02)00337-1
- Lindén, H., Pettersen, K. H., and Einevoll, G. T. (2010). Intrinsic dendritic filtering gives low-pass power spectra of local field potentials. *J. Comput. Neurosci.* 29, 423–444. doi: 10.1007/s10827-010-0245-4
- Litvak, V., Jha, A., Eusebio, A., Oostenveld, R., Foltynie, T., Limousin, P., et al. (2011). Resting oscillatory cortico-subthalamic connectivity in patients with Parkinson's disease. *Brain* 134, 359–374. doi: 10.1093/brain/awq332
- Melgari, J. M., Curcio, G., Mastroioli, F., Salomone, G., Trotta, L., Tombini, M., et al. (2014). Alpha and beta EEG power reflects L-dopa acute administration in parkinsonian patients. *Front. Aging Neurosci.* 6:302. doi: 10.3389/fnagi.2014.00302
- Michely, J., Volz, L. J., Barbe, M. T., Hoffstaedter, F., Viswanathan, S., Timmermann, L., et al. (2015). Dopaminergic modulation of motor network dynamics in Parkinson's disease. *Brain* 138, 664–678. doi: 10.1093/brain/awu381
- Miller, A. M., Miocinovic, S., Swann, N. C., Rajagopalan, S. S., Darevsky, D. M., Giron, R., et al. (2019). Effect of levodopa on electroencephalographic biomarkers of the parkinsonian state. *J. Neurophysiol.* 122, 290–299. doi: 10.1152/jn.00141.2019
- Milz, P., Faber, P. L., Lehmann, D., Kochi, K., and Pascual-Marqui, R. D. (2014). sLORETA intracortical lagged coherence during breath counting in meditation-naïve participants. *Front. Hum. Neurosci.* 8:303. doi: 10.3389/fnhum.2014.00303
- Mitsis, G. D., Anastasiadou, M. N., Christodoulakis, M., Paphanasiou, E. S., Papacostas, S. S., and Hadjipapas, A. (2020). Functional brain networks of patients with epilepsy exhibit pronounced multiscale periodicities, which correlate with seizure onset. *Hum. Brain Mapp.* 41, 2059–2076. doi: 10.1002/hbm.24930
- Molina, J. L., Voytek, B., Thomas, M. L., Joshi, Y. B., Bhakta, S. G., Talledo, J. A., et al. (2020). Memantine effects on electroencephalographic measures of putative excitatory/inhibitory balance in schizophrenia. *Biol. Psychiatry Cogn. Neurosci. Neuroimaging* 5, 562–568. doi: 10.1016/j.bpsc.2020.02.004
- Müller, E. J., and Robinson, P. A. (2018). Suppression of parkinsonian beta oscillations by deep brain stimulation: determination of effective protocols. *Front. Comput. Neurosci.* 12:98. doi: 10.3389/fncom.2018.00098
- Olanow, C. W., Stern, M. B., and Sethi, K. (2009). The scientific and clinical basis for the treatment of Parkinson disease. *Neurology* 72(21 SUPPL. 4), S1–S136. doi: 10.1212/WNL.0b013e3181a1d44c
- Olde Dubbelink, K. T. E., Hillebrand, A., Stoffers, D., Deijen, J. B., Twisk, J. W. R., Stam, C. J., et al. (2014). Disrupted brain network topology in Parkinson's disease: a longitudinal magnetoencephalography study. *Brain* 137, 197–207. doi: 10.1093/brain/awt316
- Olde Dubbelink, K. T. E., Stoffers, D., Deijen, J. B., Twisk, J. W. R., Stam, C. J., Hillebrand, A., et al. (2013). Resting-state functional connectivity as a marker of disease progression in Parkinson's disease: a longitudinal MEG study. *NeuroImage Clin.* 2, 612–619. doi: 10.1016/j.nicl.2013.04.003
- Oostenveld, R., Fries, P., Maris, E., and Schoffelen, J. M. (2011). FieldTrip: open source software for advanced analysis of MEG, EEG, and invasive electrophysiological data. *Comput. Intell. Neurosci.* 2011:156869. doi: 10.1155/2011/156869

- Pascual-Marqui, R. D. (2007). Instantaneous and lagged measurements of linear and nonlinear dependence between groups of multivariate time series: frequency decomposition. *arXiv [Preprint]*. arXiv:0711.1455.
- Pascual-Marqui, R. D., Lehmann, D., Koukkou, M., Kochi, K., Anderer, P., Saletu, B., et al. (2011). Assessing interactions in the brain with exact low-resolution electromagnetic tomography. *Philos. Trans. R. Soc. A Math. Phys. Eng. Sci.* 369, 3768–3784. doi: 10.1098/rsta.2011.0081
- Peterson, E. J., Rosen, B. Q., Campbell, A. M., Belger, A., and Voytek, B. (2017). 1/F neural noise is a better predictor of schizophrenia than neural oscillations. *bioRxiv [Preprint]* doi: 10.1101/113449
- Politis, M., and Niccolini, F. (2015). Serotonin in Parkinson's disease. *Behav. Brain Res.* 277, 136–145. doi: 10.1016/j.bbr.2014.07.037
- Pollok, B., Kamp, D., Butz, M., Wojtecki, L., Timmermann, L., Südmeyer, M., et al. (2013). Increased SMA-M1 coherence in Parkinson's disease – Pathophysiology or compensation? *Exp. Neurol.* 247, 178–181. doi: 10.1016/j.expneurol.2013.04.013
- Ridding, M. C., Rothwell, J. C., and Inzelberg, R. (1995). Changes in excitability of motor cortical circuitry in patients with parkinson's disease. *Ann. Neurol.* 37, 181–188. doi: 10.1002/ana.410370208
- Robertson, M. M., Furlong, S., Voytek, B., Donoghue, T., Boettiger, C. A., and Sheridan, M. A. (2019). EEG power spectral slope differs by ADHD status and stimulant medication exposure in early childhood. *J. Neurophysiol.* 122, 2427–2437. doi: 10.1152/jn.00388.2019
- Rockhill, A. P., Jackson, N., George, J., Aron, A., Swann, N. C., et al. (2020). *UC San Diego Resting State EEG Data from Patients with Parkinson's Disease. OpenNeuro. [Dataset]*. doi: 10.18112/openneuro.ds002778.v1.0.4
- Ruan, X., Li, Y., Li, E., Xie, F., Zhang, G., Luo, Z., et al. (2020). Impaired topographical organization of functional brain networks in Parkinson's disease patients with freezing of gait. *Front. Aging Neurosci.* 12:580564. doi: 10.3389/fnagi.2020.580564
- Rubinov, M., and Sporns, O. (2010). Complex network measures of brain connectivity: uses and interpretations. *NeuroImage* 52, 1059–1069. doi: 10.1016/j.neuroimage.2009.10.003
- Sang, L., Zhang, J., Wang, L., Zhang, J., Zhang, Y., Li, P., et al. (2015). Alteration of brain functional networks in early-stage Parkinson's disease: a resting-state fMRI study. *PLoS One* 10:e0141815. doi: 10.1371/journal.pone.0141815
- Schapira, A. H. V. (2005). Present and future drug treatment for Parkinson's disease. *Journal of Neurology, Neurosurgery and Psychiatry* 76, 1472–1478. doi: 10.1136/jnnp.2004.035980
- Schaworonkow, N., and Voytek, B. (2021). Longitudinal changes in aperiodic and periodic activity in electrophysiological recordings in the first seven months of life. *Dev. Cogn. Neurosci.* 47:100895. doi: 10.1016/j.dcn.2020.10.0895
- Sharma, A., Vidaurre, D., Vesper, J., Schnitzler, A., and Florin, E. (2021). Differential dopaminergic modulation of spontaneous cortico-subthalamic activity in parkinson's disease. *eLife* 10:e66057. doi: 10.7554/eLife.66057
- Shen, Y., Hu, J., Chen, Y., Liu, W., Li, Y., Yan, L., et al. (2020). Levodopa changes functional connectivity patterns in subregions of the primary motor cortex in patients With Parkinson's Disease. *Front. Neurosci.* 14:647. doi: 10.3389/fnins.2020.00647
- Siegel, M., Buschman, T. J., and Miller, E. K. (2015). Cortical information flow during flexible sensorimotor decisions. *Science* 348, 1352–1355. doi: 10.1126/science.1255111
- Silberstein, P., Pogosyan, A., Kühn, A. A., Hotton, G., Tisch, S., Kupsch, A., et al. (2005). Cortico-cortical coupling in Parkinson's disease and its modulation by therapy. *Brain* 128, 1277–1291. doi: 10.1093/brain/awh480
- Smith, R. J., Alipourjedi, E., Garner, C., Maser, A. L., Shrey, D. W., and Lopour, B. A. (2021). Infant functional networks are modulated by state of consciousness and circadian rhythm. *Netw. Neurosci.* 5, 614–630. doi: 10.1162/netn_a_00194
- Stam, C. J., Jones, B. F., Nolte, G., Breakspear, M., and Scheltens, P. (2007). Small-world networks and functional connectivity in Alzheimer's disease. *Cereb. Cortex* 17, 92–99. doi: 10.1093/cercor/bhj127
- Stanzione, P., Marcianni, M. G., Maschio, M., Bassetti, M. A., Spanedda, F., Pierantozzi, M., et al. (1996). Quantitative EEG changes in non-demented Parkinson's disease patients before and during L-dopa therapy. *Eur. J. Neurol.* 3, 354–362. doi: 10.1111/j.1468-1331.1996.tb00229.x
- Steiner, H., and Kitai, S. T. (2001). Unilateral striatal dopamine depletion: time-dependent effects on cortical function and behavioural correlates. *Eur. J. Neurosci.* 14, 1390–1404. doi: 10.1046/j.0953-816X.2001.01756.x
- Stoffers, D., Bosboom, J. L. W., Deijen, J. B., Wolters, E. C., Berendse, H. W., and Stam, C. J. (2007). Slowing of oscillatory brain activity is a stable characteristic of Parkinson's disease without dementia. *Brain* 130, 1847–1860. doi: 10.1093/brain/awm034
- Stoffers, D., Bosboom, J. L. W., Wolters, E. C., Stam, C. J., and Berendse, H. W. (2008). Dopaminergic modulation of cortico-cortical functional connectivity in Parkinson's disease: an MEG study. *Exp. Neurol.* 213, 191–195. doi: 10.1016/j.expneurol.2008.05.021
- Sun, S., Li, X., Zhu, J., Wang, Y., La, R., Zhang, X., et al. (2019). Graph theory analysis of functional connectivity in major depression disorder with high-density resting state EEG Data. *IEEE Trans. Neural Syst. Rehabil. Eng.* 27, 429–439. doi: 10.1109/TNSRE.2019.2894423
- Suo, X., Lei, D., Li, N., Cheng, L., Chen, F., Wang, M., et al. (2017). Functional brain connectome and its relation to hoehn and yahr stage in Parkinson disease. *Radiology* 285, 904–913. doi: 10.1148/radiol.2017162929
- Swann, N. C., De Hemptinne, C., Aron, A. R., Ostrem, J. L., Knight, R. T., and Starr, P. A. (2015). Elevated synchrony in Parkinson disease detected with electroencephalography. *Ann. Neurol.* 78, 742–750. doi: 10.1002/ana.24507
- Tahmasian, M., Betray, L. M., van Eimeren, T., Drzeżga, A., Timmermann, L., Eickhoff, C. R., et al. (2015). A systematic review on the applications of resting-state fMRI in Parkinson's disease: does dopamine replacement therapy play a role? *Cortex* 73, 80–105. doi: 10.1016/j.cortex.2015.08.005
- Tessitore, A., Cirillo, M., and De Micco, R. (2019). Functional connectivity signatures of Parkinson's disease. *Journal of Parkinson's Disease* 9, 637–652. doi: 10.3233/JPD-191592
- Tinkhauser, G., Pogosyan, A., Tan, H., Herz, D. M., Kühn, A. A., and Brown, P. (2017). Beta burst dynamics in Parkinson's disease off and on dopaminergic medication. *Brain* 140, 2968–2981. doi: 10.1093/brain/awx252
- Utianski, R. L., Caviness, J. N., van Straaten, E. C. W., Beach, T. G., Dugger, B. N., Shill, H. A., et al. (2016). Graph theory network function in parkinson's disease assessed with electroencephalography. *Clin. Neurophysiol.* 127, 2228–2236. doi: 10.1016/j.clinph.2016.02.017
- van den Heuvel, M. P., de Lange, S. C., Zalesky, A., Seguin, C., Yeo, B. T. T., and Schmidt, R. (2017). Proportional thresholding in resting-state fMRI functional connectivity networks and consequences for patient-control connectome studies: issues and recommendations. *NeuroImage* 152, 437–449. doi: 10.1016/j.neuroimage.2017.02.005
- van Wijk, B. C. M., Beudel, M., Jha, A., Oswal, A., Foltynie, T., Hariz, M. I., et al. (2016). Subthalamic nucleus phase-amplitude coupling correlates with motor impairment in Parkinson's disease. *Clin. Neurophysiol.* 127, 2010–2019. doi: 10.1016/j.clinph.2016.01.015
- Vecchio, F., Miraglia, F., Alù, F., Cotelli, M., Pellicciari, M. C., Judica, E., et al. (2021). Human brain networks in physiological and pathological aging: reproducibility of EEG graph theoretical analysis in cortical connectivity. *Brain Connect.* 12, 41–51. doi: 10.1089/brain.2020.0824
- Voytek, B., Kramer, M. A., Case, J., Lepage, K. Q., Tempesta, Z. R., Knight, R. T., et al. (2015). Age-related changes in 1/f neural electrophysiological noise. *J. Neurosci.* 35, 13257–13265. doi: 10.1523/JNEUROSCI.2332-14.2015
- Watts, D., and Strogatz, S. (1998). Collective dynamics of 'small-world' networks. *Nature* 393, 440–442. doi: 10.1038/30918
- Whitmer, D., de Solages, C., Hill, B., Yu, H., Henderson, J. M., and Bronte-Stewart, H. (2012). High frequency deep brain stimulation attenuates subthalamic and cortical rhythms in Parkinson's disease. *Front. Hum. Neurosci.* 6:155. doi: 10.3389/fnhum.2012.00155
- Wingeier, B., Tchong, T., Koop, M. M., Hill, B. C., Heit, G., and Bronte-Stewart, H. M. (2006). Intra-operative STN DBS attenuates the prominent beta rhythm in the STN in Parkinson's disease. *Exp. Neurol.* 197, 244–251. doi: 10.1016/j.expneurol.2005.09.016
- Zeng, K., Wang, Y., Ouyang, G., Bian, Z., Wang, L., and Li, X. (2015). Complex network analysis of resting state EEG in amnesic mild cognitive impairment patients with type 2 diabetes. *Front. Comput. Neurosci.* 9:133. doi: 10.3389/fncom.2015.00133
- Zhang, J., Idaji, M. J., Villringer, A., and Nikulin, V. V. (2021). Neuronal biomarkers of Parkinson's disease are present in healthy aging. *NeuroImage* 243:118512. doi: 10.1016/j.neuroimage.2021.118512

- Zhou, S., and Yu, Y. (2018). Synaptic E-I balance underlies efficient neural coding. *Front. Neurosci.* 12:46. doi: 10.3389/fnins.2018.00046
- Zhou, X., Ma, N., Song, B., Wu, Z., Liu, G., Liu, L., et al. (2021). Optimal organization of functional connectivity networks for segregation and integration with large-scale critical dynamics in human brains. *Front. Comput. Neurosci.* 15:641335. doi: 10.3389/fncom.2021.641335

Conflict of Interest: The authors declare that the research was conducted in the absence of any commercial or financial relationships that could be construed as a potential conflict of interest.

Publisher's Note: All claims expressed in this article are solely those of the authors and do not necessarily represent those of their affiliated organizations, or those of the publisher, the editors and the reviewers. Any product that may be evaluated in this article, or claim that may be made by its manufacturer, is not guaranteed or endorsed by the publisher.

Copyright © 2022 Zhang, Villringer and Nikulin. This is an open-access article distributed under the terms of the Creative Commons Attribution License (CC BY). The use, distribution or reproduction in other forums is permitted, provided the original author(s) and the copyright owner(s) are credited and that the original publication in this journal is cited, in accordance with accepted academic practice. No use, distribution or reproduction is permitted which does not comply with these terms.

Curriculum Vitae

My curriculum vitae does not appear in the electronic version on my paper for reasons of data protection.

My curriculum vitae does not appear in the electronic version on my paper for reasons of data protection.

Publication list

Publication 1: **Zhang, J.**, Idaji, M. J., Villringer, A., & Nikulin, V. V. (2021). Neuronal biomarkers of Parkinson's disease are present in healthy aging. *NeuroImage*, 243(August), 118512. <https://doi.org/10.1016/j.neuroimage.2021.118512>. Impact factor (2020) = 6.556

Publication 2: Jamshidi, M., **Zhang, J.**, Stephani, T., Nolte, G., Müller, K. R., Villringer, A., & Nikulin, V. V. (2022). Harmoni: a Method for Eliminating Spurious Interactions due to the Harmonic Components in Neuronal Data. *NeuroImage*, 252(March), 119053. <https://doi.org/10.1016/j.neuroimage.2022.119053>. Impact factor (2020) = 6.556

Publication 3: **Zhang, J.**, Villringer, A., & Nikulin, V. V. (2022). Dopaminergic Modulation of Local Non-oscillatory Activity and Global-Network Properties in Parkinson's Disease: An EEG Study. *Frontiers in Aging Neuroscience*, 14(April), 1–18. <https://doi.org/10.3389/fnagi.2022.846017>. Impact factor (2020) = 5.750

Acknowledgments

Throughout my doctoral studies, I have been supported and inspired by several people without whom this thesis would not be possible. First of all, I want to express my gratitude to my supervisor, Prof. Dr. Arno Villringer, whose influence on my thesis and personal career path is indescribable. I thank him for not only believing in and accepting me to give me the opportunity to continue my doctoral study, but also for sharing his insights and guiding me toward my growth in neuroscience, particularly in clinical neuroscience. I have really enjoyed our pleasant and inspiring meetings and conversations.

Even though words cannot express my gratitude to my supervisor Dr. Vadim V. Nikulin, I would like to give it a try. I am very thankful for his guidance toward the path I am currently on. His incredible knowledge and experiences in a wide range of topics, particularly neuroimaging data analysis, have had a huge influence on me, allowing me to gain considerable expertise in this field. He also inspires me to keep trying and improving, and he has served as a role model to me to strive for what I am pursuing.

In addition, I'd like to express my appreciation to colleagues from Charite: Amna Ghani and Paul Triebkorn. They were a pleasure and supportive resource to be around. Then, I would like to give my special thanks to Annette Winkelmann. I was able to steer and redirect my personal professional path with her support. Moreover, I would like to thank all my colleagues and friends at the Max Planck Institute for Human Cognitive and Brain Sciences for their support and company during my doctoral study: Mina Jamshidi, Simon M. Hofmann, Elena Cesnaite, Tilman Stephani, Paul Steinfath, Esra Al, Khosrov Alexander Grigoryan, Magdalena Gippert, Nikolai Kapralov, Moritz Gerster, Studenova Alina, and Maria Azanova. They have provided their valuable input to my work through official and unofficial discussions. A special thanks to Mina Jamshidi who is not only a competitive peer but also a life-long friend. She has generously shared her inspiration and caring, which has given me a lot of strength to get through the difficult times.

My dear friends, both old and new, have also been a part of my life in various ways. Among them, I would like to thank Meng Zhu, Chang Liu, Lijia Long, Yuan Yuan, Weijie Du, Yu Wang, Jie Meng, Ningfei Li, Xu Duan, Ke Chen, Yulin Chen, Fumin Pan, Zonghan Yu, Lei Wang, Ruxue Gong and Shih-Cheng Chien in particular for their

company, support and inspiration. Another person I would like to share my gratitude with is Florian Koch, who has been a constant source of support and encouragement during the years. He has witnessed almost all of my joys, successes, sorrows and frustrations.

Last but not least, I would like to thank my family for providing me conditions to pursue my professional and personal goals. Their unwavering emotional support and care are essential in guiding me through life-changing events. Even though my grandparents are no longer physically with me, I believe their spirits are always present to accompany me along the way.